TECHNICKÁ UNIVERZITA V LIBERCI
Fakulta textilní

PRODUCTION OF NONWOVEN FABRICS BY USING SILK FIBRES VIA ELECTROSPINNING TECHNIQUE

Příprava netkaných textilií s obsahem hedvábných vláken získaných metodou elektostatického zvlákňování

Dissertation

Study programme:

Study branch:

Author: Nongnut Sasithorn, M.Sc.

Supervisor: Doc. Ing. Lenka Martinová, CSc.

Declaration

I hereby certify that I have been informed the Act 121/2000, the Copyright Act of the Czech Republic, namely § 60 - Schoolwork, applies to my dissertation in full scope.

I acknowledge that the Technical University of Liberec (TUL) does not infringe my copyrights by using my dissertation for TUL's internal purposes.

I am aware of my obligation to inform TUL on having used or licensed to use my dissertation; in such a case TUL may require compensation of costs spent on creating the work at up to their actual amount.

I have written my dissertation myself using literature listed therein and consulting it with my thesis supervisor and my tutor.

Concurrently I confirm that the printed version of my dissertation is coincident with an electronic version, inserted into the IS STAG.

Date:

Signature:

Abstract

This dissertation was concerned and focused a fabrication of a silk fibroin (SF) nonwoven sheet and its blending with polycaprolactone (PCL) via a needleless electrospinning technique (technology Nanospider™). The procedure concentrated on a novel method for the preparation of a spinning solution from silk fibroin, by using a mixture of formic acid and calcium chloride as a solvent. The role of concentration of silk fibroin solution, applied voltage and spinning distance are investigated as a function of the morphology of obtained fibres and the spinning performance of the electrospinning process. Biocompatibility of the obtained fibre sheets that resulted from the experiment was evaluated by in vitro testing method, with 3T3 mouse fibroblasts, normal human dermal fibroblasts, MG 63 osteoblasts and human umbilical vein endothelial cells. Tensile strength and hydrophilicity as well as physical properties evaluation of electrospun fibre sheets were performed.

The solvent system consists of formic acid and calcium chloride that can dissolve SF at room temperature, a rate of 0.25 gram of calcium chloride per 1 gram of silk fibroin is required to obtain the completely dissolved silk fibroin solution. This solvent system could be potentially employed and used for a preparation of silk fibroin solution for a large-scale production of silk nanofibres, with a needleless electrospinning method.

The diameters of the silk electrospun fibres obtained from the formic acid-calcium chloride solvent system had a diameter ranging from 100 nm to 2400 nm depending upon the spinning parameters. Concentrations of silk fibroin in the range of 8 wt% to 12 wt% seem to be a suitable concentration for the preparation of a nanofibre sheet, with needleless electrospinning. Furthermore, increasing the concentration of the silk fibroin solution and the applied voltage improved the spinning ability and the spinning performance in needleless electrospinning. Pure silk fibroin electrospun fibres have poor mechanical properties, while research indicates blending PCL with silk fibroin can improve mechanical properties significantly. The diameters of the blended SF/PCL electrospun fibres were smaller and the elasticity was greater than the pure SF elctrospun fibres. However, an increase of PCL content in the blended solution affected the spinning performance of the process. The spinning performance of the electrospinning process tends to decrease as the polycaprolactone content in the blended solution increases.

Silk electrospun fibre sheets and its blends with PCL are promising materials for the biomedical applications such as wound dressing and bone tissue engineering. In vitro tests with living cells show very good biocompatibility of the electrospun fibre sheets, especially with MG 63 osteoblasts. In addition, the PCL/SF blend fibre sheets have been applied as supports for immobilization of laccase from *Trametes versicolor*. The blended fibre sheet were suitable for enzyme immobilization and the blended fibre sheets with the laccase immobilized showed very good results in the degradation of endocrine disrupting chemicals (bisphenol A and 17α-ethinyl estradiol). The laccase immobilization onto the PCL/SF blend fibre sheets seems to be a promising system for bioremediation of wastewater treatment.

Keywords: silk fibroin, needleless electrospinning, formic acid, calcium chloride

Abstrakt

Tato dizertační práce se zabývá výrobou nanovlákenných vrstev z fibroinu z přírodního hedvábí (silk fibroin, dále jen SF), a směsí SF s polykaprolaktonem (PCL) připravené metodou bezjehlového elektrostatického zvlákňování (technologie Nanospider^{TM}). V procesu zvlákňování byla zkoumána inovativní metoda přípravy zvlákňovacího roztoku SF za použití rozpouštědla ve formě směsi kyseliny mravenčí a chloridu vápenatého. Výzkum byl zaměřen na vliv koncentrace roztoku fibroinu, použitého napětí a vzdálenosti elektrod na morfologii vzniklých vláken i na samotný proces zvlákňování. In vitro testy za použití 3T3 myších fibroblastů, lidských kožních fibroblastů, MG 63 osteoblastů a lidských endotelových buněk z pupečníkové žíly byly zvoleny pro hodnocení biokompatibility vlákenných vrstev. Dále byla sledována pevnost v tahu a hydrofilita spolu s dalšími fyzikální vlastnostmi vytvořených vlákenných vrstev.

Rozpouštědlový systém, který sestával z kyseliny mravenčí a chloridu vápenatého, byl schopen rozpustit SF za pokojové teploty při použití poměru 0,25 g chloridu vápenatého na 1 g SF. Tento rozpouštědlový systém je vhodný pro nanovláken metodou elektrostatického zvlákňování na poloprovozní jednotce Superlab.

Průměr vláken, získaných za použití zmíněného rozpouštědlového systému, se pohyboval v rozmezí 100 nm až 2400 nm v závislosti na parametrech zvlákňovacího procesu. Pro přípravu nanovláken prostřednictvím bezjehlového zvlákňování byla optimální koncentrace SF od 8% hmot. do 12% hmot. S rostoucí koncentrací a napětím se zlepšovala zvláknitelnost roztoku a produktivita zvlákňovacího procesu. Zatímco vlákna ze samotného SF měla špatné mechanické vlastnosti, ukázalo se, že ve směsi s PCL docházelo k výraznému zlepšení. Průměr směsných nanovláken byl nižší a pružnost těchto vrstev byla vyšší než v případě čistého SF. Se zvyšujícím se podílem PCL však docházelo ke zhoršení zvlákňovacího procesu.

Nanovlákenné vrstvy z čistého SF a ze směsi SF a PCL jsou materiály s potenciálem pro využití v biomedicínských aplikacích, jako jsou kryty ran nebo tkáňové inženýrství zaměřené na regeneraci kostních tkání. In vitro testy s živými buňkami, především MG 63 osteoblasty, potvrdily velmi dobrou biokompatibilitu připravených nanovlákenných vrstev. PCL/SF nanovlákna navíc našla své uplatnění jako nosič pro imobilizaci lakázy *Trametes versicolor*. Nejen že se tato směsná nanovlákna uplatnila jako nosič pro enzym, ale zároveň měla imobilizovaná lakáza velmi dobré výsledky v oblasti degradace endokrinních disruptorů (bisfenol A a 17α-ethinyl estradiol). Imobilizace lakázy na PCL/SF nanovlákna má potenciál pro využití při čištění odpadních vod.

Klíčová slova: přírodní hedvábí, bezjehlové elektrostatické zvlákňování, kyselina mravenčí, chlorid vápenatý

Acknowledgement

I would like to express my gratitude and appreciation to my advisor, Doc. Ing. Lenka Martinová, CSc. for her kind suggestion, valuable guidance and encouragement throughout the experimental period and review my dissertation. Furthermore, I am most indebted to Prof. RNDr. Oldřich Jirsák, CSc., his excellent guidance, kind suggestion and valuable advice which has enable me to carry out the research successfully. His kindness will be long remembered.

My sincere thanks are expressed to Ing. Rattanaphol Mongkholrattanasit, Ph.D. from Department of Textile Chemistry Technology, Faculty of Industrial Textiles and Fashion Design, Rajamangala University of Technology Phra Nakhon for invaluable help and constant encouragement throughout the course of this research. I would also like thank Mgr. Jana Horáková from Department of Nonwovens and Nanofibrous Materials, Faculty of Textile Engineering, Technical University of Liberec for her help with *In vitro* testing of my material. Additionally, I would like to thank Ing. Milena Maryšková, my student from Department of Nonwovens and Nanofibrous Materials for her help with enzyme immobilization and characterization of my material.

My thanks go to Mrs. Chan Wises, the owner of silk farm in Si Sa Ket Province, Thailand, for materials support (raw silk cocoons and silk fibres). Many thanks go to my colleagues from Department of Nonwovens and Nanofibrous Materials, Faculty of Textile Engineering, Technical University of Liberec and my friends, whose names are not mentioned here, who have contributed suggestions and courteous assistance during the course of my research. In addition, my special thanks go to Rajamangala University of Technology Phra Nakhon (RMUTP) for supporting a scholarship throughout my study.

Finally, I would like to express my deepest gratitude to my family's member especially my parents and my sisters for their support and continual encouragement throughout the period of my study.

Contents

Contents

Contents

List of Figures

List of Figures

List of Figures

List of Figures

List of Tables

Notations

Å	Angstrom
ABTS	2,2′-Azino-bis(3-ethylbenzothiazoline-6-sulfonic acid) diammonium salt
ASTM	American Society for Testing and Materials
ATCC	American Type Culture Collection
AY	Activity Yield
BPA	Bisphenol A
BSA	Bovine Serum Albumine
$CaCl_2$	Calcium chloride
$CHCl_3$	Chloroform
C_2H_5OH	Ethyl alcohol
^{13}C-NMR	Carbon-13 nuclear magnetic resonance
DAPI	2-(4-amidinophenyl)-1H -indole-6-carboxamidine
DIW	Deionized water
DMF	N,N-Dimethylformamide
DMEM	Dulbecco´s Modified Eagle Medium
DSC	Differential Scanning Calorimetry
ECM	Extracellular matrix
EDCs	Endocrine disrupting chemicals
EE2	17α-ethinyl estradiol
FBM	Fibroblast Basal Medium
FBS	Fetal Bovine Serum
FGM	Fibroblast Growth Media
FTIR	Fourier Transform Infrared Spectroscopy
GA	Glutaraldehyde
HFIP	Hexafluoroisopropanol
HMD	Hexamethylenediamine
H_2O	Water
HPLC	High Performance Liquid Chromatography
HUVEC	Human Umbilical Vein Endothelial Cells
IY	Immobilization Yield
J/gK	Joules per gram-kelvin
LiBr	Lithium bromide
mN/m	millinewtons per meter
Milli-Q	Ultrapure water of "Type 1", 18 MΩ
mS/cm	milli-Siemens per centimeter

Notations

MTT test	cell viability test using 3-(4,5-dimethylthiazol-2-yl)-2,5-diphenyl-2*H*-tetrazolium bromide
$NaHCO_3$	Sodium hydrogen carbonate
NHDF	Normal Human Dermal Fibroblasts
PBS	Phopshated Buffer Saline
PCL	Polycaprolactone
PEG	Polyethylene glycol
PVA	Polyvinyl alcohol
RPM	Revolutions per minute
R_S, Ω kg/m^2	the resistance in ohms between the ends of a specimen 1 meter long and of mass 1 kilogram
RT	Retention time
SEM	Scanning Electron Microscopy
SF	Silk fibroin
StDev	Standard Deviation
W/(mK)	Watts per meter kelvin

1. Introduction

Polymer nanofibres have gained much attention as promising materials due to their unique properties, such as a high specific surface area, small pore diameters and ability to act as a barrier against microorganisms. They have shown enormous application potential in diverse areas, including filtration, energy storage, catalyst and enzyme carriers, drug delivery and release control systems and tissue engineering scaffolds. [1-3]. There are several methods to produce fibres at the nanoscale. One of these, electrospinning, has attracted a lot of interest in the last decade. Electrospinning was described as early as 1934 by Anton [5]. It is a simple but effective method to produce polymer fibres with a diameter in the range of several micrometres down to tens of nanometres, depending on the polymer and processing conditions [4-5].

Electrospinning technology can be divided into two branches: conventional or needle electrospinning and needleless electrospinning. Needle electrospinning setup normally comprises a high-voltage power supply and a syringe needle or capillary spinner connected to a power supply and a collector. During the electrospinning process, a high electric voltage is applied to the polymer solution. This leads to the formation of a strong electric field between the needle and the opposite electrode, resulting in the deformation of the solution droplet at the needle tip into a Taylor cone. When the electric force overcomes the surface tension of the polymer solution, the polymer solution is ejected off the tip of the Taylor cone to form a polymer jet. Randomly deposited dry fibres can be obtained on the collector due to the evaporation of solvent in the filament [5-6]. As a needle can produce only one polymer jet, needle electrospinning systems have very low productivity, typically less than 0.3 g/h per needle, making it unsuitable for practical uses [7].

Needleless electrospinning systems have been developed recently. In needleless electrospinning, instead of the generation of a polymer jet from the tip of the needle, polymer jets form from the surface of free liquid by self-organization [6-14]. For example, Jirsak et al. [9] invented a needleless electrospinning system using a roller or cylinder as the fibre generator, which was commercialized by Elmarco Co. (Czech Republic) with the brand name "Nanospider^{TM}". The roller electrospinning device contains a rotating cylinder electrode, which is partially immersed in a polymer solution reservoir. When the roller slowly rotates, the polymer solution is loaded onto the upper roller surface. Upon applying a high voltage to the electrospinning system, a number of solution jets are simultaneously generated from the surface of the rotating spinning electrode, thereby improving fibre productivity [5].

Silk is a fibrous protein produced by a variety of insects, including the silkworm. Silk fibres from silkworms have been used in textiles for nearly 5,000 years. The primary reasons for this longtime use have been the unique luster, tactile properties, high mechanical strength, elasticity, durability, softness and dyability of silks. Silk fibres are remarkable materials displaying unusual mechanical properties: strong, extensible, and mechanically compressible. Silks also display interesting thermal and electromagnetic responses, particularly in the UV range for insect entrapment and form crystalline phases related to processing [15]. Silk fibres were used in optical instruments as late as the mid-1900s because of their fine and uniform diameter and high strength and stability over

a range of temperatures and humidity. In addition to its outstanding mechanical properties, it is a candidate material for biomedical applications because it has good biological compatibility and oxygen and water vapour permeability, in addition to being biodegradable and having minimal inflammatory reactions [16-21]. Silks have historically been used in medicine as sutures over the past 100 years and are currently used today in this mode along with a variety of consumer product applications. Commercially, silkworm cocoons are mass produced in a process termed ‘‘*Sericulture*’’ [15].

Although the silk worm spins its cocoon from a continuous filament of silk, the rest of the silk cocoon is unsuitable for reeling, and is known as *silk waste.* Silk waste includes cocoons that are not suitable for reeling and waste silk from all stages of production from reeling through weaving. In Thailand, a large amount (36.6 tons) of this by-product is produced annually. The composition of silk waste is similar to that of good silk, which is composed of an inner core protein called fibroin that is surrounded by a glue-like protein called sericin. Silk waste have been roughly characterized by scientists and showed high value of remaining nutrients such as protein and lipid that could be transformed into high-value products. Many attempts have been emphasized on application of these silk wastes for purposes, for example handicraft, cosmetics, medical materials for human health and food additives according to its characteristics [22].

In order to discover the alternative way of value adding from silk waste in Thailand, this study interested in the fabrication of silk fibroin nanofibre sheets with needleless electrospinning techniques, concentrating on the effect of parameters on the electrospinning process.

Objective of the work

In order to utilize silk waste, as well as achieve large-scale production of electrospun fibre sheets. It is necessary to be able to regenerate silk fibres through a simple but efficient spinning process. A needleless electrospinning was chosen as a technique for a preparation of electrospun fibre sheets for these studies owning to a capability to fabricate nanofibre layers in a mass industrial scale. However, a needleless electrospinning is a new technique and most research on an electrospinning of silk fibroin has been focused on the needle electrospinning system. There was a little information on an electrospinning of silk fibroin with a needleless system; therefore, parameters of the spinning process with have not been identified.

The aim of this research is to fabricate silk fibroin nanofibres with a needleless electrospinning method, the experiment intensively concentrated on the effect of parameters on the needleless electrospinning process. In these studies the role of concentration of silk fibroin solution, applied voltage and working distance are investigated as a function of the morphology of the obtained fibres and the spinning performance of the electrospinning process. In addition, a new method for a preparation of the spinning solution by dissolving silk fibroin in a mixture of formic acid and calcium chloride is being used for a solution preparation instead of a conventional method (as described in topic 2.1.9). Furthermore, a characterisation of properties of the obtained electrospun fibre sheets and their interaction with living cells were also studied.

2. Theoretical and literature review

2.1 Silk fibre and its characteristics

Silks represent one member of a larger class of fibrous proteins in nature, which include keratins, collagens, elastins, and others. These types of proteins can be considered nature's equivalent of synthetic block copolymers. Aside from their direct use in materials applications, fibrous proteins provide experimentally accessible model systems with simpler and well controlled genetic template-based protein synthesis. Silk, a fibrous protein secreted by several species of insects for building structures external to the body known as cocoons. A wide variety of natural silks from hundreds of different silkworm species are available throughout the world. Among these, the family Bombycoidea consists of eight families of which Bombycidae and Saturniidae are commercially important. The family Bombycidae silkworm silk is categorized as *mulberry silkworms* (Bombyx species), while the Saturniidae fall under the category of *non-mulberry silkworms* (Antheraea species). Nonmulberry silks are also known as wild silks.

Commercially available mulberry silk is produced from one single species called *Bombyx mori* (as the silkworm feeds on the leaves of the mulberry plant). Mulberry silkworms are entirely domesticated, and they do not occur naturally. They need human care for their growth and reproduction. It is believed that this species originates from its native wild ancestor species, *Bombyx mandarina* by gene duplication and chromosomal fusion mechanism.

Bombyx mori scientific classification (according to Carolus Linnaeus, 1758): Kingdom: Animalia; Phylum: Arthropoda; Class: Insecta; Order: Lepidoptera; Family: Bombycidae; Genus: *Bombyx*; Species: *mori*.

Bombyx mandarina scientific classification (according to Frederic Moore, 1872): Kingdom: Animalia; Phylum: Arthropoda; Class: Insecta; Order: Lepidoptera; Family: Bombycidae; Genus: *Bombyx*; Species: *mandarina*. [23]

Bombyx mori is classified as Chinese, Japanese, European, Indian, etc. They are also classified as pure, monohybrid or polyhybrid, based on the crossings made between two pure strains or more than two pure strains [24]. The number of breeds per year greatly depends upon the climatic conditions. According to climate, these species are also classified into univoltine (generating silk only once annually), bivoltine (harvested twice annually) and multivoltine (harvested throughout the year) [25]. The univoltine breed is generally linked with the geographical area within greater Europe. The eggs of this type hibernate during winter due to the cold climate, and cross-fertilize only by spring, generating silk only once annually. The second type, bivoltine is normally found in China, Japan, and Korea. The breeding process of this type takes place twice annually, a feat made possible through the slightly warmer climates and the resulting two lifecycles. The multivoltine type of mulberry silkworm can only be located in the tropics. The eggs are laid by female moths and hatch within 9 to 12 days, so the resulting type can have up to eight separate lifecycles throughout the year [26].

2.1.1 Composition of silk

In contrast to all other natural fibres, silk does not have a cellular structure. In this respect, and in the way it is formed, it closely resembles a man-made fibre. Morphologically, silk is very simple. It consists of two single compact, continuous threads, which are extruded by the silkworm as it spins its cocoon. These are surrounded and covered by silk gum or sericin. The denier of the filament varies within the cocoon. A silkworm extrudes liquid fibre from the two excretory canals of sericteries, which unite in the spinneret in its head. Each of these two threads is known as a brin. The two brins are cemented together in the spinneret by sericin to become a single continuous fibre called the bave or filament, as illustrated in Figure 2.1. Sericin acts as a glue and fixes the fibroin fibres together in a cocoon. Fibroin and sericin protein has useful properties and has been found to possess various biological functions.

Silk of *Bombyx mori* is composed of the proteins fibroin and sericin, as well as soluble organic matter such as fats, wax, ash and mineral salts. Silk is naturally coloured yellow or green and thus contains a small amount of colouring matter. The content of all these substances is not constant and varies within wide limits, depending on the species of silkworm and on the location and conditions of rearing. Silk filament contains the following (by total weight): 72-81% fibroin, 19-28% sericin, 0.8-1.0% fat and wax and 1.0-1.4% colouring matter and ash [27].

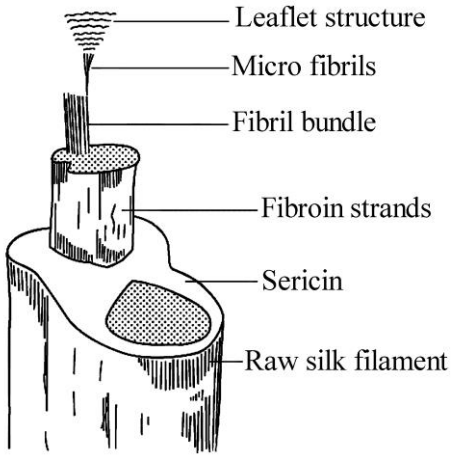

Figure 2.1 Structure of raw silk filament [27].

The fibroin and sericin are made up of chains of amino acids. The amino acid composition of both sericin and fibroin proteins differ significantly. In sericin, the amino acid chain sequences are randomly arranged and form amorphous regions. In fibroin, the amino acid chains are arranged mostly in an ordered pattern, which results in high crystalline regions. Microfibrils are the miniature protein strands composed of ordered amino acid chains. These microfibrils are found in bundles; several such bundles constitute a single fibroin filament.

2.1.2 Silk proteins

Silk is a strong and lustrous natural fibre, which mainly contains protein polymer. Silk protein obtained from different silkworm species consists of two totally different families of proteins, namely fibroin and sericin.

Figure 2.2 SEM images of silk fibres before (left) and after (right) degumming (SEM magnification 2 kx)

- *Fibroins*

Fibroin is a glycoprotein composed of two equimolar protein subunits of 370 kDa and 25 kDa covalently linked by disulphide bonds. Fibroin is secreted from the posterior gland of silkworms and sericin is secreted from the middle and anterior gland of the silkworms. During spinning, the larvae secrete two very thin (~10 μm diameter) fibroin twin strands from the two exocrine silk glands (aligned on both sides of the body) through the spinnerets, simultaneously gluing them together with sericin. In the presence of air, the protein fibre becomes stronger and harder.

Fibroin protein is the major constituent (around 72-81%) of the cocoon and the remaining 19-28% is sericin protein. Fibroin filament is made of both crystalline and amorphous domains. The amorphous domains are characterized by the presence of amino acids with bulkier side chains, whereas the crystalline domains are characterized by high percentage of alanine, glycine, and serine, which contains short side chains to permit the close packing densities for overlying sheets [23]. The crystalline part contributes to the strength and toughness and the amorphous part contributes the flexibility and elasticity to the fibre. Being a hydrophobic glycoprotein, fibroin is insoluble in water. It contains a large amount of hydrogen bonds.

- *Sericins*

Sericin is a second type of silk protein, which contains 18 amino acids including essential amino acids and is characterized by the presence of 32% of serine. The total amount of hydroxy amino acids in sericin is 45.8%. There are 42.3% of polar amino acid and 12.2% of nonpolar amino acid residues. Sericin contributes about 20-30% of total cocoon weight [28]. Their main role is to envelop the fibroin. In presence of sericin, the fibres are hard and tough and become soft and lustrous after its removal. Sericin occurs mainly in an amorphous random coil and to a lesser extent in a β-sheet organized structure [15, 29].

Sericin isolated from the cocoon has two subunits, namely α-sericin, found in the external layer, and β-sericin, found in the inner layer of the cocoon. Because of the presence of a lesser amount of C and H and a higher amount of N and O than β-sericin, α-sericin is more soluble than β-sericin. Sericin is a hydrophilic (soluble in hot water) protein, and can therefore be removed or separated from the fibroin by a simple

thermochemical process known as *'degumming'*. This protein is amorphous and glue-like in nature, which helps in adhering one fibroin to the next fibroin fibre and in maintaining the structural integrity of the cocoon. Another very rare and discrete silk protein sericin can be found in the cocoon, which is produced in the middle and posterior gland of the silkworm [23].

- *Protein from Sericin-Hope*

The improved mutant variant of *Bombyx mori* is known as Sericin-Hope, which was developed by Yamamoto and colleagues. As the posterior gland is degenerated in this species, they are able to produce threads, which contain almost 98.5% sericin protein and a negligible amount of fibroin protein. The sericin is known as virgin sericin. The protein contains eighteen kinds of hydrophilic polar amino acids with nucleophilic side groups and the presence of serine as a major amino acid (one third of the total amino acids present). The cocoon made from this thread is very thin, brittle and easily dissolvable in water with less hydrolysis. The molecular structure of virgin sericin is the same as the sericin protein isolated from a normal *Bombyx mori* cocoon. It is produced in pure conditions in comparison with normal thermochemically degraded sericin, and it has better mechanical strength and other physicochemical properties [23].

2.1.3 Chemical compositions of silk fibres

As for the chemical composition, *Bombyx mori* fibres consist of 15-16 α-amino acids linked together to form a biopolymer whose ratio varies between different areas of the supramolecular structure of fibroin. In the fibroin, glycine and alanine together account for 70% of the total composition (as shown in Table 2.1) whereas in the sericin they make up about 15%. The chief component of sericin is another amino acid, serine (30% of the total).

Silk polymer contains two structural proteins termed *fibroin heavy chain* and the *fibroin light chain*. Heavy areas of silk polymer, with a mean molecular weight of up to 350-370 kDa mainly consist of highly ordered hydrophobic macromolecules, and in looser light areas with a mean molecular weight of about 25 kDa the major components are polar amino acid residues. The majority of the polar groups in silk fibre are supplied by the hydroxyl containing amino acids serine, threonine and tyrosine. These two proteins are linked by a single disulfide bond to form a large protein chain that remains linked during protein processing into fibres by the silkworm and may play a role in the regulation of chain-folding and fibre formation. Aside from these core proteins, there is the family of sericin proteins that range in molecular weight between 20 kDa and 310 kDa that bind the fibroin chains together in the silk threads [28].

The raw silk fibre extracted from a silk cocoon is subjected to a degumming process to remove sericin from it. The silk fibre after degumming contains fibroin protein. This fibroin is composed of about 20 different amino acids. Glycine (about 44%), followed by alanine (about 29%), are the main amino acids present in the mulberry silk fibroin; whereas in wild silks, alanine (about 40%), followed by glycine (about 25%), are the highest amino acid present. Aspartic acid and glutamic acid are the acidic amino acids, while arginine, histidine and lysine are the basic amino acids that are present in

higher proportions in the silk fibroin of wild silks. Other amino acids present in silk fibroin are neutral in nature.

Table 2.1 Composition of amino acid in silk fibroin [28]

Amino acid	Symbol	Charge	Hydrophobicity/ Hydrophilicity	Composition (mol %)		
				Total	Heavy areas	Light areas
Glycine	Gly	neutral	hydrophilic	42.90	49.40	10.00
Alanine	Ala	neutral	hydrophobic	30.00	29.80	16.90
Serine	Ser	neutral	hydrophilic	12.20	11.30	7.90
Tyrosine	Tyr	neutral	hydrophilic	4.80	4.60	3.40
Valine	Val	neutral	hydrophobic	2.50	2.00	7.40
Aspartic acid	Asp	-	hydrophilic	1.90	0.65	15.40
Glutamic acid	Glu	-	hydrophilic	1.40	0.70	8.40
Threonine	Thr	neutral	hydrophilic	0.92	0.45	2.80
Phenylalanine	Phe	neutral	hydrophobic	0.67	0.39	2.70
Methionine	Met	neutral	hydrophobic	0.37	-	0.37
Isoleucine	Ile	neutral	hydrophobic	0.64	0.14	7.30
Leucine	Leu	neutral	hydrophobic	0.55	0.09	7.20
Proline	Pro	neutral	hydrophobic	0.45	0.31	3.00
Arginine	Arg	+	hydrophilic	0.51	0.18	3.80
Histidine	His	+	hydrophilic	0.19	0.09	1.60
Lysine	Lys	+	hydrophilic	0.38	0.06	1.50

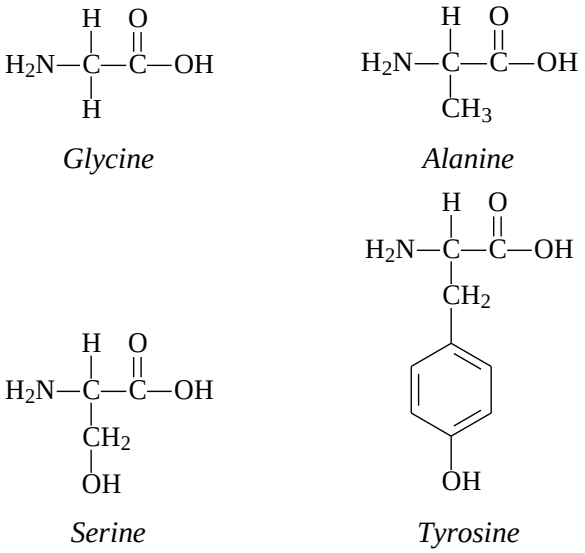

Figure 2.3 Structure of four most abundant amino acid groups found in *Bombyx mori* silk.

2.1.4 Morphological structure of silk fibroin

Silk fibroin morphological structure can be explained in four levels of observations, as explained below.

1. Primary structure (amino acid structure): The silk fibroin is composed of many microfibrils, which are composed of a large number of amino acids in ordered and disordered regions. These amino acids can be represented as -$HNCH_2RCO$-, where R is the side group specific to a different amino acid (Fig. 2.4). The amino acids in the fibroin are joined in a sequential polypeptide chain by the amide linkages (CONH), which are known as polypeptide bonds. The length of the fibroin molecular chain is about 140 nm and its molecular weight ranges from 300 kDa to 400 kDa [25].

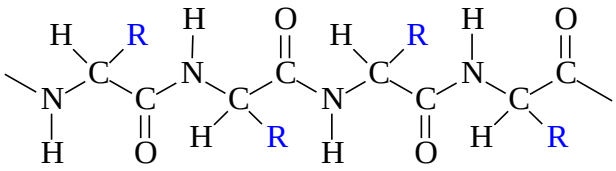

Figure 2.4 Polypeptide chain of silk fibroin molecule.

Silks are considered semicrystalline materials with 62-65% in cocoon silk fibroin from the silkworm *Bombyx mori* [27]. The crystalline portion in primary structure contains repetitive amino acids: glycine, alanine and serine as $(Gly\text{-}Ser\text{-}Gly\text{-}Ala\text{-}Gly\text{-}Ala)_n$ along its sequence (Fig. 2.5), forming a layer of antiparallel, hydrogen-bonded β-sheet and leading to the stability and mechanical properties of the fibre. The high glycine (and, to a lesser extent, alanine) content allows for tight packing of the sheets, which contributes to silk's rigid structure that cannot be stretched. A combination of stiffness and toughness make it a material with applications in several areas, including biomedicine and textile manufacture. These sections have simple branching owing to which the chains may be closely and compactly arranged. Sections containing residues of tyrosine, praline, diamine and dicarboxylic acids are characterized by bulky residues which impede regular and close packing of chains and, as a result, less oriented (amorphous) regions are formed. The degree of branching of the polypeptide chain depends on the amino acids contained in the protein. Thus, the side chains form 19% of the weight in silk fibroin. The side chains may be non-polar, as for instance hydrocarbon residues. The amorphous domains are characterized by the presence of amino acids with bulkier side chains, whereas the crystalline domains are characterized by high percentage of alanine, glycine and serine (12, 30 and 44%, respectively), which contains short side chains to permit the close packing densities for overlying sheets [28].

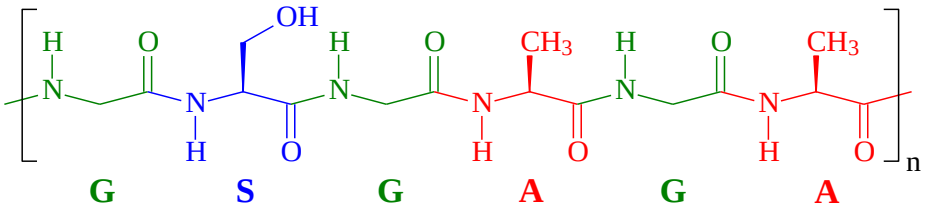

Figure 2.5 Silk fibroin primary structure.

2. Secondary structure (polypeptide chain structure): The silk fibroin is composed of simple amino acids, mostly with hydrocarbon side groups; as a result of these side groups strong hydrogen bonding and salt linkages exist between the polypeptide chains of the amino acids, resulting in a β-pleated sheet form of silk fibroin, as shown in Figure 2.6.

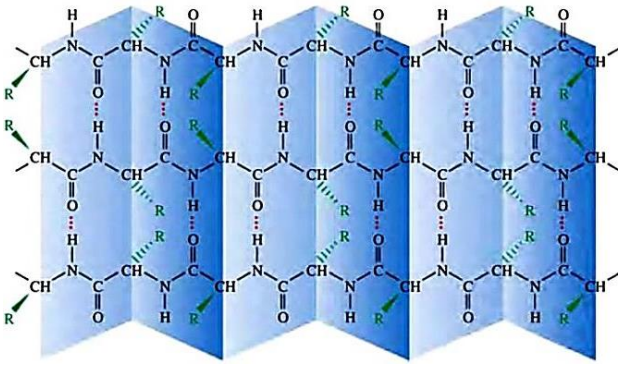

Figure 2.6 β-Pleated sheet form of polypeptide chain arrangements in silk fibroin [30].

In the β-sheet crystals the polymer chain axis is parallel to the fibre axis. The extent, to which these structures form, as well as their orientation and size, directly impact the mechanical features of silk fibres. Furthermore, the polyalanine repeats or the glycine-alanine repeats are the major primary structure sequences responsible for β-sheet formation. Other silks can also form α-helical structures (such as some bees, wasps, ants) or cross-β-sheet structures (many insects) structures. The cross-β-sheets are characterized by a polymer chain axis perpendicular to the fibre axis. Most silks assume a range of different secondary structures during processing from soluble protein in the glands to insoluble spun fibres. Infrared spectroscopy is often used to distinguish some of the polymorphs (Table 2.2). Most silkworm fibres contain assembled antiparallel β-pleated sheet crystalline structures.

Three main kinds of secondary structures of natural silk fibroin are distinguished today: in crystalline areas, α-helical and β-pleated folded structures and in amorphous areas, disordered conformation of random globules. Fibroin of natural *Bombyx mori* fibres contains 56±5% macromolecules in the β-pleated folded form and 13±5% macromolecules in the α-helical form. Thus, the fraction of highly ordered (crystalline) areas of the polymer reaches 60-70%. Three crystalline forms of silk fibroin is known to arrange itself in three structures, called Silk I (prespun), Silk II (spun), and Silk III (interfacial) [15].

- *Silk I (prespun)* is the natural form of fibroin, as emitted from the *Bombyx mori* silk glands. The prespun pseudocrystalline form in a water-soluble state, remains without a consensus structure in the field and likely represented by many partially stable states. Silk I structure is unstable and on shearing, drawing, heating, spinning, or exposure in an electric field, or exposure to polar solvents such as methanol or acetone, converts to silk II. The change in unit cell dimensions during the transition from silk I to silk II during fibre spinning is most significant in the intersheet plane, with an 18.3% decrease in distance between overlying sheets based on modeling predictions. This change results in the exclusion of water, reducing solubility.

- *Silk II (spun)* refers to the arrangement of fibroin molecules in spun silk, which has greater strength and is often used in various commercial applications, the spun form of silk that is insoluble in water. The unit cell parameters in the silk II structure are 0.94 nm (a, interchain), 0.697 nm (b, fibre axis), and 0.92 nm (c, intersheet). These unit cell dimensions are consistent with a crystalline structure in which the protein chains run antiparallel, with interchain hydrogen bonds perpendicular to the chain axis between carbonyl and amine groups and Van der Waal forces stabilize intersheet interactions (based on the predominance of short side-chain amino acids such as glycine, alanine, and serine in the crystalline regions). The β-sheets consisting of the glycine-alanine crystalline repeats in the silkworm fibreare asymmetric, with one surface primarily projecting alanyl methyl groups and the other surface of the same sheet containing hydrogen atoms from the glycine residues. In silk II, these sheets are organized back-to-back such that for every other sheet, the sheet-to-sheet interacting faces are the glycyl side-chains and the alternating interacting faces are the alanyl methyl groups. This arrangement leads to alternating intersheet spacings of 3.70 Å in the glycyl and 5.27 Å in the alanyl interacting intersheet distances. Silk II is more thermodynamically stable than silk I and the energy barrier for the transition is low, whereas the return barrier is high and considered essentially irreversible

- *Silk III (interfacial)* is a newly discovered structure of fibroin. Silk III is formed principally in solutions of fibroin at an interface i.e. air-water interface, water-oil interface. Silk III structure stabilized at interfaces optimizes the surfactancy of the silk in the core repeats of glycine, alanine and serine.

Table 2.2 Infrared spectral features to assist in clarifying structural polymorphs of silk fibroin during various stages and modes of processing [15].

Secondary structures	**Absorption bands (cm^{-1})**
α-helix	1648-1662
β-sheet	1624-1642, 1645,1699, 1703
Antiparallel	1629, 1630-1636, 1690-1693, 1696
Parallel	1630, 1640, 1645
Turns and bends	1666-1688, 1691
Random coil	1641, 1649, 1650, 1653, 1656-1660
Silk I	1641, 1645, 1649-1650
Silk II	1624-1625, 1697
Silk III	1662

3. Tertiary structure (3D arrangement of polypeptide chains): The tertiary structure of the silk fibroin details the 3D configuration of the polypeptide chains and the β-pleated sheet forms. The crystal structure of silk fibroin, in which four amino acid molecules pass through a rectangular unit cell with a = 9.37 Å, b = 9.49 Å and c = 6.98 Å [25].

4. Quaternary structure (Complex protein structure): Overall, the silk fibroin structure is reported to consist of aggregates of polypeptide chains in β-pleated sheet form, arranged parallel to the silk fibre axis. These β-pleated sheet forms are held together by lateral forces with freedom and space in disordered regions. In ordered crystalline regions, close packing of the polypeptide chains and β-pleated sheet forms are assisted by strong hydrogen bonds and further strengthened by the van der Waals forces. The morphological structure of silk fibroin has evolved through good, close packing of polypeptide chains and yields about 48% of crystalline regions in the mulberry silk fibre [25].

2.1.5 Mechanical properties

Silk is a strong fibre comparable to the medium tenacity synthetic fibres nylon and polyesters. Silk is the only natural fibre available in a filament form; coupled with good tenacity, it has unparalleled supremacy for being a niche comfort fibre with strong durability credentials. The mechanical properties of silk fibres consist of a combination of high strength, extensibility and compressibility. The mechanical properties of silk fibres are a direct result of the size and orientation of the crystalline domains, the connectivity of these domains to the less crystalline domains, and the interfaces or transitions between less organized and crystalline domains [25].

2.1.6 Thermal properties

Silk fibre is thermally stable below 100 ^{O}C. A high degree of molecular orientation of silk fibroin aids the thermal stability of the silk fibre. Yellowing begins to occur in silk fibres at 110 ^{O}C after 15 min of exposure. From the peaks of the DSC curves of silk [31] predicted that the glass transition temperature of silk is about 175 ^{O}C, and silk fibre degradation begins at 280 ^{O}C with an initial weight loss starting at about 250 ^{O}C. The amorphous regions play the major role in determining the behaviour of silk fibres subjected to heat treatments. When silk fibre is subjected to heat, no significant changes are observed in the crystalline structure of the silk but the amorphous region becomes highly oriented [25]. The strength retention of silk fibre exposed to 100 ^{O}C for 20 days and 80 days is 73% and 39%, respectively. When exposed to flame, silk fibre catches fire and burns slowly. It self-extinguishes when removed from the flame. Upon burning silk fibre, an odor of burning hair is detected.

Silk is a good insulator of heat among the textile fibres; the specific heat of dry silk fibre is 1.38 J/gK [32], which is marginally better than cotton (1.3 J/gK) and wool (1.36 J/gK). The thermal conductivity of mulberry silk fibre in longitudinal (K_L) and transverse (K_T) direction is 1.49 W/(mK) and 0.119 W/(mK) respectively, resulting in anisotropic ratio (K_L/K_T) of 12.64, which indicate high orientation of fibroin molecules along the direction of the fibre. The thermal conductivity of silk along the transverse direction is very poor compared to 0.165 W/(mK) of wool and 0.243 W/(mK) of cotton.

Due to the lower thermal conductivity and high moisture regain of silk fibres, the comfort level of wearing silken items is decreased in hot and humid conditions [25].

2.1.7 Dielectric properties

Silk fibres are insulators for electrical conduction. Therefore, under the action of friction, static electric charges tend to develop in the fibres. The high moisture regain dissipates the static charges effectively; however, under low humidity conditions, static charges pose problems for silk fibre handling. Like most textile fibres, silk fibres get positive static charges. The insulation resistance and dielectric strength of silk fibres give an indication of their dielectric constant, current leakages at certain voltages, moisture content, and stability under electric fields. Electrical and dielectric properties have gained importance with applications such as moisture measurement, evenness measurement, and the use of silk fibres in the form of fibre reinforced composites as insulating materials for special applications. The electrical resistance (R_S, Ω kg/m^2) of silk fibres is 9.8 (log R_S value) at 65% RH The electrical resistance of silk fibre drops with increased humidity and temperature [25, 32].

2.1.8 Solubility and solvent for silk fibroin [15, 29]

Natural silk fibres dissolve only in a limited number of solvents because of the presence of a large amount of intra- and intermolecular hydrogen bonds in fibroin and its high crystallinity. Silks are difficult to resolubilize due to the extensive hydrogen bonding and van der Waals interactions, and the exclusion of water from the intersheet regions. Consequently, hydrogen bonds have an important effect on the conformation and structure of fibroin. The influence of hydrogen bonding on the stability of fibroin molecules can be seen by the ease with which protein dissolution occurs in known hydrogen bond-breaking solvents.

Silk fibroins are insoluble in water, dilute acids, alkali and the majority of organic solvents but only swells to 30-40%; two thirds of the absorbed solvent is retained by the amorphous fraction of the polymer. They are also partially resistant to most proteolytic enzymes, with the exception of chymotrypsin and other V8 protease. Silk fibroin can be dissolved in concentrated aqueous solutions of acids (Hydrochloric acid, Phosphoric acid and Sulphuric acid) and in high ionic strength aqueous salt solutions, such as lithium thiocyanate (LiCNS), sodium thiocyanate (NaSCN), lithium bromide (LiBr), calcium chloride ($CaCl_2$), calcium thiocyanate ($Ca(CNS)_2$), zinc chloride ($ZnCl_2$), magnesium chloride ($MgCl_2$), magnesium thiocyanate ($Mg(SCN)_2$) and copper salts such as copper ethylene diamine ($Cu(NH_2CH_2CH_2NH_2)_2(OH)_2$), copper nitrate ($Cu(NO_3)_2$) and $Cu(NH_3)_4(OH)_2$. This kind of salts have chaotropic properties that disrupts stabilizing intra-molecular forces such as hydrogen bond by shielding charges and preventing the stabilization of salt bridges. Hydrogen bonding is stronger in nonpolar media, so salts, which increase the chemical polarity of the solvent, can also destabilize hydrogen bonding. Mechanistically this is because there are insufficient water molecules to effectively solvate the ions. This can result in ion-dipole interactions between the salts and hydrogen bonding species, which are more favorable than normal hydrogen bonds. It will make hydrophobic proteins more soluble in water.

The main disadvantage of a salt-containing aqueous solvent is the long preparation time because aqueous solutions of fibroin have to be dialyzed for several days to remove the salts and to recover the polymer as films, sponges, or powder from the aqueous solution by dry forming. The solvency of aqueous salt systems depends on the salt concentration and increases in the following order: for anions, sulfate < citrate < tartrate < acetate < chloride < nitrite < bromide < iodide < thiocyanate < dichloroacetate; for cations, $Ca^{2+} < Sr^{2+} < Ba^{2+} < Li^{+} < Zn^{2+}$. The solvency of aqueous salt systems depends on the salt concentration, although premature reprecipitation is a problem unless the solutions are kept at low temperature. In some organic solvents (e.g. hexafluoroacetone and hexafluoroisopropanol), fibroin can be dissolved only after preliminary activation by dissolution in aqueous salt systems followed by the recovery.

2.1.9 Reprocessed silks for new materials

The silk fibroin protein is a structuring molecule that has the ability to be processed into numerous forms through a variety of techniques. Due to the material's inherent biocompatibility, the protein has been recently utilized as a scaffold for developing a number of biomedical product ideas for use in clinical applications. Several different material morphologies can be formed from aqueous or solvent formulations of the natural fibre form of silk for utilization in biomaterials for biomedical applications.

Various forms of silk fibroin, such as gels, powders, fibres and non-woven membranes can be regenerated by dissolution in aqueous systems, followed by recovery and reprocessing into desired material formats [15, 29]. There are several methods to reprocess silk fibres. Dissolution methods used for solubilizing the degummed silk fibroin fibres generally rely on strong chaotropic agents, including concentrated acids, inorganic salts, fluorinated organic solvents, and ionic liquids, to neutralize the hydrogen bonds stabilizing the silk crystal structure. Consequently, the conditions of the dissolution process can influence the chemical composition and the molecular structure of the silk protein, affecting its biomaterial properties [33].

The most ubiquitous method to produce regenerated silk fibroin solution is through the use of heavy salts like LiBr or $CaCl_2$. The degummed fibres can be dissolved using a 9.3 M LiBr solution or a ternary solvent system of $CaCl_2/C_2H_5OH/H_2O$ (1/2/8 mole ratio) to disrupt hydrogen bonding between the fibroin protein chains. The solution should then be allowed to thoroughly dissolve for up to 4 hours at 60 ^{O}C to ensure complete dissolution. The heavy salts, in this case LiBr, $CaCl_2$ can then be removed from the silk solution through dialysis against deionized water over a period of 72 hours. Typically the molecular weight cut-off for the dialysis membrane is 3,500 Da, which is permeable enough to allow for the salts and water to travel freely while retaining the fibroin light and heavy protein chains, respectively. Final silk solution concentrations range from 6% to 10% (w/v) content. The silk solution can then be stored in a 4 ^{O}C refrigerated environment where the material has shown stability for up to two months post production [34].

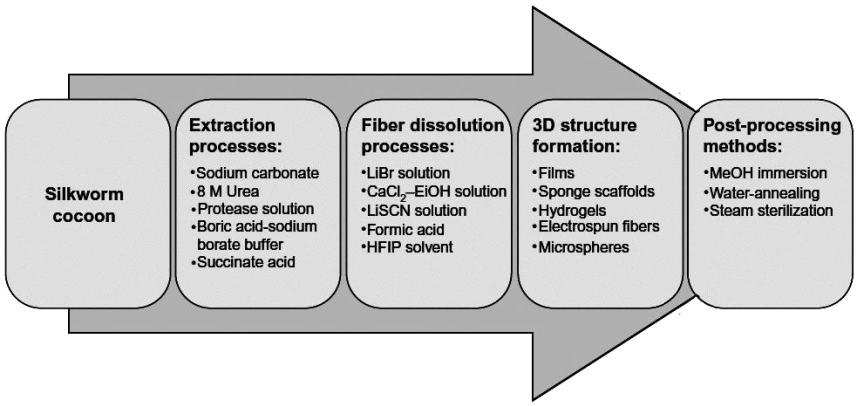

Figure 2.7 A flow chart detailing the processing steps for preparing silk-based biomaterials [33].

- *Regenerated silk fibres* [15]

Resolubilized silkworm cocoon silk and genetically engineered variants of silk have also been spun into fibres. These fibres do not exhibit the remarkable mechanical properties of the native materials. Electrospun silk has also been generated from silkworm, spider, and genetically engineered silks. These fibres can be formed with diameters in the hundreds to thousands of nanometer diameter size range, depending on spinning conditions (solids content, water or organic solvents). These fibres can also be mineralized to further stiffen the materials to expand their potential applications.

- *Nonwoven silk fibroin mats* [15, 35]

Nonwoven mats are of interest as biomaterials due to the increased surface area and rougher topography for cell attachment. Silk fibroin has been used to generate nonwoven silk mats from reprocessed native silk fibres. Nonwoven silk fibroin mats were prepared by partial solubilisation of native silk fibres, usually in formic acid and small amounts of calcium chloride. The mats were washed and planted subcutaneously in rats, where they demonstrated good biocompatibility. Nonwoven mats were studied with a variety of cells, including keratinocytes, fibroblasts, osteoblasts and cell lines from epithelial lung, colon and cervical carcinomas for up to 7 weeks. No degradation of the silk fibres was observed during culture, possibly due to low infiltration of the cells within the matrix.

- *Silk electrospun fibres* [34]

Electrospinning silk solution is a favored processing methodology for producing nanometer- to micron-scale fibres that result in a high degree of available surface area for use in creating scaffolds for tissue engineering and regenerative medicine purposes. In brief, electrospun materials are produced by applying a strong electric field between a polymer solution and a collection device (more detail in topic 2.2). In the case of silk fibroin this has been readily accomplished using both organic solvents and aqueous based processes. For example, silk fibres must dissolve in a ternary solvent system or in a LiBr solution. The solution was then dialyzed against distilled water. The silk fibroin solution was lyophilized to obtain the regenerated silk sponges. The regenerated silk sponge was dissolved in formic acid (98%) or hexafluoroisopropanol (HFIP) to obtain the

spinning solution for electrospinning process. Electrospun nonwoven meshes can be prepared as predominately random coil structure from which β-sheet structures can be formed via methanol treatment. The porosity changed from 76-68% due to dehydration after methanol treatment of these nonwoven meshes. The electrospun silk fibres have found utility in producing scaffolds for a variety of biological applications such as growing cardiac, bone, nerve and skin tissue.

- *Silk fibroin films*

Films or membranes formed from reprocessed silkworm silk have been produced by air-drying silk solutions after salts or organic solvents are removed by dialysis. Silk films prepared from aqueous silk fibroin solution had oxygen and water vapor permeability dependent on the content of silk I and silk II structures. However, rapid gelation can occur at room temperature, so the solutions must be handled carefully. Maintaining solutions of higher concentrations at 48 ^{O}C significantly slows the gelation process and provides wider processing windows. The films formed from the water-soluble protein generally contain a silk I conformation with a significant content of random coil. Many different treatments have been used to modify these films to decrease water solubility by conversion of the protein to the silk II polymorph. Most commonly, methanol has been used to induce this structural transition. This process was used successfully to entrap enzymes, although the materials embrittle with time [15]. Oxygen and water vapor transmission rates of silk fibroin films were dependent on the exposure conditions to methanol to facilitate the conversion to silk II [36]. Alteration of silk structure was induced by treatment with 50% methanol for varying times. Changes in silk structure resulted in differing mechanical and degradability properties of the films. In recent studies, methanol treatments were avoided and an all-water annealing process for the films was utilized. This process resulted in a different structural content of the films, reduced silk II content, but the films were insoluble in water and retained flexibility over time unlike the same materials when treated with methanol rapidly embrittled. These approaches have also been used to control drug release from films, since the structural state can be modified by processing conditions, leading to control of release profiles of entrapped drugs [37].

Nanoscale silk fibroin films can also be formed from aqueous solution using a layer-by-layer technique. These ultrathin films were stable due to hydrophobic interactions and predictable film thickness could be obtained based on control of solution conditions. Microstructures in films, which are advantageous for increasing surface roughness for cell attachment. Transparent films cast from a blend of silk and cellulose showed increased mechanical strength compared with silk films alone [35].

- *Silk fibroin hydrogels*

Hydrogels are three-dimensional polymer networks which are physically durable to swelling in aqueous solutions but do not dissolve in these solutions. Hydrogel biomaterials provide important options for the delivery of cells and cytokines [35]. Silk fibroin hydrogels have been prepared from aqueous silk fibroin solution and are formed from β-sheet structures. Gelation of the silk fibroin solution can be controlled by temperature (higher the temperature the more rapid the gelation), pH (lower the pH the

more rapid the gelation), solids content (higher the solids higher the rates of gelation) and polymer blending with materials like polyethylene oxide to produce a hydrogel. Cations can also enhance rates of gelation, with the specific salts dependent on the type of silk; potassium plays a role with spider dragline silk and calcium with silkworm silk. An increase in Ca^{2+} concentration decreased the time of silk fibroin gelation. The overall rate of gelation has been controlled via osmotic stress, with resulting mechanical, morphological, and structural details dependent on the rate and extent of water removal. Hydrogel pore size was controllable based on silk fibroin concentration and temperature [16].

- *Silk fibroin porous sponges* [34-35]

Regenerated silk fibroin solution may also be processed to produce three dimensional sponge scaffolds for use in tissue engineering. Sponge scaffolds provide a framework of interconnected pores with a high amount of surface area within a defined three dimensional volume, which allows for cell attachment and tissue ingrowth. Porous sponge scaffolds are important for tissue engineering applications for cell attachment, proliferation, and migration, as well as for nutrient and waste transport. Regenerated silk fibroin solutions, both aqueous and solvent, have been utilized in the preparation of porous sponges. Sponges have been formed using porogens, gas foaming and lyophilization. The nature of the process used to form the porous matrices directly influences mechanical properties, degradability, and cell and tissue formation when used as scaffolds in tissue engineering. Pore sizes in these scaffolds can be controlled from below 100 nm diameter to above 1,000 nm, depending on processing conditions.

Solvent-based sponges were prepared using salt (e.g., sodium chloride) or sugar as porogen. Solvents such as 1,1,3,3 hexafluropropanol do not solubilize salt or sugar; therefore, pore sizes in the sponges reflect the size of the porogen used in the process. A gradient of pore sizes can be generated by stacking porogens of different sizes. Sponges with varying porosity can be controlled by stacking variations of salt/HFIP-silk solutions. Solvent-based porous sponges can also be prepared by addition of a small amount of solvent (ethanol, methanol) into aqueous silk fibroin solution before pouring into a mold and freezing. Aqueous based porous silk sponges can be prepared using variable size salt crystals as porogen, with control of pore sizes from 490-940 mm, by manipulating the percent silk solution and size of salt crystals. Pore sizes are 80-90% smaller than the size of salt crystals due to the limited solubilisation of the surface of the crystals during supersaturation of the silk solution prior to solidification. Aqueous-based sponges have rougher surface morphology, based on SEM, than solvent-based sponges due to this partial solubilisation. Aqueous silk fibroin sponges demonstrated improved cell attachment than the solvent-based porous sponges, likely due to these rougher surfaces. Sponges with high porosity and better mechanical strength were obtained with aqueous-based processing [35].

- *Microspheres* [34]

Microspheres describe a general class of particulates that have diameters in the high nanometer to micron range and assume a spherical shape, which can be used for a variety of biomedical purposes such as controlled drug release applications.

Silk microspheres can be readily produced by mixing regenerated fibroin solution with lipid vesicles that act as templates to efficiently load biological molecules in an active form for sustained release. The lipid could then be subsequently removed by methanol or sodium chloride treatments that produced silk fibroin microspheres with β-sheet structure, and measured 2 μm in diameter on average.

Silk microspheres could be produced by using a fibroin and polyvinyl alcohol blend methodology to avoid the complications from the freeze-thaw cycle and use of organic solvents. Fibroin/PVA blended films were first produced by drying the solution into film form, the dried film was then rehydrated in water, and residual polyvinyl alcohol was removed by centrifugation. Controlled microsphere diameters ranging from 300 nm up to 20 μm were achieved. An additional processing method was developed in which drug-loaded silk fibroin microspheres were produced using a laminar jet break-up of aqueous solution. Sphere diameters ranging between 100 μm and 440 μm were produced depending on the diameter of the nozzle and treatment to induce water insolubility using either methanol or water annealing methods. Additionally, smaller sphere sizes ranging in the hundreds of nanometers to the lower micron size range can be similarly controlled through the use of salting-out techniques of potassium phosphate solutions.

2.1.10 Post-processing on silk-based material

Post treatments are usually carried out on silk fibroin mats to remove solvent residues and to stabilize the structure by β-sheet crystallization. Several methods, including the exposure to physical shear or heat, immersion into organic solvents such as alcohol or controlled water vapor annealing, have been used to induce β-sheet crystallization and convert the silk fibroin structure into a more hydrophobic silk II conformation, with varying degrees of crystallinity achieved based on the processing method used.

Common method to convert secondary structure of the silk fibroin from random coil to β-sheet is to add low dielectric constant organic solvents such as alcohol to the sample. Alcohols such as methanol and ethanol are well known as the crystallization reagent for the silk fibroin molecules. Methanol immersion causes rapid dehydration and allows the conformation of the silk fibroin peptide to shift toward a silk II structure. The rate and degree of crystallinity induced by methanol immersion can be examined as a function of treatment time and concentration of methanol used. Structural changes and crystallinity of silk fibroin can also be induced using water-annealing technique. This technique was producing water insoluble silk fibroin materials by increasing the presence of β-sheet secondary structure of the silk. This method exploits the plasticizing effect of water to induce the conformational transition from silk I structure to a predominant silk II conformation. Absorption of water molecules lowers the glass transition temperature (T_g) and induces molecular movement of the silk fibroin peptide chains, permitting the formation of β-sheets. Elevated temperature and pressure conditions during steam sterilization can also induce crystallization and increase of β-sheet content within the silk fibroin bulk material [34].

2.2 Electrospinning process

Electrospinning, which may be considered to be a variant of the electrostatic spinning (or spraying) process, is currently the only technique that is able to produce continuous ultrafine fibres from submicrometre to nanometer diameters [39]. Electrospinning is applied predominantly to polymer-based materials including natural and synthetic polymers, but it has been extended towards the production also of metal, ceramic and glass nanofibres exploiting precursor routes. The production either of individual fibres, of random nonwovens or of orientation ally highly ordered nonwovens is achieved by an appropriate selection of electrode configurations [38].

The original idea of using high electric potentials to induce the formation of liquid drops can be traced back more than 100 years [39]. The first patent that described the operation of electrospinning appeared in 1934, when Formhals disclosed an apparatus for producing polymer filaments by taking advantage of the electrostatic repulsions between surface charges (Formhals, 1934). Despite these early discoveries, the procedure was not utilised commercially with any great success. In the early 1990s, several research groups revived interest in this technique by demonstrating the fabrication of thin fibres from a broad range of organic polymers. At this time, the term '*electrospinning*' was coined and is now widely used in the literature [39].

2.2.1 Basic concepts and apparatus

In a typical electrospinning process, a high voltage is used to create an electrically charged jet of polymer solution or melt, which dries or solidifies on extrusion to leave a polymer fibre. Three major components are needed to complete the process (Fig. 2.8): a high voltage power supply, a capillary tube with a spinneret and a collector, which is normally earthed. Most often, the spinneret is connected to a syringe, which supplies the polymer solution, and the solution can be fed through the spinneret at a constant rate using a syringe pump. When a high voltage is applied, the drop of polymer solution at the nozzle of the spinneret becomes statically charged and the induced charges are evenly distributed over the surface.

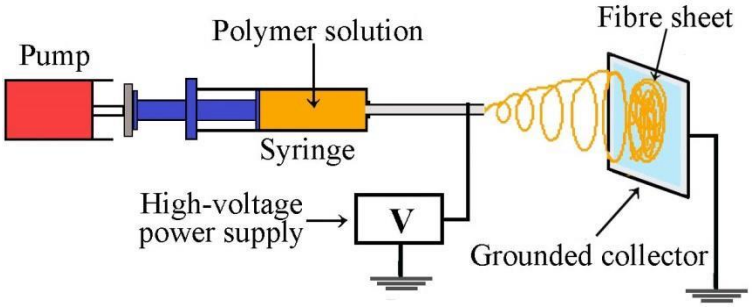

Figure 2.8 Schematic illustration of the setup used for electrospinning

The surface tension of the droplet would normally result in a sphere at equilibrium but it is distorted in the electric field, because charges within the droplet migrate to the surface that faces the collector. The accumulation of charge causes a protrusion to appear on the end of the droplet, distorting the droplet into a conical shape known as the *Taylor cone*. With increasing field strength, the repulsive electrostatic force

overcomes the surface tension and a charged jet of fluid is ejected from the tip of the Taylor cone when a critical value is attained. The polymer solution is discharged as a jet, which then undergoes a stretching, and whipping process, leading to the formation of a long thin thread. As the solvent evaporates, solid polymer fibres with diameters ranging from micrometres to nanometres are formed and lay themselves on a grounded collecting.

In spite of the wide applications, electrospun nanofibres are produced at a low production rate when conventional needle electrospinning setup is used, which hinders their commercialization. Electrospinning with large-scale nanofibre production ability has been explored [5]. Variation in fibre assemblies and morphologies can be effected through the design and construction of the electrospinning apparatus (or setups) and, obviously, the key to making reproducible fibres and assemblies is to control the spinning environment. In many cases, the purpose of modifications to the process is to improve control or tailor the process to suit the needs of specific materials and applications [39].

There are three main categories of modification to the apparatus for electrospinning: the spinneret, manipulation of the electric field (controlling fibre deposition) and the collector (Fig. 2.9). Recent developments in electrospinning apparatus have been discussed in several good reviews. By modifying the spinneret design, different properties can be introduced into the ultrafine fibre. Coaxial spinneret design [40-46] has been utilised by various researchers either to protect or to exhibit functionalising agents or to electrospin material that cannot otherwise be electrospun perhaps owing to high surface tension or low molecular weight. For commercial activities in the fibre production and utilisation industries, one important consideration is the rate of production of fibre assemblies. Much work has been done on the use of multiple spinnerets for fabricating fibres [47-50]. Another method to obtain a high rate production of fibres is using a needleless spinning setup [8-14, 51], which ensures constant renewal of the solution surface without the problem of needle clogging or droplet setting and enables spinning over a larger area. Needleless electrospinning process with rotating spinneret can be summarized as that, the rotation of spinneret loads a thin layer of polymer solution onto the spinneret surface. The rotation and perturbance create conical spikes on the surface of this solution layer. When a high voltage is applied to the spinneret, these spikes tend to concentrate charges and amplify the perturbance and the fluid around the spikes is drawn to these spikes under high electric force. Taylor cones are thus formed. Fine solution jets are then ejected from the tips of these Taylor cones, when the electric force is large enough [5].

There are significant differences between the needle and needleless electrospinning processes. In the needleless electrospinning, Taylor cones are created on the surface of polymer solution. If the Taylor cone is stable, it will move together with the surface of rotating roller and produces a solution jet under the strong electric field. Therefore, there must be strong inter-molecular interactions among polymer macromolecules in the solution to stabilize the Taylor cone given that Taylor cone is stretched into a fine jet and deposited on the collector as solid fibres. Different to the conventional needle electrospinning in which Taylor cone is generated and stabilized

through constantly feeding polymer solution through the needle, the needleless electrospinning forms its Taylor cones by sucking up the solution covering the surrounding fibre generator [14]. In spinning, solutions with a low concentration cannot be loaded on the surface of the electrode because of their lack of viscosity. When Taylor cones do not form on the surface of a roller, the electrospinning process results in non-fibrous formations [51]. Therefore, the solution must have a suitable rheological property. Furthermore, a higher electric voltage is required to initiate the needleless electrospinning, because Taylor cone is formed due to the wave fluctuation [5].

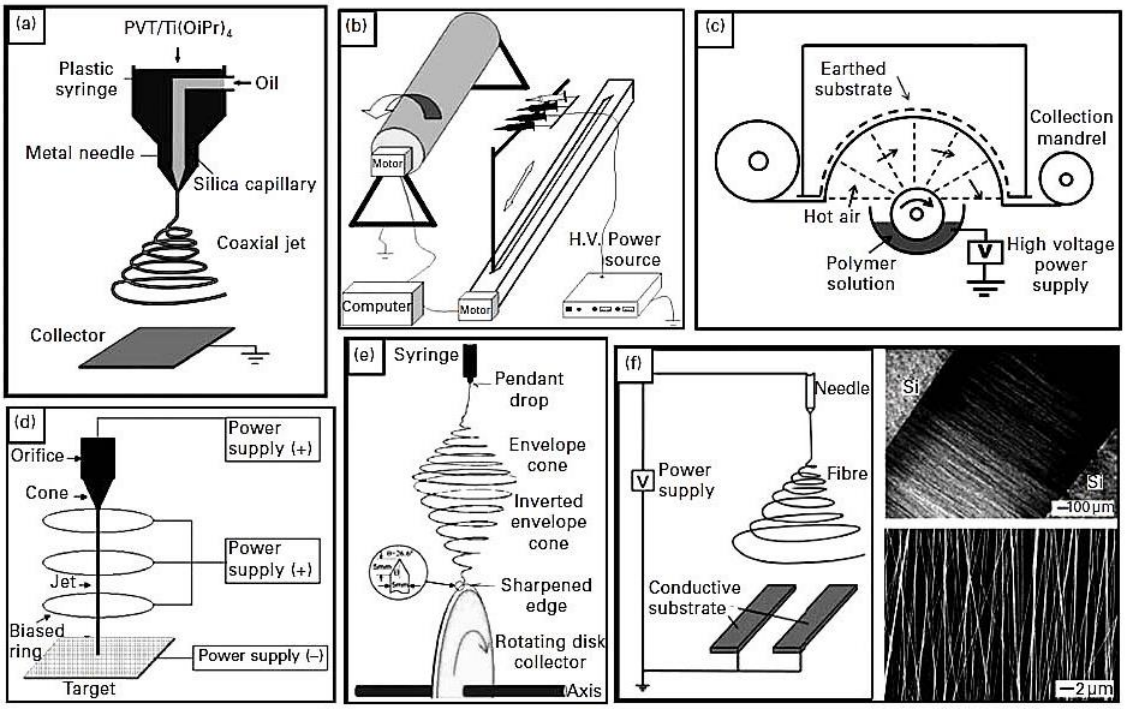

Figure 2.9 Schematic illustration of different electrospinning setups (a) coaxial or dual-capillary spinneret, (b) multiple spinnerets, (c) needleless spinning setup (d) electrostatic lens (e) wheel-like rotating collector and (f) parallel strip collector and parallel-aligned fibres [39].

2.2.2 Parameters for electrospinning process [52]

Process control in the electrospinning process is typically limited to identifying the operating conditions that produce fibres with acceptable properties. However, within a laboratory setting, even with these conditions identified, it is reported that there still remains significant variation in the quality of the produced materials. There are many factors influencing the morphology of the fibres or fibrous constructs produced, from beaded fibres to fibres with pores on its surface. These can be divided into solution parameters, process parameters and ambient parameters. Substance parameters, including the properties of polymer itself and the intrinsic solution properties such as concentration (or viscosity), conductivity and surface tension. Process parameters, including operational conditions such as the applied electrical potential and the distance between tip and collector and ambient parameters such as temperature and humidity. These factors form a complex web of interaction and changes in any one of them can affect the impact of the others. However, the following general comments may be made :

- The electric potential must be large enough to overcome the surface tension of the solution.

- The longer the polymer jet takes to solidify and the further it travels before solidification, the thinner the fibre will be. This is because the droplet has to stretch over the distance the fibre is travelling (elongation of a fixed volume) and the material is only able to flow while it possesses some fluidity.

- To produce discernible fibres rather than an interlocking web, the jet must have solidified by the time it reaches the collector. This means that a combination of the time-in-flight, which is related to the spinneret-collector separation, and the evaporation rate of the solvent must, in combination, allow the polymer to solidify before hitting the collector.

2.2.2.1 Polymer solution parameters [52-53]

The properties of the polymer solution have the most significant influence in the electrospinning process and the resultant fibre morphology. Generally the polymer solution must have a concentration high enough to have a sufficient number of polymer entanglements, yet not so high that the viscosity prevents sufficient polymer flow and sufficient stretching being induced by the electrical field. The solution must also have a low enough surface tension, a high enough charge density and be sufficiently viscous to prevent the jet from coalescing into droplets (via the Rayleigh instability) before the solvent has evaporated. It has been recognised that the intrinsic properties of the polymer such as molecular weight, molecular weight distribution and architecture of the polymer could affect the concentration range that is suitable for electrospinning fibres. The methods that can be employed to alter the solution properties are numerous and include altering the concentration, the choice of solvent, the molecular weight of the polymer and using additives. Moreover, considerably increasing the conductivity, by addition of salts or increasing the polarity of a solvent mixture increases the net charge density and results in a marked increase of Coulombic repulsion and electrostatic forces, which cause the charged jet to be more stretched or extended and to form thinner fibres.

- *Viscosity, molecular weight and polymer concentration* [52-54]

One of the conditions necessary for electrospinning to occur where fibres are formed is that polymer must have both a sufficiently high average molecular weight as well as an open chain-like geometry in solution to allow the development of a degree of jet elasticity via chain entanglement. Generally, electrospinning can only occur with moderately concentrated solutions, as the process of jet formation relies on the entanglement of polymer chains. As a result, monomeric polymer solution does not form fibres when electrospun. The molecular weight of the polymer represents the length of the polymer chain, which in turn have an effect on the viscosity of the solution since the polymer length will determine the amount of entanglement of the polymer chains in the solvent. The greater polymer chain entanglements within the solution, which is necessary to maintain the continuity of the jet during electrospinning.

In addition, the solution viscosity is also dependent on the concentration (percentage of polymer in solution), ambient temperature and presence of impurities in the solution. The viscosity can be altered by adjusting any of these parameters. A reduced

viscosity has been reported to be a major factor in the formation of beads along the fibre length, along with several other parameters. The ability of the solution to flow is related to how fast and how far individual polymer chains can move in relation to each other and can influence the fibre diameter. To produce consistent fibres, a constant solution viscosity should be maintained. If the same polymer and solvent combination are used to make a solution of the same concentration, the viscosity will only be comparable between batches at a specified temperature. The viscosity of solution can be manipulated by using additives such as salts. Du and Zhang [55] demonstrated the effect that salt inclusion had on the viscosity of a polymer solution, as well as subsequent changes to fibre morphology.

- *Surface Tension* [52-54]

As a standalone factor, surface tension can be very important, as the electric field needs to overcome surface tension in terms of energy to produce the solution jet. Surface tension is the primary force opposing coulomb repulsion and its role in determining electrospinnability cannot be overstated. In the instability region of the jet that obtains fibre extension, electrostatic forces are countered primarily by surface tension forces. It is this balance between surface tension cohesive forces and the surface electrostatic repulsion that determine the curvature in bending of the jet during whipping instability. The initiation of electrospinning requires the charged solution to overcome its surface tension. The critical electric field intensity, E_c (equation 2.1) [6] to initiate jet formation, is proportional to surface tension, suggesting that electrospinning is possible at lower critical electric field intensity when the surface tension of the solution is reduced.

$$E_c = \sqrt[4]{\frac{4\gamma\rho g}{\varepsilon^2}} \tag{2.1}$$

All other factors being equal, lower surface tension is therefore a desirable solvent characteristic. However, the surface tension of polymer solutions changes with concentration as well as with the chemical nature of the polymer. Surface tension is temperature-dependent and is affected by the presence of an electric field, making it one of the more elusive factors to quantify in an electrospinning model.

Surface tension can be manipulated by changing the material used or by the addition of surfactants to the solution. It is also a very important factor in beading along the fibre as a solution with a high surface tension will favour the formation of beads. Surface tension has the effect of decreasing the surface area per unit mass of a fluid. In this case, when there is a high concentration of free solvent molecules, there is a greater tendency for the solvent molecules to congregate and adopt a spherical shape due to surface tension. Beads have a higher volume to surface area ratio than a continuous fibre and, by forming beads, the surface energy of the material is lowered as less surface is created. This is counter-productive to the common aim of electrospinning, which is to create very low volume to surface area ratio fibres. If the surface tension is too high or if the viscosity is too low, fibres will not form at all and droplets will be created instead in a process known as electrospraying. Solvent such as ethanol has a low surface tension thus it can be added to encourage the formation of smooth fibres. Another way to reduce the surface tension is to add surfactant to the solution. The addition of surfactant was found to

yield more uniform fibres. Even when insoluble surfactant is dispersed in a solution as fine powders, the fibre morphology is also improved. It is often the surface tension and viscosity of the solution that determine the window within which a specific polymer/solvent combination can be electrospun.

- *Solution Conductivity*

The electrospinning process fundamentally requires the transfer of electric charge from the electrode to the spinning droplet at the terminus of the tip. A minimal electrical conductivity in the solution is therefore essential for electrospinning; solutions of zero conductivity cannot be electrospun. Solvents commonly used in electrospinning have conductivities that are much lower than that of even distilled water. On dissolving a polymer in the solvent, however, the solution conductivity generally increases due to the availability of conducting ionic species (mostly from impurities or additives) from the polymer [54].

Conductivity may be altered by changing the polymer/solvent, the concentration of the solution, or by the addition of additives such as salts. The net charge density (measure of the amount of charge carried from the spinneret to the collector, per volume of material deposited) has been found to be related to both bead formation and fibre diameter. Having a high current flow seems to favour the formation of thin, beadless fibres. Generally, the conductivity of the solution will be difficult to modify without altering other characteristics of the solution [52].

- *Dielectric constant* [52-54]

The dielectric constant ε of a material is essentially a measure of how effectively it concentrates the electrostatic lines of flux when placed in an electric field. In a practical sense, it is a measure of how much electrical charge the solvent is capable of holding. Solvents with different values of ε used in electrospinning will interact very differently with the electrostatic field and it is therefore an important material parameter in electrospinning. It has been reported that the dielectric constant of the solution can have an effect on both the speed of deposition and the diameter of the fibres. This is believed to be a result of the interaction of the internal electrical field created in a dielectric material and the external applied electric field. Generally, a solution with a greater dielectric property reduces the beads formation and the diameter of the resultant electrospun fibre.

The extent to which the choice of solvent affects the nanofibre characteristics is well illustrated in the electrospinning of poly(ε-caprolactone) (PCL) from $CHCl_3$/DMF mixed solvent. As the volume fraction of dimethylformamide in the mix is increased from 0 to 10 wt%, the average diameter at the same polymer concentration was shown to decrease from 450 nm to 150 nm. This was likely a result of the increased dielectric constant of the solvent due to addition of dimethylformamide [$\varepsilon(DMF) \approx 36.7$ and $\varepsilon(CHCl_3) \approx 4.8$]. The bending instability of the electrospinning jet also increases with higher dielectric constant. This may also facilitate the reduction of the fibre diameter due to the increased jet path. However, it is important to appreciate that changing solvents affects not only ε, but also the conductivity, surface tension, and the chain conformation of the polymer in solution.

- *Solvent choice* [52]

The choice of solvent used in the production of fibres can have a major impact on their properties. More volatile solvents will evaporate quicker, which will reduce the required spinning distance. Different solvents will result in polymer-containing solutions that have varying viscosities, which can influence the final morphology of fibres. It has also been shown that for the same process conditions, changing the solven from acetone to hexafluoroisopropanol (HFIP) can eradicate the presence of beading in poly-ε-caprolactone, as well as alter the mechanical properties of the materials produced.

2.2.2.2 Process parameters [52]

Another important parameter that affects the electrospinning process is the various external factors exerting on the electrospinning jet. The structure and morphology of electrospun fibres is also affected by the applied electrical potential and the distance between tip and collector because these parameters directly affect the deposition time, evaporation rate and whipping or instability regions. In general, for a given solution viscosity and polarity, a higher electrical potential ejects more fluid in a jet, resulting in a larger fibre diameter whereas a shorter electrode-collector distance tends to produce wetter fibres and thus beaded structures. Evaporation rate affects the fibre formation process because the loss of solvent increases the viscosity during spinning. Aqueous polymer solutions require longer distances to form dry cylindrical fibres than systems that use highly volatile organic solvents. Ambient temperature and humidity are also very important process parameters, owing to their influence on the solvent evaporation process and the resultant fibre morphology. These parameters have a certain influence in the fibre morphology although they are less significant than the solution parameters.

- *Electric field strength (Voltage)* [53-54]

A crucial element in electrospinning is the application of a high voltage to the solution. The high voltage will induce the necessary charges on the solution and together with the external electric field, will initiate the electrospinning process when the electrostatic force in the solution overcomes the surface tension of the solution. The columbic repulsive force in the jet will then stretch the viscoelastic solution. If the applied voltage is higher, the greater amount of charges will cause the jet to accelerate faster and more volume of solution will be drawn out. These have the effect of reducing the diameter of the fibres and also encourage faster solvent evaporation to yield drier fibres. When a solution of lower viscosity is used, a higher voltage may favor the formation of secondary jets during electrospinning. This has the effect of reducing the fibre diameter. Another factor that may influence the diameter of the fibre is the flight time of the electrospinning jet. A longer flight time will allow more time for the fibres to stretch and elongates before it is deposited on the collection plate. Thus, at a lower voltage, the reduced acceleration of the jet and the weaker electric field may increase the flight time of the electrospinning jet which may favor the formation of finer fibres. In this case, a voltage close to the critical voltage for electrospinning may be favorable to obtain finer fibres.

The effect of high voltage is not only on the physical appearance of the fibre, it also affects the crystallinity of the polymer fibre. The electrostatic field may cause

the polymer molecules to be more ordered during electrospinning thus induces a greater crystallinity in the fibre. However, above a certain voltage, the crystallinity of the fibre is reduced. With increased voltage, the acceleration of the fibres also increases. This reduces the flight time of the electrospinning jet. Since the orientation of the polymer molecules will take some time, the reduced flight time means that the fibres will be deposited before the polymer molecules have sufficient time to align itself. Thus, given sufficient flight time, the crystallinity of the fibre will improve with higher voltage.

- *Distance between electrode and collector* [53-54]

Varying the distance between the spinning electrode and the collector will have a direct influence in both the flight time and the electric field strength. For independent fibres to form, the electrospinning jet must be allowed time for most of the solvents to be evaporated. When the distance between the electrodes is reduced, the jet will have a shorter distance to travel before it reaches the collector plate. Moreover, the electric field strength will also increase at the same time and this will increase the acceleration of the jet to the collector. As a result, there may not have enough time for the solvents to evaporate when it hits the collector. The excess solvent may cause the fibres to merge where they contact to form junctions resulting in inter and intra layer bonding. Depending on the solution property, the effect of varying the distance may or may not have a significant effect on the fibre morphology. In some cases, changing the distance has no significant effect on the fibre diameter. Decreasing the distance has the same effect as increasing the voltage supplied and this will cause an increased in the field strength. If the field strength is too high, the increased instability of the jet may encourage beads formation. In other circumstances, increasing the distance results in a decrease in the average fibre diameter. The longer distance means that there is a longer flight time for the solution to be stretched before it is deposited on the collector. However, there are cases where at a longer distance, the fibre diameter increases. This is due to the decrease in the electrostatic field strength resulting in less stretching of the fibres. When the distance is too large, no fibres are deposited on the collector.

- *Collectors* [52]

The type of collector that is used in the process affects the morphology of the collected fibres. A simple collector plate will form an unwoven mat of fibres in a random orientation, whereas other specifically designed collectors can collect aligned fibres. Specialised collectors include spinning disks, drums and mandrels for which the speed of rotation is an important factor that affects the fibre deposition rate. If the collector is moving faster than the fibres are being deposited, the fibres will stretch or break into small fragments as the fibre sticks to the collector and is accelerated away.

2.2.2.3 Ambient parameters [52-53]

As previously mentioned, the ambient parameters can change on a day to day and laboratory to laboratory basis. These parameters offer the opportunity for enabling fibres to be produced more consistently.

- *Humidity*

The humidity of the electrospinning environment may have an influence in the polymer solution during electrospinning. The surrounding humidity will affect each solution differently, depending on the solvent used and the hydrophilicity of the polymer solution. At high humidity, it is likely that water condenses on the surface of the fibre when electrospinning is carried out under normal atmosphere. As a result, this may have an influence on the fibre morphology especially polymer dissolved in volatile solvents. The humidity of the environment will also determine the rate of evaporation of the solvent in the solution. At a very low humidity, a volatile solvent may dries very rapidly. Aqueous solutions are obviously most affected as the humidity is a measure of the vapour pressure of the solvent in the atmosphere and it can be expected that the water in solution and in the atmosphere will interact. It has been reported that increased humidity slows the solidification process for aqueous solutions, increasing both beading defects and fibre diameters. A higher humidity will slow the evaporation rate of water, thus increasing the drying time, which would produce thinner fibres given enough time for the water to evaporate completely before the jet hits the collector. Non-aqueous solutions can be affected in several ways. If the relative vapour pressure of water is too high, evaporation will be slowed by a saturation effect even if there is no solvent present in the atmosphere. There will be a limit to how much liquid the atmosphere can hold at a certain pressure before either water or solvent start to condense back into liquid form. This factor can have several consequences, thinner fibres can be produced as longer solidification times may result or a congealed mat of fibres may form owing to incomplete solidification.

- *Temperature*

The ambient temperature in which the spinning is performed has a substantial effect on the fibres produced. There are two main effects resulting from an increase in temperature: the solvent evaporation rate increases and the viscosity decreases. A warmer environment, individual molecules of solvent will have more energy and thus more molecules will have the energy required to jump from liquid to gaseous form, making the solution dry faster. The viscosity decreases with an increase in temperature. This is attributed to several properties of the polymer solution. Softening of polymers occurs at higher temperatures, with two major steps occurring at two particular points: the glass transition and the melting point. The higher the temperature, the more flexibility is displayed by each individual polymer molecule. The polymer chains have a greater degree of freedom to move owing to the increase in energy breaking or weakening cross-linkages, Van der Waals forces and hydrogen bonding between the chains. Overall, the temperature has two opposing effects on the electrospinning process relating to a change in solvent evaporation rate and in solution viscosity. At high temperatures, the solution dries quickly, leaving little time for elongation and thinning. However, at increased temperature, the decrease in viscosity will cause the solution to flow faster before drying, allowing the fibre to elongate faster.

2.3 Literature review

2.3.1 Method for the preparation of nonwoven silk fibroin fabrics (US patent 7285637) [56]

Armato *et al.* were invented nonwoven silk fibre fabrics. In this invention relates to a method for the preparation of silk fibroin nonwoven fabrics forming structures suitable to be used as implant biomaterials, cell culture scaffolds for tissue engineering applications, cell carriers and even biological fluid-filtering systems and protein adsorption.

The process according to the invention comprises the initial degumming of silk fibroin using a treatment based on a $NaHCO_3$ solution. Silk fibroin, for example either from silk cocoons or silk textiles or waste silk were used as raw material. The degummed silk undergoes then a treatment breaking the disulfide bonds between heavy (350 kDa) and light (27 kDa) chains of silk fibroin by partially dissolving the silk fibroin in a formic acid solution (formic acid mixed with water) having a concentration of formic acid from 88 wt% to 99 wt%, The formic acid solution used in the process contains 0.1 wt% to 10 wt% by weight of a mixture of salts selected from the group consisting of calcium chloride, zinc chloride, potassium chloride, lithium bromide, lithium thiocyanate, magnesium chloride, copper nitrate and sodium chloride. Silk fibroin concentrations in said solution are in a range between 0.1 wt% and 10 wt%. Dissolve process is carried out at room temperature. The resulting solution was poured onto clean glass or polystyrene dishes and then stirred at 100 rpm for 30 minutes in order to obtain homogeneously distributed fibres. The resulting solution was left under atmospheric conditions in order to remove the formic acid. Once the formic acid had been removed by evaporation at room temperature, the resulting silk fibroin fabrics were washed several times with double distilled water and next dried inside a vacuum oven at 50 ^{O}C. A three-dimensional fibroin fibre fabric was prepared according to the following method. A first layer 200 μm thick with a mean pore diameter of 15 μm was coupled to a second layer having 1200 μm thick with a mean pore diameter of 40 μm. The two layers were prepared separately and joined together applying a suitable pressure forming a fabric with a total thickness of 1.5 mm.

Since the raw silk filament is not soluble in formic acid due to the presence of an external sericin layer, silk must be first degummed, to eliminate the sericin layer. In this context, solutions having from 88 wt% to 99 wt% of formic acid could be used, with the 99 wt% formic acid solutions being preferred. According to the invention, the best result are obtained with concentrations between 0.5 wt% to 5.0 wt%. An advantageous form of embodiment of the present invention the degree of solution of the silk fibroin can be increased in order to obtain highly tightened fabrics. Preferably, the salts to be used are calcium chloride and lithium bromide. In accordance with a preferred form of embodiment of the process the silk fibroin is dipped into formic acid at room temperature; nevertheless, the process can be carried out at higher temperatures, for example up to 60 ^{O}C.

2.3.2 An experimental study on electrospinning of silk fibroin [18]

Amiralian *at el.* were studied about preparation of nonwoven matrices of silk fibroin nanofibres by electrospinning technique. Effects of electric field and silk concentration in formic acid on the nanofibres uniformity, morphology and diameter were studied.

In these work, silk fibroin solution was prepared by dissolving degummed silk fibre in a ternary solvent system of $CaCl_2/C_2H_5OH/H_2O$ (1:2:8 in molar ratio) at 70 ^{O}C for 6 hours. Then dialyzed with cellulose tubular membrane in water for 3 days, the solution was filtered and lyophilized to obtain the regenerated silk fibroin sponges. Spinning solution was prepared by dissolving the regenerated silk fibroin sponges in 98% formic acid for 30 min. Concentrations of silk fibroin solutions for electrospinning was in the range from 8 wt% to 14 wt%.

In electrospinning process, a high electric potential was applied to a droplet of silk fibroin solution at the tip of a syringe needle (0.7 mm in external diameter), the electrospun nanofibres were collected on a target plate, which was placed at a distance of 10 cm from the syringe tip. A high voltage in the range from at 10, 15 and 20 kV was applied to the droplet of silk fibroin solution at the tip. After spinning process, Electrospun silk fibroin nanofibre matrices were treated with solvent, including methanol, and ethanol. Solvent vapor-treated samples were prepared by placing silk nanofibre matrices in palates saturated with solvent for 1 hour and then dried in air at room temperature for 2 hours.

From result, the electrospinning of silk fibroin in formic acid was successful and thin and rod like fibres with diameters ranging from 80 nm to 500 nm were obtained depending on electrospinning conditions. It was found that, at 8% silk solution, nanofibres were formed at 20 kV. Below the silk concentration of 8% as well as at low electric filed in the case of 8% solution, droplets were formed instead of fibres. The obtained fibres are not uniform and branched off. The average fibre diameter is 80 nm and a narrow distribution of fibre diameters is observed. Above silk concentration of 8% continues nanofibres were formed regardless of the applied electric field and electrospinning condition. A significant increase in mean fibre diameter with the increasing of the silk concentration, which shows the important role of silk concentration in fibre formation during electrospinning process.

In addition, it was found that 10% concentration of silk solution in formic acid (at 15 kV) was the lower critical concentration limit for fibre formation in electrospinning process. Below this critical concentration, application of electric field to a polymer solution results electrospraying and formation of droplets to the instability of the ejected jet. As the polymer concentration increased, a mixture of beads and fibres is formed. Further increase in concentration results in formation of continuous fibres. Furthermore, in order to study the effect of the electric field, silk solution with the concentration of 12% was electrospun at 10, 15 and 20 kV. Variation of applied electric field had not a significant effect on the mean fibre diameter but the narrowest fibre diameter distribution was obtained at lower electric field (10 kV). It is suggested that, higher applied voltage causes multiple jets formation, which would provide non-uniform fibre diameter and broad fibre diameter distribution.

2.3.3 Effects of some electrospinning parameters on morphology of natural silk-based nanofibers [3]

Amiralian *at el.* were examined about electrospinning of silk fibroin. The solutions of silk fibroin in formic acid were electrospun into nanofibres and the effects of electrospinning temperature, solution concentration and electric field on the formation nanofibres were studied.

In these work, silk fibroin solution was prepared by dissolving degummed silk fibre in a ternary solvent system of $CaCl_2/C_2H_5OH/H_2O$ (1:2:8 in molar ratio) at 70 ^{O}C for 4 hours. Then dialyzed with cellulose tubular membrane in water for 3 days, the solution was filtered and lyophilized to obtain the regenerated silk fibroin sponges. The regenerated SF sponge was dissolved in 98% formic acid for 30 min to prepare 8-14% (W/V) solutions. In electrospinning process, a high electric potential was applied to a droplet of silk fibroin solution at the tip of a syringe needle (0.35 mm in external diameter). The electrospun nanofibers were collected on an aluminum foil, which was placed at a distance of 10 cm from the syringe tip. A syringe pump was used to form a constant amount of silk fibroin solution on the tip. The output of the injection pump was 20 μl/min. The processing temperature was adjusted at 25, 50 and 75 ^{O}C. A high voltage in the range from 10 to 20 kV was applied.

From result, the electrospinning temperature, the solution concentration and the electric field have a significant effect on the morphology of the electrospun silk nanofibres. About an effect of electrospinning temperature on the morphology and texture of electrospun silk nanofibres, 12% silk solution was electrospun at various temperatures. Results are shown the electrospinning of silk solution showed flat fiber morphology at 50 and 75 ^{O}C, whereas rounded cross section circular structure and a smooth surface was observed at 25 ^{O}C. Their diameter showed a size range of 100 nm to 300 nm with 180 nm being the most frequently occurring. With increasing the electrospinning temperature to 50 ^{O}C, The morphology of the fibers was slightly changed from circular cross section to ribbon-like fibres. Fibre diameter was also increased to a range of 20 nm to 320 nm with 180 nm the most occurring frequency. At 75 ^{O}C, The morphology of the fibers was completely changed to ribbon-like structure. Furthermore, fibres dimensions were increased significantly to the range of 500 to 4,100 nm with 1,100 nm the most occurring frequency. Since nanofibres are resulted from evaporation of solvent from polymer solution jets, the fibre diameters will depend on the jet sizes, elongation of the jet, and evaporation rate of the solvent. In this work, believe that ribbon-like structure in the electrospinning of silk solution at higher temperature thought to be related with skin formation at the jets. With increasing the electrospinning temperature, solvent evaporation rate increases, which results in the formation of skin at the jet surface. Nonuniform lateral stresses around the fiber due to the uneven evaporation of solvent and/or striking the target make the nanofibers with circular cross section to collapse into ribbon shape. With increasing the temperature of electrospinning process, the balance between the surface tension and electrical forces can shift so that the shape of a jet becomes unstable. Such an unstable jet can reduce its local charge per unit surface area by ejecting a smaller jet from the surface of the primary jet or by splitting apart into two smaller jets. Branched jets,

resulting from the ejection of the smaller jet on the surface of the primary jet were observed in electrospun fibres of silk fibroin.

A series of experiments were carried out when the silk fibroin concentration was varied from 8% to 14% at the 15 kV constant electric field and 25 ^{O}C constant temperature. Continues nanofibres were formed above silk concentration of 8% at the applied electric field of 10 kV to 20 kV. Similar sets of experiments were performed when the electrospinning temperature was 50 ^{O}C and 75 ^{O}C. As the solution concentration increases, the fibre diameter increases and there is gradual shift from circular to ribbon-like fibres when the electrospinning temperature was increased (occurs at 10% silk fibroin concentration). Furthermore, the average size of the fibres increases and thick fibres with broader distribution of the size was collected on the target at this temperature (75 ^{O}C). There is a significant increase in mean fibre diameter with increasing of the silk concentration. Experimental observations in electrospinning confirm that for fibre formation to occur, a minimum polymer concentration is required. Below this critical concentration, application of electric field to a polymer solution results electro spraying and formation of droplets to the instability of the ejected jet. It seems that the critical concentration of the silk solution in formic acid for the formation of continuous silk fibres is 10% when the applied electric field was in the range of 10 kV to 20 kV.

To examine the effect of the electric field at higher electrospinning temperature, silk fibroin solution with concentration of 14% was electrospun at 10, 15 and 20 kV at 50 ^{O}C. Result showed a gradual shift in nanofibre morphology from ribbon-like structure to circular cross section. There is also a significant decrease in the nanofibre diameter, which may be due to changing of the flattened fiber structure to the circular cross section. Increasing the electric field strength will increase the electrostatic force on the fluid jet, which favors the more elongation of the jet and the formation of thinner fibers. On the other hand, at higher electric field, a larger amount of solution would be removed from the capillary tip, which results in the increase of the fibre diameter. As the results of this finding, it seems that electric field shows different effects on the nanofibre morphology. This effect depends on the solution concentration and electrospinning conditions. It can be imagined that the noncircular and flat ribbons fibres form in two distinct processes. First, the polymer molecules leave the solvent and form the skin of the fibres. Then the solvent evaporates and makes the fibres to collapse into flattened form. It is expected that temperature have effects on the ribbon formation in these two distinct process involved. It has effect on molecular interactions between formic acid and polar groups in silk fibroin molecules that make the skin and it has effects on the rate of evaporation of solvent that causes the skin to collapse into flattened forms. Then increasing the temperature would increase the possibility of the formation of flattened fibres. Nevertheless, increasing the electric field strength will increase the elongation rate and traveling speed of the jet in the distance between nozzle and collecting plate. Therefore, the fluid jet may reach the collector before the formation of any skin on the surface of the jet and the fibres would have circular cross section. The same trend was observed at the silk concentration of 10 and 12%. Flattening of the electrospun nanofibres increases fibre dimensions. Hence, thicker nanofibres are resulted at lower applied voltage.

2.3.4 Preparation of non-woven mats from all-aqueous silk fibroin solution with electrospinning method [57]

Chuanbao *et al.* were studied about preparation of nonwoven mats from aqueous silk fibroin solution with electrospinning technique. In this study tried to develop the regenerated silk fibre with two major purposes. First, to avoid the use of organic solvents can enhance the potential biocompatibility of the electrospun fibers or blending with any other polymers. Water was used as electrospinning solvent in order to avoid the problem that derived from residual organic solvents when the silk fibroin fibers were exposed to cell *in vitro* or *in vivo* and improve the potential biocompatibility of the silk fibroin nonwoven mats. Second, to simplify the process of electrospinning, instead of lending with other materials, the concentrated solution that was appropriate for electrospinning was prepared by concentrating the silk fibroin solution.

In these work, aqueous silk fibroin was prepared by dissolving degummed silk fibre in $CaCl_2/C_2H_5OH/H_2O$ (1:2:8 in molar ratio) for 40 minutes at 80 ^{O}C and dialyzed to remove salts in a cellulose tube against distilled water for 3 days at room temperature. Then the silk solution was filtered. The silk solution was prepared about 28, 30, 32, 34 and 37 wt% with slow continuous stirring at 50-60 ^{O}C, in order to prevent solution from turning into gel during the concentrating process. The electrospinning process was operated by needle system. The capillary with axis tilted about 45^{O} from horizontal direction was connected to a syringe filled with 5 ml solution. A high voltage in the range from 12 kV to 20 kV was applied at the tip. A grounded aluminum foil was placed at a distance of 18 cm from the capillary tip. Spun silk fibroin mats were immersed into a 90/10 (v/v) methanol/water solution for 10 minutes and then dried under vacuum at room temperature for 24 hours.

From result, electrospinning process of a stable aqueous solution at a high concentration was conducted successfully. It was found that the gelation time for the silk solution decreases with increasing concentration, for the silk fibroin/water system studied here, the gelation time is 4 days at 25 ^{O}C when the concentration is 37% (w/w), which is stable enough to be used in electrospinning. Silk fibroin fibres deposited randomly and the thickness was from 500-10 mm. Fibres intersected each other to make up numerous pores, whose size reached up to several tens of microns. At concentration of 28%, fibers together with droplets and beaded fibres were observed; at a higher concentration of 32%, droplets disappeared and the beaded fibers became fewer; no droplets or beaded fibres were observed at the concentration of 34% and 37%. However, there was a high concentration end because the solution with concentration of about 37% (w/w) was proved difficult to flow through the syringe needle of the apparatus and the droplet of solution suspended at the end of the syringe needle dried readily in the electrospinning process.

The beads were found in the electrospun products when the applied voltage was not higher than 16 kV and there were few beads at the voltage of 18 kV or 20 kV. Because the distance was fixed, higher voltage resulted in a higher charge density on the surface of the solution jet during the electrospinning process. That higher net charge density resulted from higher voltage on the jet also imposed higher elongation forces to the jet, which resulted in small beads and smooth fibers were produced; however, further

increasing voltage may decrease the stability of the initiating jet and the fibres became rough. The suitable condition for a fabrication of nonwoven mats

The solution with a concentration of 34% was chosen to fabricate at the voltage of 20 kV with a spinning distance of 18 cm. The fibers had a belt-like morphology, resulted from the presence of a thin, mechanically distinct polymer skin; in brief, after the skin formed, the solvent inside escaped, atmosphere pressure tended to collapse the tube formed by the skin as the solvent evaporated, the circular cross section became elliptical and then flat, forming a ribbon with a cross-sectional perimeter nearly the same as the perimeter of the jet.

2.3.5 Electrospun silk fibroin mats for tissue engineering [58]

Alessandrino *et al.* were studied about a preparation of electrospun silk fibroin mats for tissue engineering. Aims of this work were to to investigate the best experimental set-up related to the dimension and uniformity of the fibres in the electrospun silk fibroin mats and to study their interaction with living cells.

In these work, silk fibroin solution was prepared by dissolving degummed silk fibre in a LiBr solution (9.3 M) for 3 hours at 60 ^{O}C, then dialyzed for 3 days against distilled water. Silk fibroin films were prepared by pouring 10 mL of the ~1 wt% silk fibroin aqueous solution in Petri dishes. Spinning dopes at different polymer concentrations were prepared immediately before spinning by dissolving the films in formic acid. The electrospinning process was operated by needle system. A high electric potential was applied to the silk solution at the tip of a syringe needle (0.5 mm in internal diameter). Three different solutions were realized solving different concentrations of silk fibroin in formic acid (5%, 7.5% and 10% w/v). A high voltage in the range from 20 kV to 24 kV was applied. The electrospun nanofibres were collected on a collector, which was placed at a distance of 7 and 10 cm. The silk electrospun mats were removed from the substrate by treatment with water at 37 ^{O}C for 5-10 minutes followed by isopropanol for 10 minutes. After an overnight drying at room temperature, the silk electrospun mats were immersed in methanol for 5, 10 and 15 minutes to induce crystallization of silk fibroin.

From the results, SEM observations showed that more uniform mats with regular morphology and fibres in the nanometric range were obtained by using a polymer concentration of 7.5 wt%, a voltage of 24 kV, a flow rate of 3 ml/h and a spinneret-collector distance of 10 cm. Lower polymer concentration, shorter spinneret-collector distance, and higher flow rate led to various kinds of defects, such as non-continuous fibres, beads and fusing of wet fibres. Thus leading to poor quality silk electrospun mats. Ribbon-like fibres were also produced at low and high values of the voltage/distance ratio, indicating that this is a key parameter for the production of silk fibroin nanofibres with uniform size and cylindrical shape.

FTIR and DSC analyses showed that the structure of the silk electrospun mats was improved at the molecular level by a methanol treatment which was effective in increasing the degree of crystallinity and the thermal stability of silk fibroin nanofibres by inducing the conformational transition of amorphous domains into more crystalline ones.

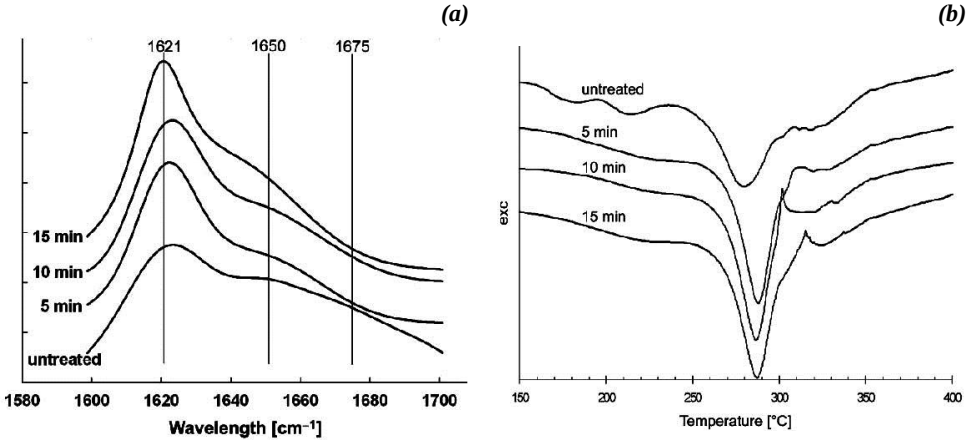

Figure 2.10 FTIR spectra (a) and DSC thermograms (b) of silk electrospun mats before and after the treatment with methanol for different times.

To study the cytocompatibility of silk fibroin electrospun mats, tests with L929 murine fibroblasts were carried out. Samples were seeded with the cells and incubated for 1, 3 and 7 days at 37 ^{O}C. It was found that silk fibroin electrospun mats were able to promote adhesion, spreading and proliferation of L929 cells. Just after day 1, cells showed good adhesion and after day 7, layered cells were observed and cells confluence was almost achieved. After 7 days in cell culture, some cells were noticed on the bottom side of the samples and points out that the porosity of the electrospun silk fibroin mats allows cells to penetrate and colonize the whole matrix.

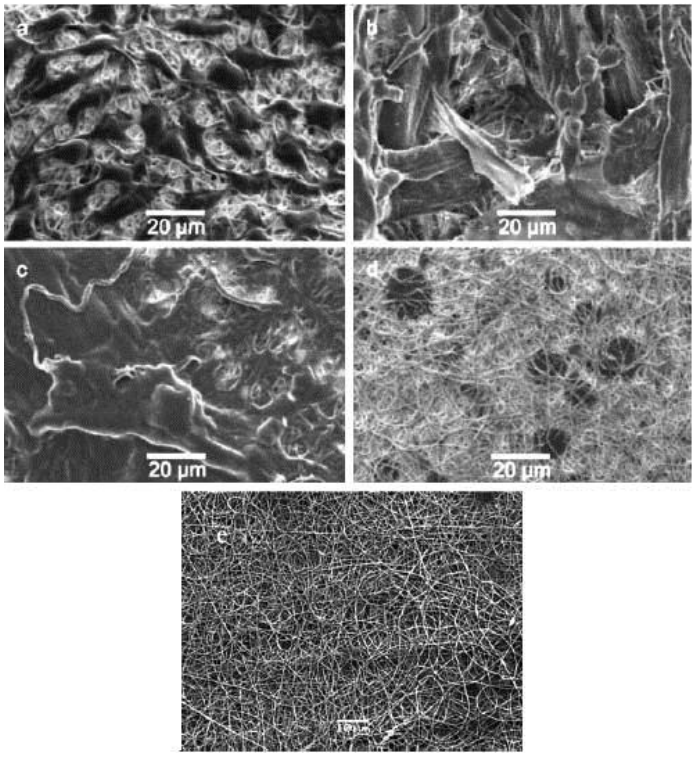

Figure 2.11 SEM micrographs of L929 cells seeded onto the silk fibroin electrospun mats after (a) 1 day, (b) 3 days, (c) 7 days, (d) 7 days (side in contact with the bottom of the well) and (e) the control silk fibroin electrospun structure.

2.3.6 Regeneration of Bombyx mori silk by electrospinning - part 1: processing parameters and geometric properties [59]

Sukigaraa *at el.* studied the effect of electrospinning parameters on the morphology and fibre diameter of regenerated silk from *Bombyx mori*. Effects of electric field and tip-to-collection plate distances of various silk concentrations in formic acid on fibre uniformity, morphology and diameter were measured.

In these work, silk fibroin solution was prepared by dissolving degummed silk fibre in 50% aqueous $CaCl_2$ (100 ^{O}C, then cooled) to obtain silk concentration of 6% solution. The solution (22 g) was poured into regenerated cellulose dialysis tubing to carry out dialysis against 1,000 ml of deionized water (for 48 hours at 23 ^{O}C). The regenerated silk fibroin sponge was obtained by lyophilisation. The silk sponge solution (5, 8, 10, 12, 15 and 19.5%) was electrospun in formic acid (98-100%). In electrospinning process, the silk-formic acid solution was placed in a syringe (18-G and spinning angle 45^{O}). The tip-to-collection plate (covered with aluminum foil) distance varied from 5 to 10 cm vertically under the needle tip. The electric field expressed in terms of voltage/distance between the collection plate (cathode) and the needle tip (anode) ranged from 2 to 5 kV/cm. Spinning distance 5, 7 and 10 cm.

The electrospinning of *Bombyx mori* silk fibroin in formic acid was processed and fibre diameters ranging from 12 nm to 1500 nm were obtained depending on the electrospinning conditions. Silk concentration plays a major role in fibre diameter. No fibres were formed at less than 5% silk concentration for any electric field and spinning distances. At 8% concentration less than 30 nm diameter fibres were formed with beads. At 10% concentration with 5 cm spinning distance and 2, 3 and 4 kV/cm electric fields, drops were formed instead of fibres. Continuous fibres were obtained above 12% regardless of electric field and distance. Fibre diameters less than 100 nm were successfully electrospun at each concentration. Solution concentration was found to be the most significant factor controlling the fibre diameter in the electrospinning process. In the short distance as well as low concentration (10%), the solution reaches the collection plate before the solvent fully evaporates.

This explains the formation of droplets and beads at the low concentration and distance. Increase in the regenerated silk concentration in the formic acid increases the solution viscosity. At low concentrations beads are form instead of fibres and at high concentrations the formation of continuous fibres are prohibited because of inability to maintain the flow of the solution at the tip of the needle resulting in the formation of larger fibres. Relationship between mean fibre diameter and electric field with concentration of 15% at spinning distances of 5, 7 and 10 cm. The mean fibre diameter obtained at 2 kV/cm is larger than other electric fields. Relationship between the fibre diameter and concentration at 2, 3 and 4 kV/cm is shown the concentration apparently has more effect on the fibre diameter than electric field.

2.3.7 Preparation of electrospun silk fibroin nanofibers from solutions containing native silk fibrils [60]

Liu, *et al.* were studied about preparation of electrospun silk fibroin nanofibres from regenerated silk fibroin film obtained by $CaCl_2$/formic acid solvents. In these work, the dried degummed silk was then directly dissolved in $CaCl_2$/HCOOH for 3 hous at room temperature to prepare 6% w/v silk solution. The dissolution time of silk is sensitive to $CaCl_2$ concentration, which decreased from 600 minutes to 40 minutes when increasing $CaCl_2$ concentration from 1 to 2%. Then the obtained solutions were cast on polystyrene Petri dishes to prepare silk fibroin films. After dried, the silk fibroin films were immersed in deionized water to remove the $CaCl_2$ for 10 hours, and then dried in air.

The electrospinning solutions were prepared by dissolving the regenerated silk fibroin films above in formic acid for 3 hours. A high electric potential of 12 kV was applied to a droplet of silk fibroin solution at the tip of a syringe needle (0.8 mm in internal diameter). The electrospun nanofibres were collected on flat aluminum foil, which was placed at a distance of 10 cm from the syringe tip. A constant volume flow rate of 1 ml/h was maintained using a syringe pump. For post-treatment, the electrospun silk fibroin nanofibres were immersed in 75% (v/v) ethanol for 1 hour and then dried in air. The thickness of the obtained regenerated silk fibroin mats is from 48 μm to 92 μm.

As a part of nature silk components, native silk fibrils make the electrospinning solutions having many good qualities. The states of silk fibroin in $CaCl_2$/HCOOH solution were observed by SEM, as shown in Figure 2.12. From the results observed, native silk fibrils were obtained in dissolving process, and we could clearly know the change of silk fibroin nanofibrils as the increase of $CaCl_2$ content. The diameter and length of fibres decreased with the increased content of $CaCl_2$. The nanofibrils with diameters of 20-170 nm are important components in the hierarchical structure of native silk fibre. It can be seen that nanofibrils aggregated together, forming bunches of fibres [Fig. 2.12 (a)] and plenty of nanofibrils were observed, 20-80 nm in diameter. They aggregated together through a node (the bigger diameter of silk fibroin).

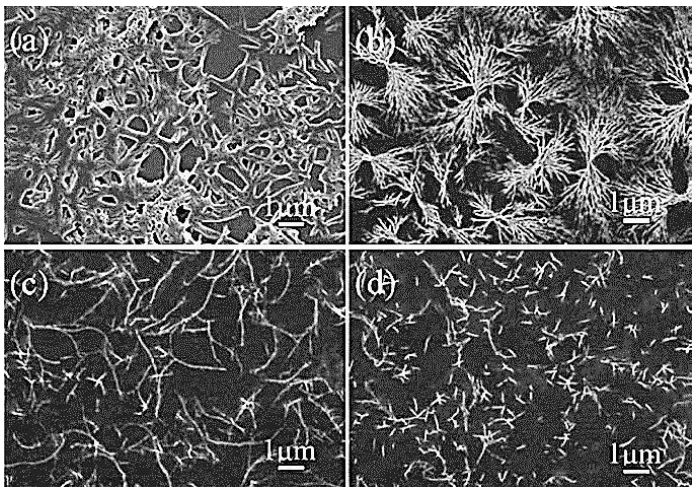

Figure 2.12 SEM images of silk fibroin state in the electrospinning solutions prepared by dissolving (a) 1% $CaCl_2$-film, (b) 2% $CaCl_2$-film, (c) 5% $CaCl_2$-film and (d) 10% $CaCl_2$-film in formic acid.

The morphology of the electrospun silk fibroin nanofibres from the silk films were examined by SEM, as shown in Figure 2.12. The fibre formation was closely related to the protein aggregate structure in spin solution. All silk solutions produced sub-micrometer fibres with less than 600 nm average diameter. The fibre diameter decreased from 543 nm to 273 nm as $CaCl_2$ concentration increased from 1% to 10%. The higher concentration of $CaCl_2$ resulted in the nanofibril with smaller diameter and short length, which makes the regenerated silk fibroin nanofibres with smaller diameter. To further investigate the spinnability, the solution containing silk nanofibrils was diluted to different concentrations, 10%, 8%, 6%, 4% and 2%. Figure 2.13 shows SEM micrographs of electrospun silk fibroin nanofibres derived from different solution concentrations.

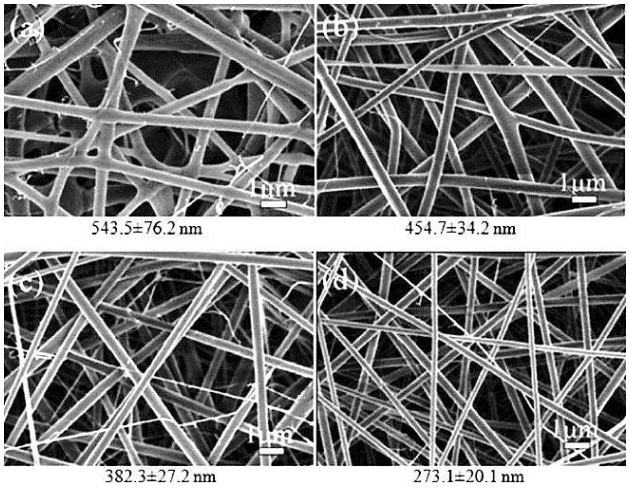

Figure 2.13 SEM images of silk fibroin nanofibres electrospun from 6 wt% silk fibroin solutions prepared by dissolving (a) 1% $CaCl_2$-film, (b) 2% $CaCl_2$-film, (c) 5% $CaCl_2$-film and (d) 10% $CaCl_2$-film in formic acid.

All exhibits good spin ability, even at low concentration of 2%. With the increase of silk fibroin concentration from 2 to 10%, the diameter of electrospun nano fibres increased from 42 nm to 1771 nm. The good spin ability of these solutions indicated the important role of silk structure in electrospinning solutions. Moreover, the results demonstrated the feasibility of fibre size control over a wide range in such system.

2.3.8 Current research on electrospinning of silk fibroin and its blends with natural and synthetic biodegradable polymers [61]

Zhang and Mo were described about aresearch on electrospinning of silk fibroin and its blends with natural and synthetic biodegradable polymers. In these, work gave a brief review about the structure, properties and applications of silk fibroin and blend nanofibres in biomedical application.

Silk fibroin blends with natural polymers

Electrospinning nanofibres can mimic the nanofibrous structure of native extracellular matrix, while the components of the native extracellular matrix (ECM) are mainly collagens and glycosaminoglycans, which remind people to use the blends of protein and polysaccharides electrospun into nanofibres for biomimicing the native

extracellular matrix both in components and in structure. Silk fibroin as a protein has also been investigated to blend with natural polymers, such as chitosan, collagen and gelatin for those purposes.

- *Silk fibroin blends with chitosan and chitosan derivative*

Chitosan is a cationic copolymer of β-(1-4)-linked D-glucosamine and N-acetyl-D-glucosamine, which is obtained from chitin. Chitosan is a biodegradable natural polymer that has been used for cosmetic and pharmaceutical applications due to its biocompatibility, good biodegradability and excellent antibacterial properties. Due to its structural resemblance with glycosaminoglycan, it has been blended with silk fibroin for nanofibre fabrication to biomimic the native extracellular matrix.

In the chitosan and silk fibroin blends, the addition of silk fibroin enhanced the mechanical properties of chitosan/silk fibroin nanofibres, the tensile strength of the cross-linked nanofibrous membranes increased from 1.3 MPa to 10.3 MPa and the elongation at break of the cross-linked nanofibrous membranes showed an increased trend with the increasing of silk fibroin content. However, chitosan has poor solubility in common organic solvents, which gives a challenge during the electrospinning process. Many laboratories have attempted to modify the properties of chitosan. Hydroxybutyl chitosan is fabricated by conjugation of hydroxybutyl groups to the hydroxyl and amino reactive sites of chitosan. This modification could increase the solubility of chitosan in water or organic solution and enhance the electrospinability of chitosan solutions.

Silk fibroin and hydroxybutyl chitosan blend nanofibres were fabricated by electrospinning using 1,1,1,3,3,3-hexafluoro-2-propanol and trifluoroacetic acid mixture as solvents to biomimic the native extracellular matrix. Scanning electron microscopy (SEM) revealed that the average nanofibre diameter increased when the content of hydroxybutyl chitosan in silk fibroin/hydroxybutyl chitosan blends was raised from 20% to 100%. FTIR and ^{13}C-NMR spectroscopy clarified that hydrogen bonding interactions exist in silk fibroin/hydroxybutyl chitosan blend nanofibres and hydroxybutyl chitosan did not induce conformation of silk fibroin transforming from random coil form to the β-sheet structure. Differential thermogravimetric analyses demonstrated that the thermal stability of silk fibroin/hydroxybutyl chitosan blend nanofibrous scaffolds was improved. The mechanical properties were tested for the blend nanofibres with different silk fibroin/hydroxybutyl chitosan blend weight ratios (100∶0, 80∶20, 50∶50, 20∶80, 0∶100).

Pure silk fibroin nanofibrous scaffolds showed a typical brittle fracture; the elongation at break was only 3.85±0.30 % and the tensile strength was 2.72±0.60 MPa. At the silk fibroin/hydroxybutyl chitosan blend ratio of 20:80, the elongation at break and the tensile strength of silk fibroin/hydroxybutyl chitosan blend nanofibres increased up to 11.42±0.88% and 4.35±0.45 MPa, respectively. The electrospun silk fibroin/hydroxybutyl chitosan nanofibre scaffolds could provide a preferable matrix for cell adhesion and proliferation by the method of mimicking the native extracellular matrix in the body.

It was revealed that all the nanofibrous scaffolds had good cell viability in comparison with coverslip. The proliferation on pure silk fibroin, silk fibroin/ hydroxybutyl chitosan (80:20) and silk fibroin/hydroxybutyl chitosan (50:50) nanofibre scaffolds was increased significantly compared to hydroxybutyl chitosan nanofibres, tissue

culture plate and coverslip. So, scaffolds fabricated by pure silk fibroin and silk fibroin/hydroxybutyl chitosan exerted positive effects on cell growth and proliferation compared to tissue culture plate.

- *Silk fibroin blends with collagen and gelatin*

Collagen is extracted from mammal organizations and has been widely used for tissue engineering scaffolds due to its excellent biocompatibility and biodegradability. Collagen is better than silk fibroin for cell adhesion and proliferation. Hence, the structural and biological properties of pure silk fibroin scaffolds were often needed to be improved by blending with collagen or gelatin. Zhou et al. [62] reported a silk fibroin/collagen tubular scaffold via electrospinning and found that the addition of collagen could induce silk fibroin conformation from the α-helix to the β-sheet that is good for cell adhesion.

Gelatin is a natural biopolymer derived from collagen, which was silk fibroin and type B gelatin blend for long-term drug release application. The diameter and morphology of the obtained silk fibroin/gelatin nanofibre were investigated. It has been found that the average diameter of silk fibroin/gelatin nanofibres tended to increase as the silk fibroin content in the blends increased and the fibre morphology turned to ribbon-like shape when the silk fibroin content was more than 60 wt%.

- *Silk fibroin blends with other polysaccharides and proteins*

Hyaluronic acid is a linear polysaccharide consisting of alternating, disaccharide units of (1,4)-linked α-D-gluconic acid and (1,3)-linked β-N-acetyl-D-glucosamine. As one of the main components of the extracellular matrix, hyaluronic acid is conducive to cells growth, adhesion and proliferation. Hyaluronic acid and its derivatives have been widely used in biomedical areas, such as wound dressing, drug delivery systems and implanted materials.

Garcia-Fuentes et al. [63] prepared the hyaluronic acid and silk fibroin blend scaffold by freeze-drying and found that hyaluronic acid improved the cell adhesion and proliferation when culturing human mesenchymal stem cells on the blended scaffolds. Zhang et al. [64] fabricated nanofibre scaffolds from the aqueous solutions of silk fibroin and Hyaluronic acid blends to biomimic the natural ECM by electrospinning. Figure 2.14 shows the SEM images of electrospinning nanofibres and the average width of nanofibres at different volume ratios when blending 30 wt% silk fibroin water solution with 4 wt% hyaluronic acid water solution. From the SEM images, it can be observed that electrospun silk fibroin/hyaluronic acid nanofibres were ribbon-shaped and their average width obviously decreased with the increase of hyaluronic acid content. Furthermore, there is no fibre that can be spun out when the hyaluronic acid content increased up to 60%, indicating that pure hyaluronic acid solution was hard in fabricating nanofibres. The cell proliferation speed on silk fibroin/hyaluronic acid nanofibres with different blend ratios. it is seen that silk fibroin/hyaluronic acid blend nanofibres are more suitable for the cell proliferation than coverslips.

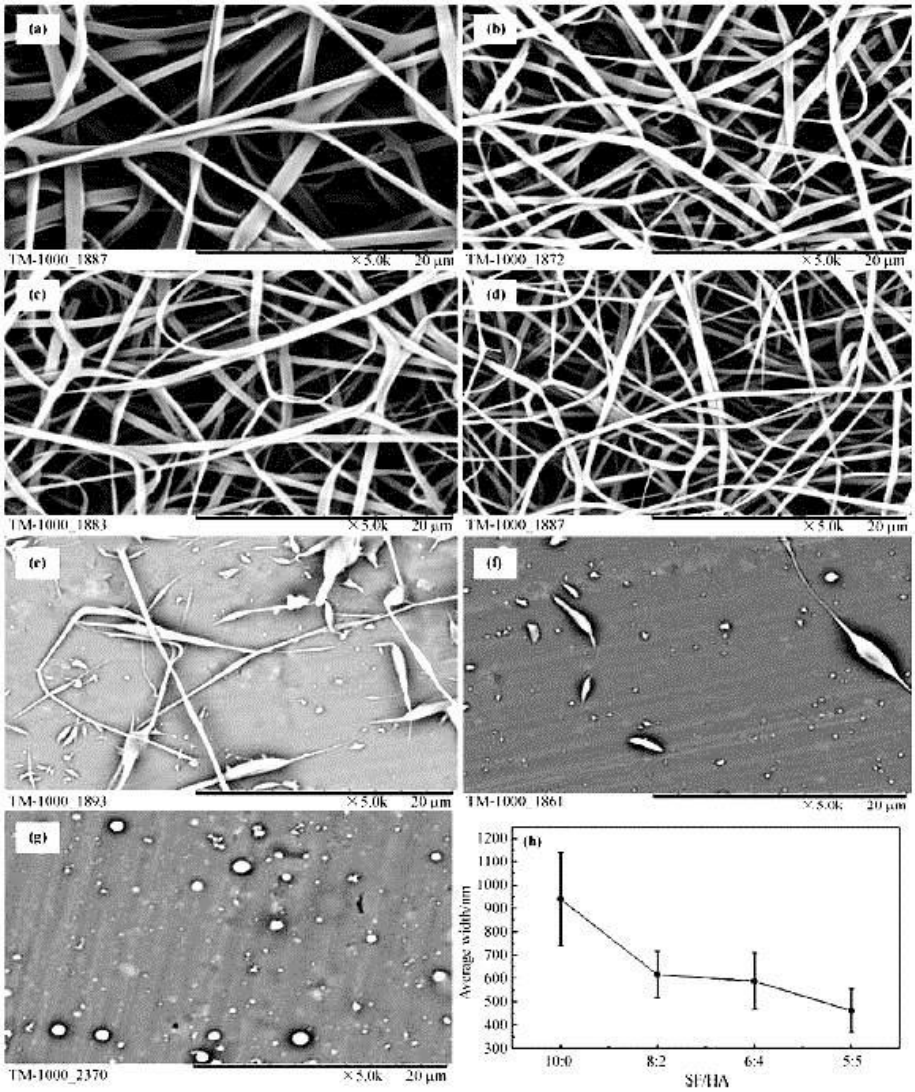

Figure 2.14 SEM images of blends with the volume ratio of 30 wt% silk fibroin solution to 4 wt% hyaluronic acid solution at (a) 10:0, (b) 8:2, (c) 6:4, (d) 5:5, (e) 4:6, (f) 2:8, and (g) 0:10. (h) Variation of width of silk fibroin/hyaluronic acid blended nanofibres with volume ratio.

Keratin is one of the most abundant proteins in animal population. Blends of silk fibroin with wool keratose have been electrospun into nanofibres from their formic acid solution, and the as-spun fibres are smooth with diameters between 160 nm and 900 nm, which fibres can absorb the heavy mental ion for water purification application.

Silk fibroin blends with synthetic biodegradable polymers

Generally, the scaffold should also have mechanically supportiveness for tissue regeneration. Although natural polymers exhibit good biocompatibility and biodegradability, they do not possess strong mechanical properties. In order to improve mechanical properties, synthetic biodegradable polymers blended with silk fibroin are widely studied for tissue engineering application, which are poly(ε-caprolactone) (PCL), polylactic acid (PLA), polyglycolic acid (PGA) and their copolymers.

- *Silk fibroin blends with polycaprolactone*

Polycaprolactone was proven to be able to degrade by microorganisms in 1985. It was also reported as a biodegradable nanofibre matrix for bone regeneration in 2004, as the electrospun polycaprolactone scaffolds provided an environment for tissue formation. Li et al. [65] generated nanofibres with a core-shellstructure that was composed of polycaprolactone as shell and silk fibroin as core via emulsion electrospinning. The tensile strength of polycaprolactone/silk fibroin nanofibres increased, but the elongation at break decreased when the silk fibroin content in blends increased. Methanol-treated polycaprolactone/silk fibroin (7:3) nanofibres give higher tensile strength 2.25±0.6 MPa and larger elongation at break 100% comparing with untreated polycaprolactone/silk fibroin (7:3) nanofibres. Furthermore, the cell proliferation speed was higher on polycaprolactone/silk fibroin nanofibre scaffolds than that on polycaprolactone nanofibre scaffolds, suggesting that the incorporation of silk fibroin into polycaprolactone was beneficial for cell proliferation.

- *Silk fibroin blends with polylactic acid*

Polylactic acid is another biodegradable polymer, which is biocompatible and undergoes scission in the body to lactic acids. Lactic acid is a chiral molecule existing in two steroisomeric forms that are L-lactic acid and D-lactic acid. Two stereoregular polymers, poly(D-lactide) and poly(L-lactide), could be polymerized separately from D-lactic acid and L-lactic acid. Usually, poly(L-lactide) is more frequently used than poly(D-lactide), since the hydrolysis of poly(L-lactide) yield L-lactic acid, which is the naturally occurring stereoisomer of lactic acid in the body. The big disadvantage of polylactic acid used in body is that it can induce an inflammatory response. Silk fibroin blended with polylactic acid could reduce the inflammatory response. It has been reported that the poly(L-lactide)/silk fibroin hybrid scaffold promoted the hepatocyte proliferation and decreased the macrophage responses. Wang et al. [66] fabricated a bi-layer tube scaffold by electrospinning. The Polylactic acid layer (outside layer) is responsible for the mechanical properties and the silk fibroin-gelatin layer (inner layer) supports cell growth. The polylactic acid/silk fibroin-gelatin tubular scaffolds, with the porosity of approximately 82±2%, possessed appropriate breaking strength 2.21±0.18 MPa and suture retention strength 4.58±0.62 N. The burst pressure strength of the composite scaffolds reached 1596±20 mmHg, which is similar to that of the native vessels.

- *Silk fibroin blends with poly(L-lactic acid-co-ε-caprolactone)*

Poly(L-lactic acid-co-ε-caprolactone) is a copolymer of L-lactic acid and ε- caprolactone. It can show different mechanical properties and biodegradability by changing the weight ratio of Lactic acid to ε-caprolactone in the copolymer. Although poly(L-lactic acid-co-ε-caprolactone) has been electrospun into nanofibres for different tissue engineering applications, it is still week in cell attachment because of the lacking of cell recognition sites. Blending silk fibroin wit poly(L-lactic acid-co-ε-caprolactone) will lead to an ideal scaffold with both good mechanical properties and biocompatibility.

Zhang and Mo [61] fabricated silk fibroin and poly(L-lactic acid-co-ε-caprolactone) blend nanofibres with different weight ratios and investigated the morphology, structure and properties of silk poly(L-lactic acid-co-ε-caprolactone) nanofibre scaffolds. The mechanical properties of silk fibroin/poly(L-lactic acid-co-ε-caprolactone) nanofibres were investigated. It found that pure silk fibroin nanofibres were week and brittle in mechanical properties with the tensile strength of 2.72 MPa and the elongation at break of 3.85%, while, pure poly(L-lactic acid-co-ε-caprolactone) nanofibres are elastic materials with the tensile strength of 6.96 MPa and the elongation at break of 458%. Interestingly, with a small amount of silk fibroin blended into poly(L-lactic acid-co-ε-caprolactone), the silk fibroin/ poly(L-lactic acid-co-ε-caprolactone) nanofibres with the ratio of 25:75 showed the highest tensile strength of 10.6 MPa, even though its elongation at break reduced to 279%. However, with further increasing the silk fibroin content in the silk fibroin/poly(L-lactic acid-co-ε-caprolactone) nanofibres, both the tensile strength and the elongation at break went to decrease. So, silk fibroin/poly(L-lactic acid-co-ε-caprolactone) (25:75) blended nanofibre scaffolds exhibited best mechanical properties, which can be considered for tissue engineering application.

Water contact angle is usually used for testing the wet ability of a material surface, which can be used to estimate the biocompatibity of a biomaterial. The pure poly(L-lactic acid-co-ε-caprolactone) nanofibres showed an water contact angle at around 120°, indicating that poly(L-lactic acid-co-ε-caprolactone) nanofibrous scaffolds were hydrophobic. If increasing the ratio of silk fibroin in the blended nanofibres, the contact angle of the nanofibrous scaffolds decreased continuously from 120° to 0°. Blending silk fibroin in poly(L-lactic acid-co-ε-caprolactone) improved the biocompatibity of poly(L-lactic acid-co-ε-caprolactone). The cells proliferated much faster on silk fibroin/poly(L-lactic acid-co-ε-caprolactone) nanofibres comparing with those on poly(L-lactic acid-co-ε-caprolactone) and silk fibroin nanofibres, especially for silk fibroin/poly(L-lactic acid-co-ε-caprolactone) (25:75). The silk fibroin/poly(L-lactic acid-co-ε-caprolactone) nanofibre scaffolds were further used for peripheral nerve regeneration in vivo.

Silk fibroin as a natural biomaterial has good biocompatibility, which is extracted from silkworm cocoons and much cheaper than other natural biomaterials like collagen. Silk fibroin has been blended with many different natural materials for nanofibre fabrication, which includes chitosan and its derivative and hyaluronic acid as polysaccharides, collagen and gelatin as protein. Silk fibroin blended with polysaccharide forming the nanofibres can biomimic the structure and components of native extracellular matrix and can give good mechanical properties and cell biocompatibility. For instance, silk fibroin/hydroxybutyl chitosan blend nanofibres show higher tensile strength and elongation at break than the pure silk fibroin nanofibres, and the cell proliferation speed on silk fibroin/hydroxybutyl chitosan nanofibres is faster than that on pure hydroxybutyl chitosan nanofibres.

Pure natural materials and its blend nanofibres cannot give enough mechanical properties as scaffolds like blood vessel and nerve conduit yet, while blending synthetic polymers with silk fibroin can improve mechanical properties significantly. Furthermore, with small amount of synthetic polymer blending with silk fibroin the cell proliferation

ability on the nanofibres can also be improved. Poly (L-lactide), poly (ε-caprolactone) and poly(L-lactic acid-co-ε-caprolactone) are all tried to be blended with silk fibroin for the nanofibre fabrication. For silk fibroin/poly(L-lactic acid-co-ε-caprolactone) nanofibres when the poly(L-lactic acid-co-ε-caprolactone) content is 25%, it gives the highest tensile strength of 10.6 MPa, which is higher than that of pure poly(L-lactic acid-co-ε-caprolactone) nanofibre and silk fibroin nanofibres. Meantime these nanofibres show the highest cell proliferation rate. Therefore, combining silk fibroin with natural or synthetic polymers to make complex nanofibres is an effective way to get a new kind of materials with good mechanical properties and biocompatibility. Electrospun silk fibroin blended nanofibres with either natural or synthetic biomaterials have shown great potential for different tissue regeneration, such as nerve, blood vessel, skin, tendon, bone and cartilage.

3. **Experimental**

3.1 Materials

- *Raw silk cocoon and silk fibroin*

Waste cocoons of *Bombyx mori* Linn. Thai silkworm (Nang-Noi Srisakate 1) were supplied from Chan farm, Amphoe Mueang Chan, Si Sa Ket Province, Thailand. Waste silk cocoons in the form of pierced cocoons* were obtained from the supplier. Thai silkworm is typical in its cocoons, i.e. intense yellow color and oval in shape. The filament is coarser and has more silk gum (e.g., up to 37%) than normal mulberry silk (e.g. 20-25%) [24].

**Pierced cocoons: cocoons from which the moth of the silkworm has emerged-and damaged cocoons*

Figure 3.1 Raw Thai silk cocoons

Silk fibroin was obtained by degumming process. Briefly, pierced cocoons were cleaned by first removing the contaminants manually and were then washed twice with water. The cleaned raw cocoons were then dried in in the sun for about 2 days. Raw silk cocoons were degummed twice with 1.0% of sodium carbonate (Merck Ltd.) and 0.5% of standard reference detergent (ECE Phosphate Reference Detergent FBA free, Union TSL Co., Ltd., Thailand) at 100 ^{O}C for 30 minutes (the ratio of raw silk cocoon over degumming solution was 1:30). After the degumming, silk fibroin was washed in boiling water for 30 minutes to remove remaining sericin from the surface of the fibre, then washed again with warm water and dried at room temperature.

Figure 3.2 Degummed cocoons (silk fibroin) used in the experiment.

The content of amino acids in the degummed silk fibre was analyzed by high performance liquid chromatography (HPLC). The result is described in Figure 3.3 and Table 3.1.

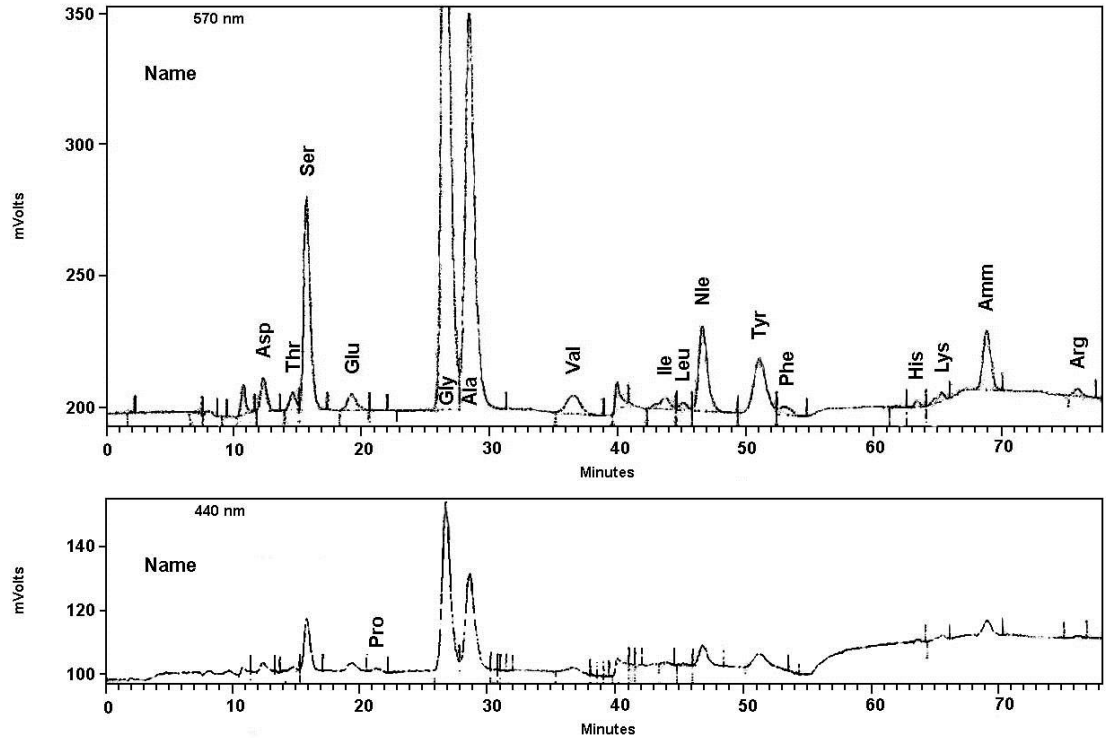

Figure 3.3 Chemical composition of silk fibroin (Institute of Organic Chemistry and Biochemistry AS CR, v.v.i.; Martin Šafařík)

Table 3.1 Composition of amino acid in silk fibres

Peak	Name	RT (min)	Area	Amount (nmol)
570 nm	Asparagin	12.27	390313	0.712
	Threonin	14.57	213669	0.387
	Serin	15.67	2767840	4.120
	Glutamic acid	19.17	315127	0.560
	Glycin	26.50	11902384	20.506
	Alanin	28.33	7917475	13.466
	Valin	36.40	552803	1.003
	Isoleucin	43.63	271790	0.480
	Leucin	45.06	124665	0.215
	Methionine	46.63	1570880	2.632
	Tyrosin	51.06	1453145	2.508
	Phenylalanin	53.16	236683	0.419
	Histidin	63.33	68220	0.110
	Lysin	65.30	142977	0.222
	Arginin	76.03	133201	0.217
440 nm	Prolin	21	47892	0.226

- *Poly(ε-caprolactone) (PCL)*

Polycaprolactone (M_n 70,000~90,000 g/mol) was purchased from Sigma Aldrich (Germany). PCL is prepared by the catalytic ring-opening polymerization of the cyclic monomer ε-caprolactone at 140 to 150 ^{O}C. Catalysts such as stannous octoate are used to catalyse the polymerization and low molecular weight alcohols can be used to control the molecular weight of the polymer. PCL is a semi-crystalline polymer having a glass transition temperature (T_g) of about -60 ^{O}C and melting point ranging between 59 ^{O}C and 64 ^{O}C. The number average molecular weight of PCL samples may generally vary from 3,000 to 80,000 g/mol and can be graded according to the molecular weight.

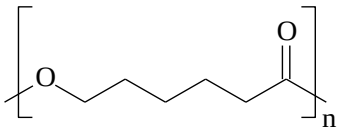

Figure 3.4 Structure of polycaprolactone

PCL is soluble in chloroform, dichloromethane, carbon tetrachloride, benzene, toluene, cyclohexanone and 2-nitropropane at room temperature. It has a low solubility in acetone, 2-butanone, ethyl acetate, dimethylformamide and acetonitrile and is insoluble in alcohol, petroleum ether and diethyl ether. PCL is a biodegradable polyester with elastomeric properties. PCL can be decomposed by hydrolysis of the ester bond even under physiological conditions and it is therefore possible to use this polymer in the implant technique. It belongs to a group of non-toxic, thermoplastic polymers and at the same time. Using PCL in medicine has been approved in some countries, and therefore can be used for example as a drug carrier such as tablets with sustained release of the active substance, or as a material for the suture of internal organs, i.e. biodegradable sutures. This polymer is also a suitable candidate for the production of scaffolds used in tissue engineering. PCL can be blended with other polymers to improve stress crack resistance, dyeability and adhesion and has used in combination with polymers such as cellulose propionate, cellulose acetate butyrate, polylactic acid and polylactic acid-co-glycolic [67].

3.2 Chemicals for a preparation of a spinning solution

- *Calcium chloride anhydrous ($CaCl_2$)*

Calcium chloride was purchased from Fluka AG (Switzerland). Calcium chloride is an inorganic salt, which exists in a solid form or as a liquid solution. The density of calcium chloride is 2.15 gm/cm^3. It is soluble both in inorganic solvents like water, as well as in organic solvents like ethanol. Calcium chloride is a good conductor of electricity, but it is a bad conductor of heat. Calcium chloride is hygroscopic in nature, ability to attract moisture from the air and surroundings and dissolve at very low temperatures. If exposed to open air, it tends to turn into liquid. Due to its exothermic properties, that is, it releases heat during any chemical reaction.

Calcium chloride has a chaotropic property, the property of being able to disrupt intra-molecular forces such as hydrogen bonds, van der Waals forces and reduce

the stability of the native state of proteins by weakening the hydrophobic effect. This increases the entropy of a substance, which correlates with the increase in kinetic energy, or movement, of its molecules. This means that ordered structures are made disordered, chaotic. Macromolecules are normally most affected: protein tertiary structure is destroyed, nucleic acids are denatured, carbohydrate (sugar) gels are solubilized.

- *Formic acid (HCOOH)*

Formic acid (Penta, Czech Republic) was used as a solvent for the preparation of the spinning solutions. Formic acid is the simplest and has the lowest mole weight of the carboxylic acids. It occurs naturally in the body of ants and in the stingers of bees. Functionally, it is not only an acid but also an aldehyde; it reacts with alcohols to form esters as an acid and it is easily oxidized which imparts some of the character of an aldehyde.

Formic acid is a colorless liquid having a highly pungent, penetrating odor at room temperature. It is miscible with water and most polar organic solvents, and is somewhat soluble in hydrocarbons. It irritates the mucous membranes and blisters the skin. Formic acid is used as a chemical intermediate and solvent, and as a disinfectant. Formic acid is freezing at 8.4 ^{O}C and boiling at 100.7 ^{O}C. The dielectric constant of formic acid is 57.9 at 20 ^{O}C and the surface tension is 37.67 mN/m at 20 ^{O}C.

3.3 Analytical methods and apparatus

3.3.1 Characterization of spinning solution properties

Conductivity and surface tension properties were determined by a conductivity meter (CON 510 Bench Conductivity/TDS Meter, Eutech Instruments, Netherlands) and a tensiometer (Digital Tensiometer K9, Krüss, Germany) using a plate method. Rheological properties of spinning solutions were measured by a rheometer (HAAKE™ RotoVisco™ 1 Rotational Rheometer, Thermo Scientific, Germany). All measurements were conducted at room temperature (approximately 22-25 ^{O}C).

3.3.2 Morphology analysis and fibre diameter

The morphological appearance of the electrospun fibres was observed with a scanning electron microscope (SEM) Vega 3 (Tescan, Czech Republic) at an accelerated voltage of 20 kV and observed at different magnification to enable image analysis of fibrous morphology. All the samples were sputter-coated (Q150R ES, Quorum Technologies Ltd., England) with gold at a thickness of 7 nm. The diameter of nanofibres was measured by counting image pixels with image software, NIS-Elements AR software (LIM s.r.o., Czech Republic). The average fibre diameter and its distribution were determined from 200 random fibres obtained under each spinning condition. Statistical analysis was performed with the software Minitab 16.2.

3.3.3 Post-treatment of electrospun fibre sheets

Electrospun fibre sheets were treated with alcohol to achieve the solvent-induced crystallization of the silk fibroin and to reduce the water solubility of the fibre sheets. Briefly, the obtained fibre sheets were immersed in ethanol for 30 min. After drying at room temperature, the treated fibre sheets were removed from the backing

substrate and immersed in distilled water overnight, followed by rinsing in distilled water to remove residual salts and then finally dried again.

3.3.4 Spinning performance of the electrospinning process

- Mass per unit area of electrospun fibres sheet

A method for determine the mass per unit area of fibres sheet was evaluated by ASTM D6242-98 (2004) standard test method for mass unit area of nonwoven fabrics. Calculate the mass per unit area (M) expressed in gram per square metre (g/m^2), using the equation (3.1)

$$M = \frac{S}{A \times C} \tag{3.1}$$

Where S is the mass of specimen in gram (g), A is the area of specimen, in square millimetre (mm^2) and C *is* the conversion factor from square millimetre (mm^2) to square metre (m^2) equal 0.000001.

- Polymer throughput of the process

Spinning performance (polymer throughput) is one of the most important parameters of the needleless electrospinning method. The spinning performance of the electrospinning process was calculated from the mass per unit area and width of the electrospun fibre sheets and the velocity of the backing material, using the equation (3.2) [11].

$$P = \frac{G \times W \times V_f}{L_r} \tag{3.2}$$

Where P is a spinning performance (g/min/m), G is a mass per unit area of electrospun fibres sheet in gram per square metre (g/m^2), W is a width of fibre layer in metre (m), V_f is a take up cylinder speed in metre per minute (m/min) and L_r is a length of spinning electrode in metre (m).

3.3.5 Conformational characterization of silk fibroin scaffolds

The analyses were done in cooperation with Ing. Jana Mülerová, Ph.D. from Department of Chemistry, Faculty of Science, Humanities and Education, Technical University of Liberec. Conformational characterization of silk electrospun fibre sheets was performed by Fourier transform infrared spectroscopy (FTIR) analysis with a Thermo Nicolet iZ10 FT-IR Spectrometer (Thermo Scientific, USA) equipped with an ATR (Attenuated Total Reflectance) accessory and Ge crystal. For each measurement, IR spectra of the specimen were taken by Spectrometer at a resolution of 2 cm^{-1} and the wavenumber ranged from in the region of 4000-700 cm^{-1}.

3.3.6 Physical properties

- Tensile properties

Tensile properties of the electrospun fibre sheets were examined with a tensile tester (Labor-Tech) at an extension rate of 3 mm/min with 15 mm gauge length. Ten samples of rectangular shape (10 mm width x 40 mm length) were cut along the same direction of width and length in the fibre sheet for each sample. The result of tensile strength and elongation at break were averaged and reported.

- *Hydrophilicity measurement*

Contact angle measurement is widely used to measure the degree of hydrophilicity of the given surface. The hydrophilicity of the electrospun fibre sheets was evaluated by water contact angle measurements using an instrument for contact angle measurement (See System, Advex Instruments, s. r. o., Czech Republic). A distilled water droplet size of ~20 μL was placed carefully onto the surface of the scaffolds at room temperature. After a period of 20 seconds, the contact angle was recorded. The mean value and standard deviation were calculated through testing at ten different positions on the same sample.

3.4 Experimental process

3.4.1 Preliminary investigation of the effect of calcium chloride on dissolution behavior and properties of silk fibroin solution

In this dissertation, a novel method for a preparation of a silk fibroin solution by dissolving silk fibre in a mixture of formic acid and inorganic salt is being used instead of a ternary solvent system of $CaCl_2/C_2H_5OH/H_2O$, which has been widely used to dissolve silk fibroin. Generally, formic acid cannot dissolve silk fibroin at all. However, from a previous study showed that silk fibroin can be dissolved by the adding of a small quantity of inorganic salts into formic acid and makes it an effective solvent for dissolution of silk fibroin [56, 60, 68]. In this work, calcium chloride was chosen for improve solubility of silk fibroin in formic acid due to its chaotropic property.

Firstly, in order to find out the appropriate amount of calcium chloride for dissolution of silk fibroin in formic acid and the effect of calcium chloride on the properties of a silk fibroin solution. Degummed silk fibres were directly dissolved in formic acid (98%) with various concentration of calcium chloride to prepare 8 wt% of silk solution. The ratio of silk fibroin to calcium chloride was 1:0.15, 1:0.20, 1:0.25, 1:0.30, 1:0.35, 1:0.40, 1:0.45 and 1:0.50 (w/w), respectively. All solutions were magnetically stirred at room temperature for 6 hours. Solution properties such as conductivity, surface tension and viscosity were determined, and then solutions were electrospun into fibre sheets.

A schematic representation of the equipment used in the experiment is illustrated in Figure 3.5. During the spinning process, the silk fibroin solution was placed on the surface of the spinning electrode (10 mm in diameter), which was connected to a high-voltage DC power supply (Spellman SL150). A high voltage of 50 kV was applied to the silk solution. The electrospun fibres were collected on a collector, which was placed at a distance of 100 mm from the electrode. The processes were carried out at room temperature and 40±2% humidity. The morphology of electrospun fibres was investigated by SEM.

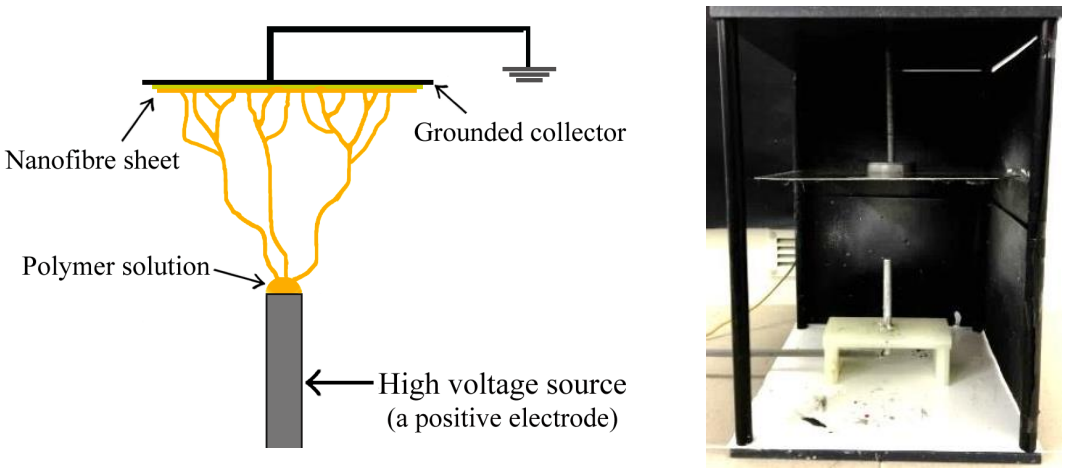

Figure 3.5 Schematic of a simple electrospinning experiment.

3.4.2 Fabrication of silk fibroin nanofibres by needleless electrospinning method

The main objective of these experiments is to fabricate silk fibroin nanofibre and to study the processing parameters in needleless electrospinning (silk fibroin concentration, applied voltage and spinning distance). The goal is to obtain a detail of the effects of the electrospinning parameters on the morphology and spinning performance of the process and optimization of the needleless electrospinning process.

The spinning solutions were prepared by the dissolution of degummed silk fibres in a mixture of formic acid and calcium chloride. The ratio of silk fibre to calcium chloride was 1:0.25 (w/w), which is used throughout the remaining experiment. All solutions were magnetically stirred at room temperature overnight. The properties of spinning solutions were measured. Subsequently, the solution was electrospun into fibre sheets without any further treatment.

For comparison, a traditional silk spinning solution was prepared as follows: the degummed silk fibres were dissolved in a tertiary solvent system of $CaCl_2$/ C_2H_5OH/H_2O solution (1/2/8 in molar ratio) at 85 ^{O}C for 40 minutes to attain silk fibroin solution. The ratio of silk fibre over dissolving solution was 1:10 (w/v). Then, the silk fibroin solution was dialyzed against deionized water in dialysis tubing cellulose membrane (Sigma, molecular cutoff 12,000-14,000) at room temperature for 3 days. The dialyzed silk solution was filtered and spray dried to obtain silk powders; finally, the dried silk powders were dissolved in formic acid for 4 hours to prepare 12% (w/w) silk solution for electrospinning.

A schematic representation of the equipment used in the spinning process is depicted in Figure 3.6. The electrospinning device contains a rotating electrode, the electrode was made of stainless steel wire with 125 mm in length (wire diameter 0.02 mm) and a solution reservoir. The solution reservoir, which has a high voltage connected to the bottom of the solution bath, was filled with the silk fibroin solution. The process parameters are shown in Table 3.2. The electrospun fibres sheet was collected on the backing material (polypropylene nonwoven fabric) moving along the collector electrode by a velocity 10 mm/min.

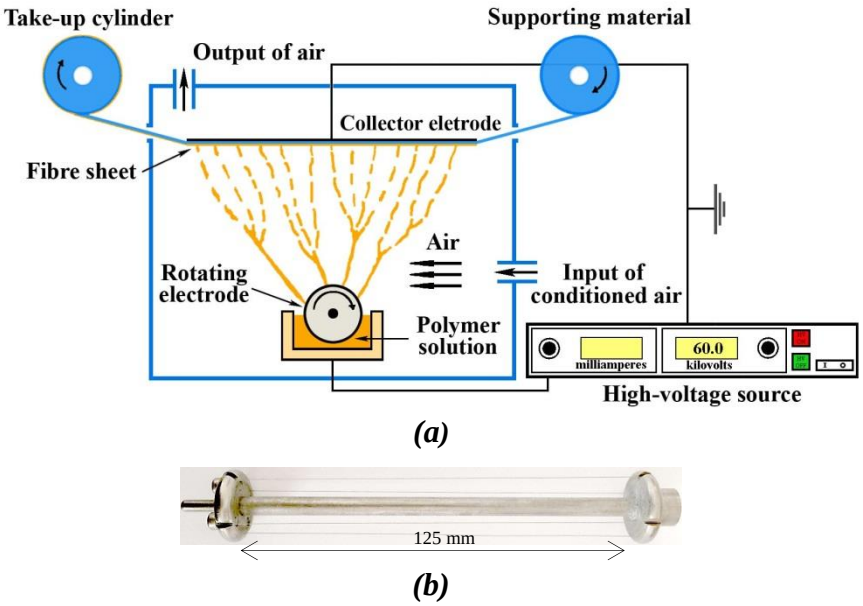

Figure 3.6 (a) Schematics of needleless electrospinning setup and (b) a spinning electrode.

Table 3.2 Spinning parameters of an electrospinning experiment

Parameters	Parameters level
Silk fibroin concentration (wt %)	6, 8, 10,12, 14
Applied Voltage (kV)	30, 35, 40, 45, 50, 55, 60
Distance between electrodes (mm)	100, 125, 150
Roller angular velocity (rpm)	15
Backing fabric take up speed (mm/min)	10
Air humidity (%)	35 - 40
Temperature (^{O}C)	20 - 25

After spinning, the electrospun fibre sheets were treated with ethanol, as described in topic 3.3.3. The morphological appearance of the silk electrospun fibres was observed with SEM. The spinning performance of the electrospinning process was calculated by using the equation 3.2.

3.4.3 Preparation of silk fibroin-polycaprolactone blend fibres with needleless electrospinning method

Although silk fibroin nanofibres were successfully fabricated with needleless electrospinning, the obtained fibre sheet is usually fragile. It is brittle in the dry state, which is a disadvantage and would be unsuitable for practical use. However, if the dry state is required and the brittleness is undesirable, mechanical properties of silk fibre sheet can be improved by blending with other synthetic polymers. Blending of two polymers is a simple method to retain their both characteristics within one material and to compensate the drawbacks of one component in blend [61, 69-70].

In these studies, polycaprolactone has been used for blending with silk fibroin owning to its good mechanical properties, non-toxicity and biocompatibility. Various blend ratios of silk fibroin and polycaprolactone could be investigated for the fabrication and evaluation. The effect of blend ratio of silk fibroin and polycaprolactone in spinning solution is investigated as a function of the properties of the blend solution, the morphology of electrospun fibres and the spinning performance of the process.

For a preparation of spinning solutions, polycaprolactone pellets were dissolved in formic acid to prepare 15 wt% and 20 wt% of polycaprolactone solutions. The solutions were continuously stirred with a magnetic stirrer at ambient temperature for 4 hours. Silk fibroin solution was prepared as described in topic 3.4.2. The silk fibroin concentration was fixed at 12 wt%. The SF/PCL blend solutions were prepared by mixing the silk fibroin solution with the polycaprolactone solutions at weight ratios of 9/1, 8/2, 7/3, 6/4 and 5/5 (w/w), respectively. After that, all solutions were magnetically stirred at room temperature. The properties of blend solutions were measured.

Subsequently, the blend solution was electrospun at a high voltage of 55 kV. The equipment used for these studies is same as a previous experiment (topic 3.4.2). The electrospun fibre sheets were collected on the backing material moving along the collector electrode by a velocity 10 mm/min. Electrospinning was carried out at a distance of 100 mm; the temperature was 22 ± 2 ^{O}C and air humidity was 38 ± 2%. After spinning, the obtained electrospun fibre sheets were post-treatmented and characterised as same as the electrospun silk fibroin fibres. Moreover, the physical properties of these blend electrospun fibre scaffolds were characterized when compared to silk fibroin fibre sheets.

3.5 *In vitro* testing of electrospun fibre sheets from silk fibroin and its blend with polycaprolactone

In vitro tests were done in cooperation with Mgr. Jana Horáková from Department of Nonwovens and Nanofibrous Materials, Faculty of Textile Engineering, Technical University of Liberec. In order to evaluate interaction between the electrospun fibre sheets with living cells; 3T3 mouse fibroblasts, normal human dermal fibroblasts, MG 63 osteoblasts and human umbilical vein endothelial cells were seeded on silk fibroin (SF) and silk fibroin/polycaprolactone (SF/PCL) blend fibre sheets [prepared from SF/PCL blend solutions at weight ratios of 7/3 and 5/5 (w/w)]. To test cell adhesion and proliferation, MTT test was used for measurement of cell viability during the cultivation time. The morphologies of cellular on the fibre sheets were analysed by fluorescence microscopy and scanning electron microscope (SEM).

3.5.1 Preparation of scaffolds

The fibre sheets were cut into small disks with a diameter of 6 mm to fit each well of 96-well plate. The specimens were sterilized by immersion in 70% aqueous ethanol solution for 30 minutes followed by double washing in phosphate buffer saline (PBS, Lonza).

3.5.2 Cell sources and seeding

- 3T3 mouse fibroblasts (ATCC) were cultivated in Dulbecco´s Modified Eagle Medium (DMEM, Lonza) supplemented by 10% fetal bovine serum (FBS, Lonza) and 1% Penicillin-Streptomycin-Amphotericin B Solution (Lonza).

- Normal human dermal fibroblasts (NHDF) were cultivated in Fibroblast Basal Medium (FBM-2, Lonza) supplemented by containing FBS, growth factors, and antibiotics.

- MG 63 osteoblasts in Eagle's Medium (EMEM, Lonza) supplemented by 10% fetal bovine serum (FBS, Lonza) and 1% antibiotics.

- Human umbilical vein endothelial cells (HUVEC) were cultivated in Endothelial Basal Medium (EBM-2, Lonza) supplemented by EGM-2 Sigle Quots (Lonza) containing human Epidermal Growth Factor (hEGF), hydrocortisone, bovine brain extract (BBE), ascorbic acid, fetal bovine serum (FBS) and gentamicin/amphotericin-B (GA).

The cells were placed in humidified incubator at an atmosphere of 5% CO_2 at 37 ^{O}C. When cells became confluent, they were suspended using trypsin-EDTA solution (Lonza), centrifuged and re-suspended in fresh complete medium. Number of cells was determined by Luna^{TM} cell counter (Logis Biosystems). 3T3 mouse fibroblasts, normal human dermal fibroblasts and MG 63 osteoblasts were seeded on the fibre sheets placed in 96-well plate at density of $5x10^3$ per well plate. During the experiment, a medium was changed 3 times per week. On the other hand, human umbilical vein endthelial cells were seeded on the scaffolds placed in 96-well plate at density of $1x10^4$ per well plate and a medium was changed 3 times during the 7 days experiment.

3.5.3 MTT assay

Cell viability seeded on the scaffolds were analysed by MTT method after the culture time. Briefly, after cell cultured, MTT solution (Sigma Aldrich) in amount of 50 µl was added to 150 µl of DMEM and the specimens were incubated at 37 ^{O}C for 4 hours. When MTT (3-(4,5-dimethylthiazol-2-yl)-2,5-diphenyl-2*H*-tetrazolium bromide) has been reduced to purple formazan by mitochondrial dehydrogenase in cells indicating normal metabolism. Then, formed violet crystals of formazan were solubilised with acidic isopropanol. Optical density of suspension was measured (λ_{sample} 570 nm, $\lambda_{reference}$ 690 nm) using Absorbance Reader ELx808 (BioTek). For each testing day, 4 samples of each material were incubated with MTT solution and average absorbance was calculated as the difference between absorbance measured by 570 nm and by reference wavelenght 690 nm.

3.5.4 Fluorescence microscopy analysis

After the cultivation peroid, the samples were washed twice in PBS and fixed in frozen methanol for 30 minutes followed by double washing with PBS and staining with propidium iodide (PI dilution 2 g/l PBS, Sigma Aldrich) for 10 minutes in the dark. Stained cells were observed by inverted fluorescence microscope (Nikon). For evaluation of cellular adhesion, the results after 1 day are depicted in result section. For proliferation assessment, the results in the end of the experiment of cell culture are presented.

3.5.5 SEM analysis

After days of cultivation, the samples for SEM analyses were washed twice in PBS and fixed in 2.5% glutaraldehyde in PBS for 30 minutes at 4 ^{O}C. The samples were dehydrated by ethanol gradient (60%, 70%, 80%, 90%, 96% and 100%, respectively).

After water removing, the scaffolds were transferred to SEM holder, sputter-coated with gold and observed under the SEM. The results after 1 day are depicted in result section for cellular adhesion evaluation. The results in the end of the experiment are presented for proliferation rate assessment.

3.6 Supplementary experiment

3.6.1 Fabrication of silk nanofibres with needle and needleless electrospinning

The objective of these experiments is to fabricate silk electrospun fibres with two different spinning systems: a needle and a roller, concentrating on the effect of the spinning electrode on the electrospinning process. The influences of the spinning electrode and spinning parameters (silk concentration and applied voltage) on the spinning process, morphology of the obtained fibres and the production rate of the spinning process were examined.

For a preparation of spinning solution, silk solutions were prepared as described in topic 3.4.2. The silk fibroin concentration varied from 8 wt% to 12 wt%. The properties of spinning solutions were measured. Subsequently, the solution was electrospun into fibre sheets without any further treatment. A schematic representation of the equipment used in the experiment is illustrated in Figure 3.7. During the needle electrospinning, the silk fibroin solution was placed in a 10 ml syringe with a stainless steel needle, which was connected to a high-voltage DC power supply. The flow rate of the spinning solution was 1.5 ml/h using a syringe pump (KDS 100 CE, KD Scientific Inc.) The syringe used in the experiment had an 18-gauge needle (capillary diameter 1.2 mm). The roller electrospinning device contains a rotating cylinder, 85 mm in length and 15 mm in diameter and a solution reservoir. The solution reservoir, which has a high voltage connected to the bottom of the solution bath, was filled with the silk fibroin solution. The rotating cylinder was then partially immersed in the solution.

During electrospinning, the spinning solution was slowly loaded onto the roller surface (rotation ~ 7 rpm). Electrospinning of the silk fibroin solutions was carried out at a high voltage in the range of 35 kV to 50 kV, and the electrospun fibres were collected on a collector, which was placed at a distance of 100 mm from the spinning electrode. All the processes were carried out at 22 $\pm$ 2 ^{O}C and 35 $\pm$ 2% humidity. After spinning, the electrospun fibre sheets were treated with ethanol, as described in 3.3.3. The production rates of the electrospun fibres with both spinning techniques were determined based on the mass of the obtained electrospun fibre sheet per unit time (the size of the samples was 10 cm × 10 cm) and then normalised to obtain the fabrication rate in grams per hour (g/h).

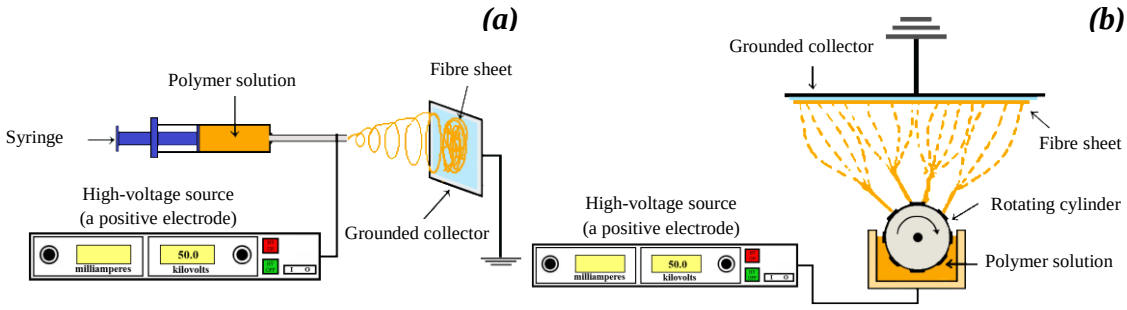

Figure 3.7 Schematic of an electrospinning experiment (a) needle electrospinning and (b) roller electrospinning

3.6.2 Immobilization of laccase on polycaprolactone/silk fibroin blend fibre sheets

This experiment was done in cooperation with Ing. Milena Maryšková, from Department of Nonwovens and Nanofibrous Materials, Faculty of Textile Engineering, Technical University of Liberec [The experiment in this section is a part of diploma thesis of Ing. Milena Maryšková, in a topic "Enzyme immobilization on microfibrous or nano fibrous materials and their application in biotechnology" and N. Sasithorn was a superviser of this diploma work, which was evaluated by rector prize (2015)].

- *Preparation of polycaprolactone/silk fibroin nanofibre sheets*

For a preparation of blend solution, PCL pellets were dissolved in formic acid to prepare 20 wt% of polycaprolactone solution. Silk solution was prepared as described in topic 3.4.2. The silk fibroin concentration was fixed at 12 wt%. The blend solution was prepared by mixing the polycaprolactone solution with the silk fibroin solutions at weight ratios of 8/2 (w/w). After that, the solution was magnetically stirred at room temperature overnight. Subsequently, the resulting solution was electrospun using Nanospider™ NS 1WS500U. The process parameters are shown in Table 3.3. After spinning, the electrospun fibre sheets were treated with ethanol.

Table 3.3 Spinning parameters of an electrospinning with Nanospider™ NS 1WS500U

Parameters	Parameters level
Applied Voltage (kV)	-10 / +50
Distance between electrodes (mm)	140
Wire speed (mm/s)	3
Backing fabric take up speed (mm/min)	15
Carriage speed (mm/s)	450 - 500
Wire distance (mm)	500
Air humidity (%)	23.5
Temperature (^{O}C)	21.7

- *Enzyme activity assay*

The catalytic activity of the laccase from *Trametes versicolor* was measured according to Arnold and Georgiou [71] and Hassani et al. [72] at 25 ^{O}C using a microplate reader (BioTech Synergy HTX). The substrate for the catalytic reaction was 0.5 mM ABTS [2,2′-Azino-bis(3-ethylbenzothiazoline-6-sulfonic acid) diammonium salt)] and the buffer was 100 mM McIlvaine buffer with pH 3.0. The activity of the soluble laccase was measured in 96-well plates where the contents were following: 160 µl of buffer, 20 µl of the laccase solution and 20 µl of 0.5 mM ABTS.

From the moment, ABTS was added in the reaction mixture it began to be oxidized by the laccase producing the stable cation radical ABTS cation with green color, which was measured by absorbance at 420 nm. The activity was expressed as 1 U (enzyme unit) which corresponds to the amount of laccase that converts 1 micro mole of ABTS per minute. The formula for the expression of 1 U is derived from the Lambert-Beer law;

$$ABS = c \cdot \varepsilon \cdot d \tag{3.3}$$

ABS stands for absorbance, c is concentration, ε is a molar extinction coefficient and d is a path length of the beam passing through the testing material or the thickness of the layer.

The molar extinction coefficient for ABTS cation at 420 nm is 0.036 µmol^{-1}cm^{-1} [73], the layer thickness of 200 µl of the reaction solution using 96-well plate was measured to be 0.6 cm and *df* represents the dilution factor. With the slope deducted from the linear part of the absorbance, growth in time the final formula for the activity measurement was following:

$$1\,U = \left(\frac{slope\ (ABS/min)}{\varepsilon\ (\mu mol^{-1} \cdot cm^{-1})\ \times\ d\ (cm)} \right) \times V\ (L) \times df \tag{3.4}$$

The activity of the immobilized laccase was measured likewise using either DR 6000 UV-Vis spectrophotometer (Hach) with cuvette or the microplate reader with 6-well plate (Fig. 3.8). The cuvette had a volume of 3.0 ml. The volume of the sample was neglected so the reaction mixture consisted of 2.7 ml of buffer and 300 µl of ABTS. The fibre sheets with the immobilized laccase were placed on the bottom of the cuvette and weighed down by a stainless steel wire so that the sample did not float and deflect the beam during measurement. On the other hand, the 6-well plate had 6 beakers with the volume of 10.0 ml and the beam coming top down through the plate. The reaction mixture consisted of 7.2 ml of the buffer and 800 µl of ABTS. The fibre sheets ware attached to wall of the beaker by a stainless steel wire and the reaction was attended by linear shaking which insured sufficient distribution of the oxidation product. The thickness of the layer *d* was 1 cm in both methods.

(a) a cuvette

(b) a 6-well plate

Figure 3.8 Measurement of the catalytic activity of the immobilized laccase using a cuvette and a 6-well plate.

The efficiency of the immobilization procedure was expressed by three values. The immobilization yield *(IY).* This value is given be following formula:

$$IY\ [\%] = \left(\frac{IN\ -\ SN}{IN}\right) \times 100 \tag{3.5}$$

The IN represents the activity of the laccase initially added to the reaction and the SN is the activity of the laccase remaining in the supernatant after the fibre sheets are removed from the immobilization bath. IY represents the amount of laccase immobilized on the fibre sheets.

The *activity yield (AY)* represents the actual activity of the laccase immobilized on the matrix. This value predicates of the catalytic activity of the final product. It is given by following formula:

$$AY\ [\%] = \left(\frac{Activity\ on\ the\ fibre\ sheet}{IN}\right) \times 100 \tag{3.6}$$

The *loading* stands for the amount of laccase immobilized on 1 gram of the matrix. Usually the activity is measured just in milligrams of the samples so the final loading is given by the activity (U) on the matrix divided by the mass of the sample in grams (g).

- *Enzyme immobilization on polycaprolactone/silk fibroin nanofibre sheets.*

Laccase from *Trametes versicolor* was immobilized on the blend nanofibre sheets by covalent attachment method. Due to covalent attachment method was suitable for a polymer that had a free amine groups, which enabling a modification via glutaraldehyde. In addition, bovine serum albumin and hexamethylenediamine are also used as a chemical for a modification. Bovine serum albumin worked as a biocompatible layer that separated the immobilized enzyme from a direct contact with the nanofibrous matrix and in substance, it extended the linkage together with two layers of glutaraldehyde. The main reason for making a longer linkage from the matrix was to provide a larger space for the biocatalyst molecule with a more flexible attachment. Before the bovine serum albumin was applied it was denatured by heat (100 ^{O}C, 1 hour) in order to fix its structure and prevent it from its conformational changes that could damage the attached enzyme molecule. Hexamethylenediamine had a similar role to extend the

linkage with the enzyme. This reactive molecule did not provide a biocompatible environment however; it did not require any treatment before it was applied [74].

In an immobilization process, the blend fibre sheet was cut into small pieces. Each of them weighed 5 mg. These samples were washed with ethanol and distilled water and after that, modified via glutaraldehyde or combinations of glutaraldehyde and bovine serum albumin or hexamethylenediamine. After modification, the fibre sheets were thoroughly washed with distilled water. Bovine serum albumin was denaturized by heat (80 ^{O}C for an hour). Modified fibre sheets according to techniques described by Silva et al. [75] were placed into the enzyme solution for certain time and then washed with a buffer several times until there was no activity detected in the washing buffer. After that, the washed samples were placed in 100 mM McIlvaine buffer with pH 3.0 to measure the activity of the laccase immobilized on the fibre sheets. Supernatant (reaction mixture) and the washings were kept for the calculation of the immobilization yield. Immobilization procedure was optimized by changing following parameters as shown in Table 3.4.

Table 3.4 Variable parameters for immobilization of laccase via covalent attachment on the blend nanofibrous layer.

Buffer	McIlvaine buffer	20 mM - 100 mM pH 3.0 - 7.8
	Sodium-acetate buffer	20 mM - 100 mM pH 3.0 - 6.0
Enzyme	Laccase from *Trametes versicolor*	0.5 mg/ml - 2.0 mg/ml Solution volume 0.25 - 2.0 ml
Modification methods	Glutaraldehyde (GA)	10% - 25% (v/v) Reaction time 2 - 4 hours
	Bovine serum albumin (BSA)	5 mg/ml and 10 mg/ml Reaction time 3 - 5 hours
	Hexamethylenediamine (HMD)	0.1 M Reaction time 2 - 4 hours
	Combinations	GA; GA-BSA-GA; GA-HMD-GA;
Time of the enzyme attachment	5 - 20 hours	
Additional crosslinkers	Glutaraldehyde	0.5% - 1% (v/v) Time 1 - 2 hours
Additional chemicals	Polyethylene glycol (PEG)	0.5 g/ml - 1.0 g/ml
Temperature	4 ^{O}C and 20 ^{O}C	

- Determination of degradation of endocrine disrupting chemicals (EDCs) by immobilized laccase on PCL/SF blend fibre sheets

A detail of selected blend fibre sheets for degradation of endocrine disrupting chemicals are shown in table 3.5.

Table 3.5 Selected samples for degradation of endocrine disrupting chemicals

Modification method	Enzyme solution	Time/ Temperature	IY [%]	AY [%]	Loading [U/g]
GA (2 h, 20 ^{O}C, milli-Q, 12.5 %v/v)-BSA (14 h, 20 ^{O}C, milli-Q, 1 mg/ml)-GA (2 h, 20 ^{O}C, milli-Q, 12.5 %v/v)	0.5 ml, 2 mg/ml, 20 mM McIlvaine pH 3.0	20 hours 4 ^{O}C	25.1 ± 6.7	4.3 ± 1.2	65.0 ± 8.4

Remark: GA, BSA and Milli-Q refer to glutaraldehyde, bovine serum albumin and ultrapure water

The fibre sheets with immobilized laccase and five solutions with different concentrations of the free laccase were tested for the degradation of micropollutant mixture. Bisphenol A (BPA) and 17α-ethinyl estradiol (EE2) were selected as a endocrine disrupting chemical for these studies. The micropollutant mixture consisted of 50 µM bisphenol A and 50 µM 17α-ethinylestradiol (EE2). Stock solutions with a concentration of 500 µM of these two chemicals were prepared separately by dissolving in methanol. These two solutions were mixed together and diluted with ultrapure water. All samples were placed into glass vials with 3 ml of micropollutant mixture and these vials were constantly shaken in a water bath at 37 ^{O}C. Blank samples that were prepared alike to the actual samples but in their case the immobilized laccase was inhibited by 10% sodium azide. The blanks were tested for possible absorption of the endocrine disruptors into the nanofibre sheets. Additional vials contained certain amount of free laccase that approximately corresponded to the units of laccase immobilized on the samples. In selected time intervals, the supernatant from all vials was collected and measured by HPLC. The sampling consisted of 70 µl of the supernatant diluted by 140 µl of methanol and 1.5 µl of 2.8% sodium azide, which was added to stop the degradation in case some of the laccase was collected within the supernatant. After the first use, all samples were removed from the reaction mixture, washed with ultrapure water and stored in ultrapure at 4 ^{O}C until they were used the next day.

4. Results and discussion

4.1 Effect of calcium chloride on dissolution behavior and properties of silk fibroin solutions

In this study, silk fibroin was directly dissolved in formic acid with various concentration of calcium chloride. To find a proper amount of calcium chloride was added to formic acid for a preparation of a spinning solution. Therefore, the preliminary investigation of the effect of calcium chloride on solubility and properties of silk fibroin solutions was carried out as follows:

4.1.1 Effect of calcium chloride on solubility of silk fibroin in formic acid

Figure 4.1 exhibits the difference dissolution of silk fibroin in formic acid with different amounts of calcium chloride. It was observed that silk fibroin insoluble in formic acid, but soluble in a mixture of formic acid and calcium chloride. This shows that calcium chloride can improve the solubility of silk fibroin in formic acid. It is suggested that calcium chloride has a chaotropic property that disrupts stabilizing intra-molecular forces such as hydrogen bonds, van der Waals forces and hydrophobic interactions in protein structures by shielding charges and preventing the stabilization of salt bridges. Hydrogen bonds are stronger in nonpolar media. Calcium chloride that increases the chemical polarity of the solvent can also destabilize hydrogen bonding in silk fibroin structure and ion-dipole interactions between the salts and hydrogen bonding species, which are more favorable than normal hydrogen bonds. It will make hydrophobic proteins more soluble in the solvent [29, 68].

(a) *without $CaCl_2$* | *(b)* *1:0.15* | *(c)* *1:0.20* | *(d)* *1:0.25*

Figure 4.1 Photograph of dissolution of silk fibroin in formic acid with different amounts of calcium chloride; [SF : $CaCl_2$ (w/w)]

In dissolution process, in order to obtain a homogenous solution that suitable for a spinning process, silk fibroin should be completely dissolved in formic acid. Thus, the proper ratio of calcium chloride and silk fibroin required. From the results show that silk fibroin could dissolve completely in weight ratios ranging from 1:0.25 to 1:0.50 of silk fibroin : calcium chloride.

4.1.2 Effect of calcium chloride on properties of silk fibroin solution

The properties of silk fibroin solution including conductivity, surface tension and viscosity with different amounts of calcium chloride were measured and summarized in Table 4.1 and Figure 4.2. The results show that the variation of weight ratio of calcium chloride in the solution had a significant effect on properties of the solution. It is obviously clear that the conductivity and surface tension of solutions increase with the increasing weight ratio of calcium chloride. Increasing amount of calcium chloride also affected a viscosity of silk fibroin solution.

Table 4.1 Effect of concentrations of $CaCl_2$ on properties of silk fibroin solution 8 wt%

SF : $CaCl_2$ (w/w)	Dissolution behaviour	Conductivity (mS/cm)	Surface tension (mN/m)
1 : 0.15	Partially soluble	-	-
1 : 0.20	Partially soluble	-	-
1 : 0.25	Soluble	6.13	38.51
1 : 0.30	Soluble	6.52	39.06
1 : 0.35	Soluble	6.90	39.89
1 : 0.40	Soluble	7.29	40.65
1 : 0.45	Soluble	7.71	41.32
1 : 0.50	Soluble	8.03	41.97

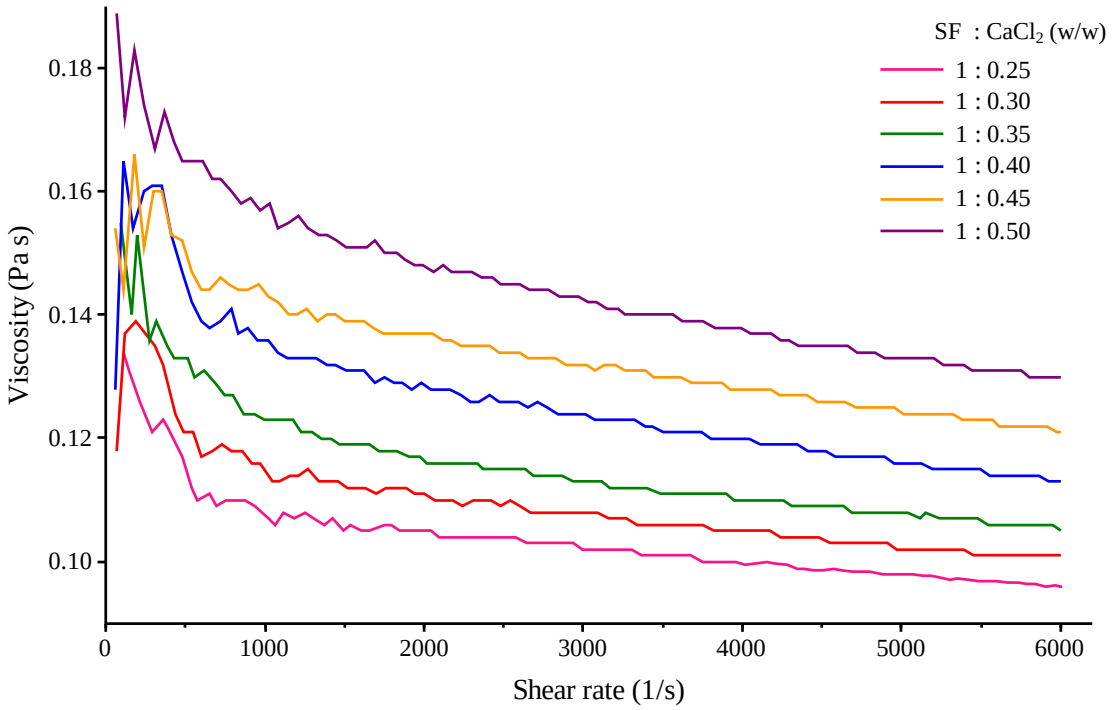

Figure 4.2 Rheological behaviour of silk fibroin solutions 8 wt% with different amounts of calcium chloride.

As shown in Figure 4.2, the viscosity of silk fibroin solutions gradually increases with increasing amounts of calcium chloride. This increase in viscosity of the solution could be owing to the complex bonds between the calcium cation and silk fibroin. It can assume that calcium chloride is a Lewis acid and it can complex with amides (Lewis base). In dissolving process, calcium ions comes close to the silk fibroin due to the intermolecular interaction, then the oxygen atoms of the carbonyl groups in the peptide bonds of silk fibroin make coordination bonds with calcium cations. When the amount of calcium chloride increased, the number of hydrogen bond in silk fibroin decrease gradually due to the increase of complexation of calcium chloride with amide groups [76-78]. The complexation of calcium ion with amide groups in silk fibroin has an effect on a viscosity of the silk solution, with higher degree complexation yielding silk solution with higher viscosity.

4.1.3 Effect of concentration of calcium chloride on fibre diameter

The SEM micrographs and diameter distribution of the silk fibroin electrospun fibres prepared from silk solutions with different amounts of calcium chloride are shown in Figure 4.3. The results show that there is a significant increase in the average fibre diameter with an increase in the concentration of calcium chloride. It is possible that the addition of ionic salt may cause an increase in the viscosity of the solution. Thus, although the conductivity of the solution is improved, the viscoelastic force is stronger than the columbic force resulting instead in an increase in the fibre diameter [53].

Moreover, increasing the weight ratios of silk fibroin to calcium chloride affected the morphology of the obtained fibres. The morphology of electrospun fibres was slightly changed from circular cross section to flat (ribbon-like) fibres. Average fibre diameter was also increased to a range of 360 nm to 720 nm. It is assumed that adding a large quantity of calcium chloride can cause a change in the evaporation of solvent. Due to calcium chloride has an ability to attract moisture from the air and surroundings, then the ability to absorb water of the silk fibroin solution was increased when an amount of salt was increased. As the result, the solution can absorb more ambient water during electrospinning. The absorption of water does not allowed to complete the drying process during the time of flight of the solution jet and this phenomenon could cause a slowing in evaporation of the solvent, which may cause an increase in fibre diameter and produce congealed mats instead of unwoven fibres [52, 79].

Therefore, the weight ratio of 1:0.25 and 1:0.30 (w/w) of silk fibre to calcium chloride seem to be a suitable ratio for a preparation of silk fibroin solution, which used for a electrospinning process. Eventually, the weight ratio of 1:0.25 (w/w) was preferred and used throughout the remaining experiment.

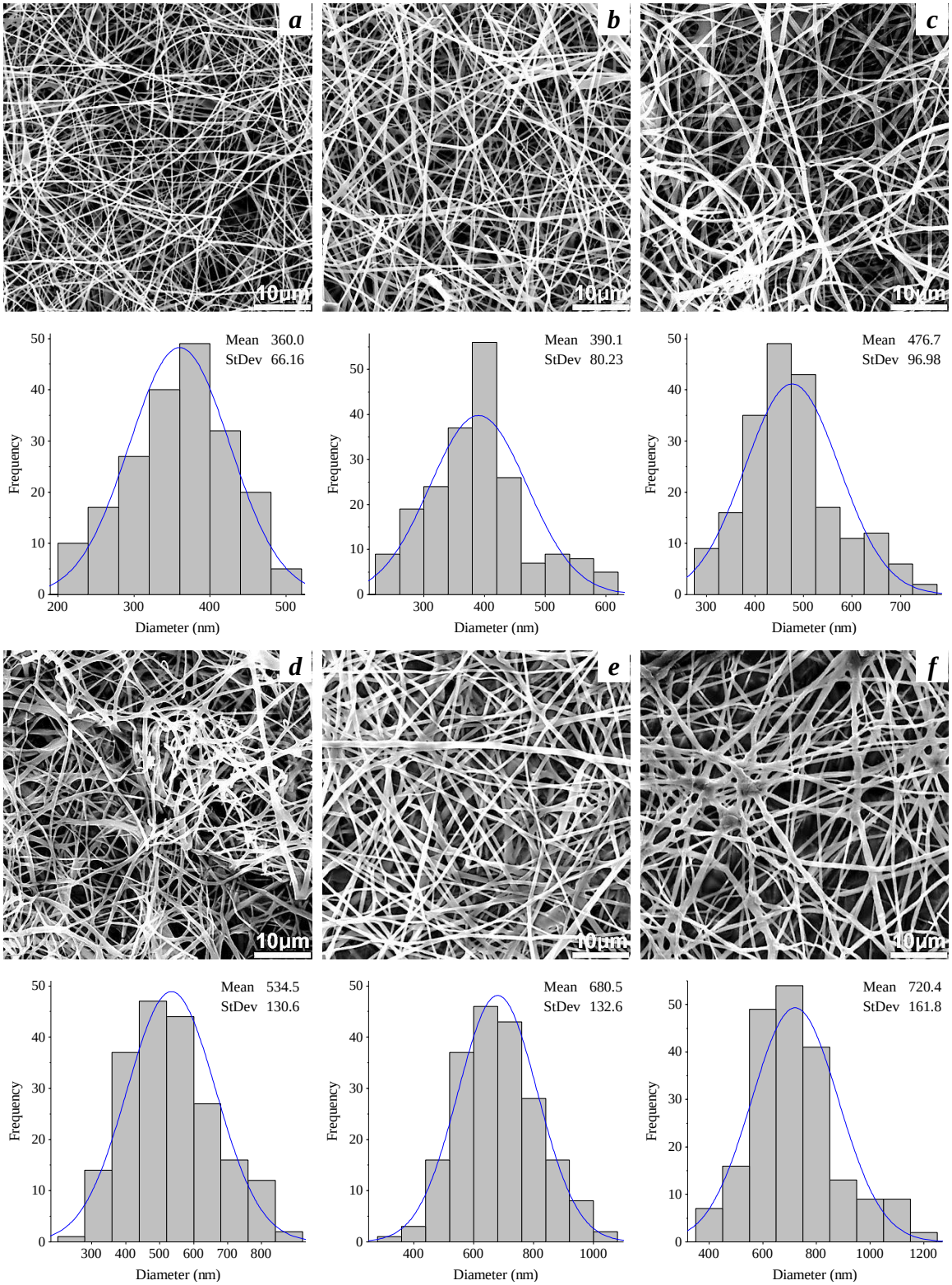

Figure 4.3 SEM micrographs and diameter distribution of electrospun fibres prepared from silk fibroin 8 wt% with different amounts of $CaCl_2$. a) 1:0.25; b) 1:0.30; c) 1:0.35; d) 1:0.40; e) 1:0.45; f) 1:0.50 (SEM magnification 5 kx).

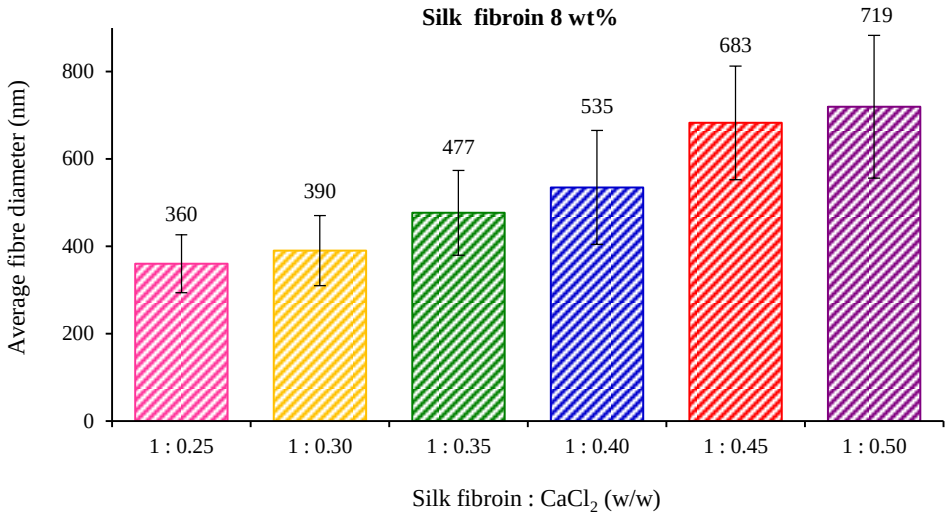

Figure 4.4 Effects of concentrations of $CaCl_2$ on average fibre diameter of silk fibroin electrospun fibres.

4.2 Effect of parameters on needleless electrospinning of silk fibroin

4.2.1 Effect of silk fibroin concentration

- Properties of silk fibroin solution at various concentrations

In electrospinning process, various solution properties play an important role in the morphology of the obtained electrospun fibres. The properties including conductivity, surface tension and viscosity of silk fibroin solution at various concentrations were measured and shown in Figure 4.5 and 4.6, respectively. The results show that the variation of silk fibroin concentration had a less significant effect on surface tension but produces an influence on conductivity and viscosity of the solution. It is obviously clear that conductivity and viscosity of the solution increase with increasing concentration of silk fibroin. It is possible that viscosity and conductivity of silk fibroin solution are affected by calcium chloride in the solution. In an electrospinning, processing parameters of the process were the same for all the solution. It can assume that conductivity and viscosity of spinning solutions are responsible for significant differences in spinnability, fibre morphology and spinning performance of the process.

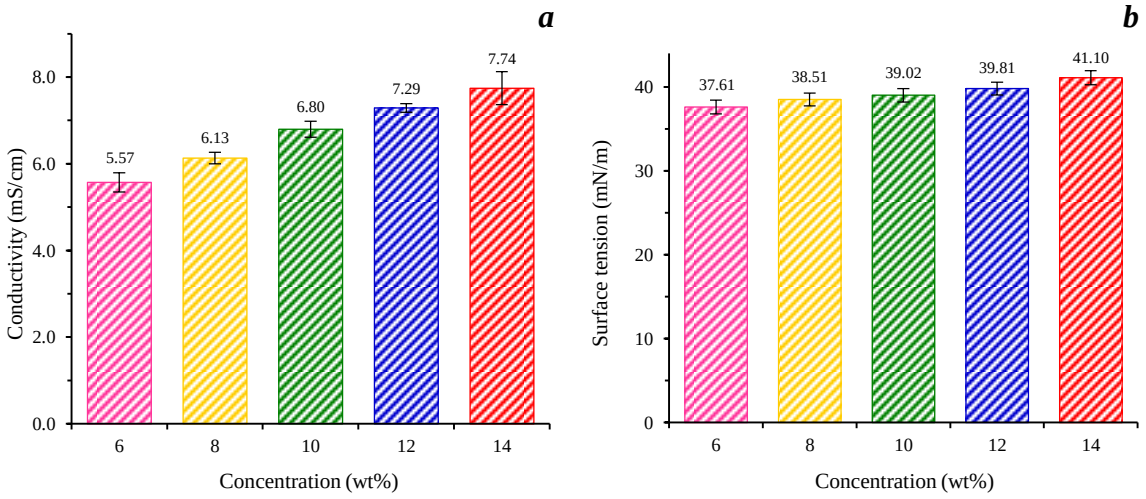

Figure 4.5 Effects of silk concentration on (a) conductivity and (b) surface tension.

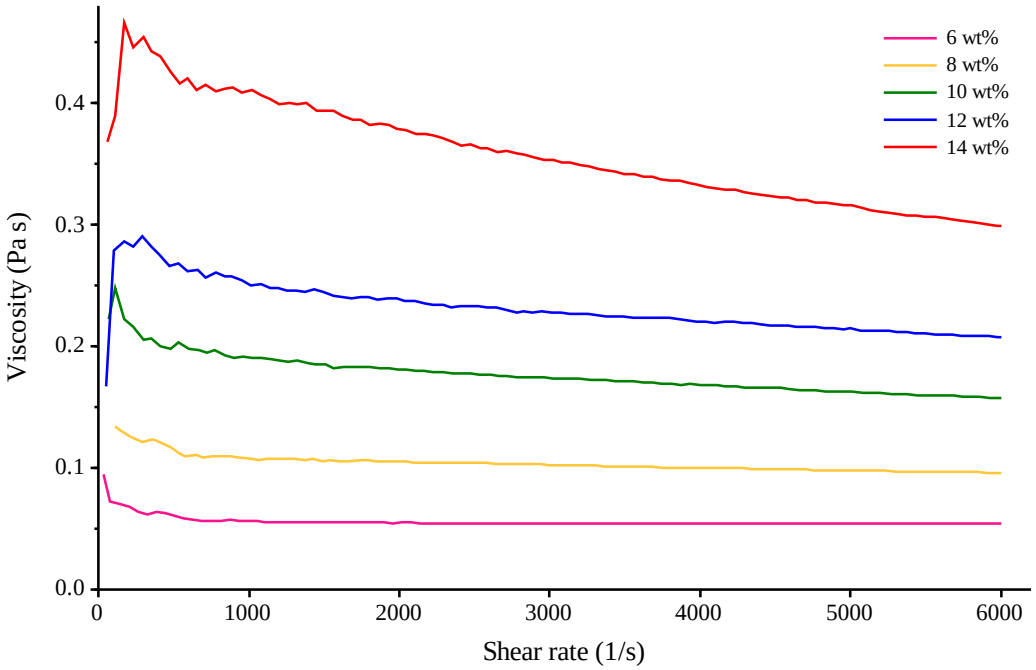

Figure 4.6 Rheological behaviour of spinning solutions prepared from different concentrations of silk fibroin.

- *Morphology of the obtained electrospun fibres*

Among the parameters of the process, the concentration of the polymer was found to be the most important factor in determining the spinnability of the solution and in deciding the morphologies and average diameters of the nanofibres after the electrospinning process. Considered the effect of concentration of spinning solution on fibre morphology with the applied voltage of 60 kV, when the silk fibroin concentration increased from 6 wt% to 14 wt%. The effect of silk concentration on the morphological appearance and diameter of the electrospun fibres was investigated by SEM, as shown in Figures 4.7.

It was found that an increase in the concentration of silk fibroin solution produces a significant effect on the average fibre diameter and the uniform diameter distribution of the obtained electrospun fibre. The results show that under the same electrospinning conditions, the fibre diameter and non-uniform fibre diameter distribution of the obtained electrospun fibres increased with an increase in the silk fibroin concentration, demonstrating the important role of the concentration of the spinning solution in fibre formation during the electrospinning process. When the concentration increased from 6 wt% to 14 wt%, the average fibre diameter increased from 191 nm to 1500 nm, respectively.

The concentration of the polymer solution reflects the number of entanglements of polymer chains in the solution, which, in turn, affect the viscosity of the solution. An increase in the concentration of the silk solution will result in greater polymer chain entanglement in the solution. Thus, the viscosity of the solution also increases. At higher concentrations, the diameter of the fibre is greater. In addition, the interaction between the solution and the charges on the jet determine the distribution of the fibre diameters obtained. This is probably due to the number of jets that form during

electrospinning. Multiple jets may form from the main electrospinning jet, which is stable enough to yield fibres of smaller diameter at certain concentrations, thereby generating fibres with various diameters [51, 53].

In this study, the concentration of the silk solution played an important role in the spinnability of the needleless system. At low concentrations of the spinning solution, nonfibrous formations were produced instead of nanofibres with beads. It is possible that Taylor cones are created in needleless electrospinning by picking up the spinning solution covering the surrounding spinning electrode [5, 14]. Generally, in spinning solutions with a low concentration, the viscosity of the solution is also low. Such solutions cannot be loaded on the surface of the spinning electrode because of their lack of viscosity. When Taylor cones do not form on the surface of an electrode, the electrospinning process results in nonfibrous formations [51, 80].

It was observed that no fibres were formed when silk fibroin concentration less than 5 wt% for this spinning condition. This was because at this concentration, there obviously were not sufficient molecular chain entanglements in the solution. When concentration of the silk solution was increased to 6 wt%, nanofibres were formed. Figure 4.7 (a) shows morphology of the obtained fibres from 6 wt% silk solution at 60 kV. The average fibre diameter is 191 nm and a narrow distribution of fibre diameters is observed. Experimental observations in electrospinning confirm that for fibre formation to occur, a minimum polymer concentration is required. Although, silk fibroin solution with the concentration of 6 wt% can spin into nanofibres with needleless system, the spinning solution still has a low viscosity. There some droplets were observed on the obtained fibre sheet. Further increase in concentration of silk fibroin up to 8 wt% results in continues nanofibres and droplets disappeared. The average fibre diameter is 393 nm and a narrow distribution of fibre diameters is observed. This was due to the fact there were sufficient molecular chain entanglements in the polymer solution to prevent the breakup of the electrically driven jet and to allow the electrostatic stresses to further elongate the jet to form fibres. Therefore, the silk fibroin solution should has a concentration at least 8 wt% to produce continuous silk fibres with a nanometer diameter under the experimental conditions of this study. Concentrations of silk fibroin in the range of 8 wt% to 12 wt% seem to be a suitable concentration for a preparation of nanofibre sheets with needleless electrospinning.

For comparison, silk electrospun fibres prepared by using silk powder (12 wt%) from the ternary solvent system of $CaCl_2/C_2H_5OH/H_2O$, was also electrospun by needleless system. Under the same operating conditions, the diameters of the silk electrospun fibres obtained from the ternary solvent system were smaller and the diameter distribution was narrower than those obtained from the solvent system composed of formic acid and calcium chloride (see Fig. 4.8). However, the disadvantage of the ternary solvent system is time-consuming and complicated preparation process.

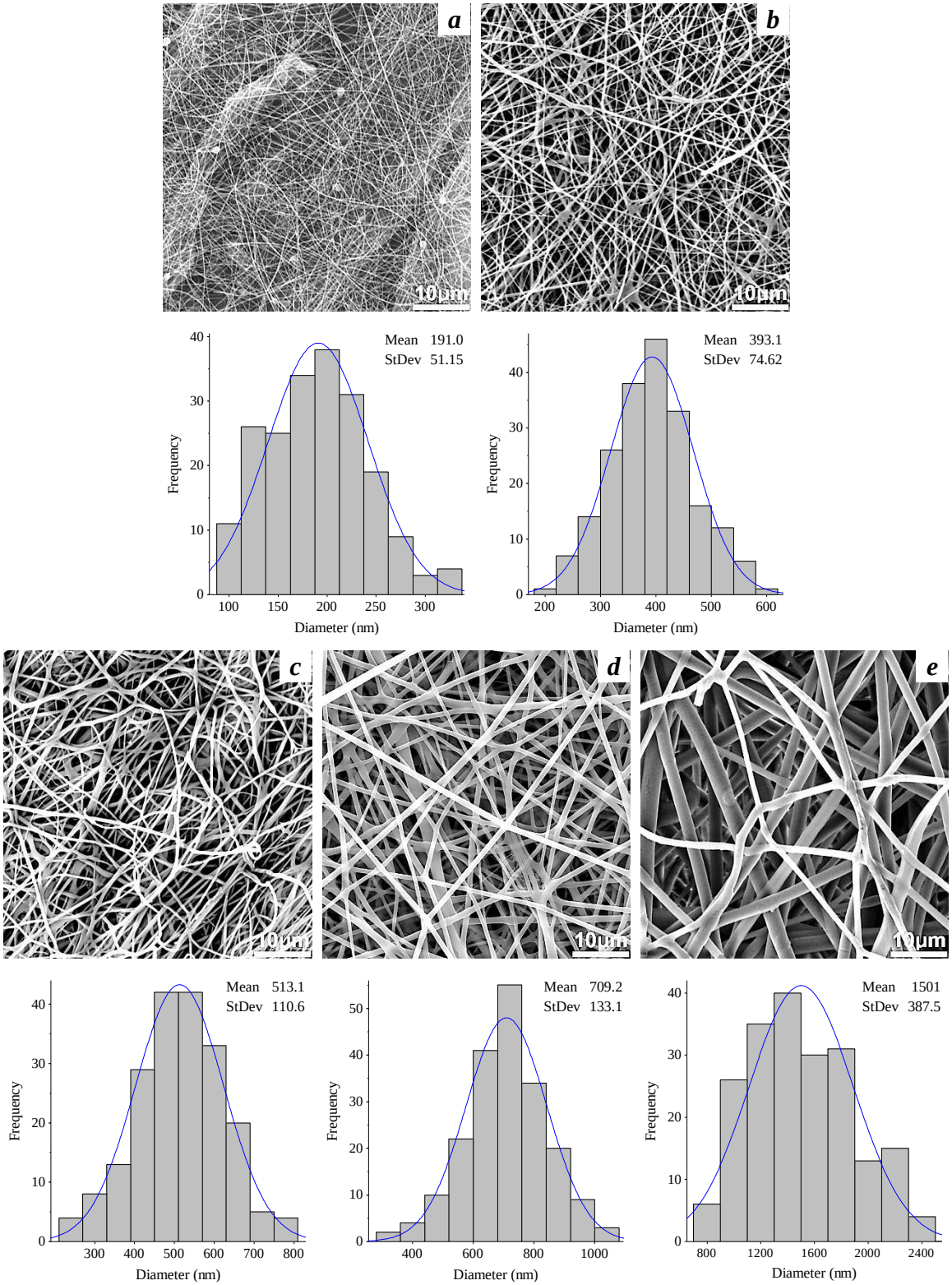

Figure 4.7 SEM micrographs and diameter distribution of electrospun fibres produced by needleless electrospinning with silk fibroin solution at various concentrations. (a) 6 wt%, (b) 8 wt%, (c) 10 wt%, (d) 12 wt%, (e) 14 wt% (magnification 5 kx).

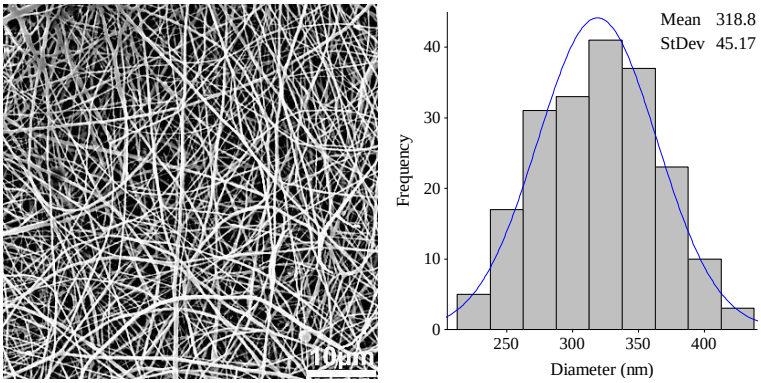

Figure 4.8 SEM micrograph and diameter distribution of electrospun fibres produced by needleless electrospinning with 12 wt% silk powder from the ternary solvent system (SEM magnification 5 kx).

In addition to affecting the fibre morphology and spinnability, the concentration of the spinning solution also influenced the spinning performance. Under the same processing parameters, with the increase in the silk fibroin concentration, the spinning performance increased constantly. The spinning performance of the electrospinning process increased from 0.224 g/min/m to 2.051 g/min/m when the concentration increased from 6 wt% to 14 wt%. The reason for the increased spinning performance of the process at the increased silk fibroin concentration was the high solution viscosity, which facilitated jet/filament formation.

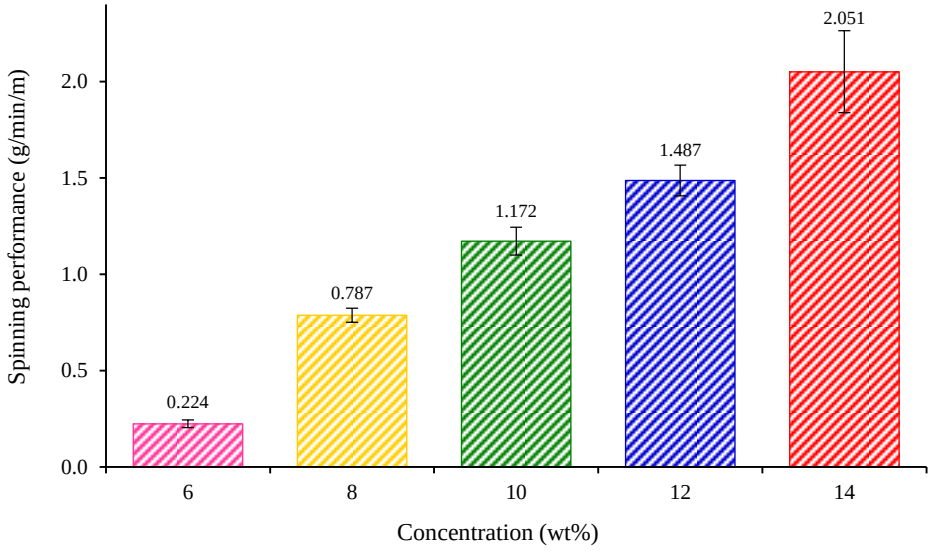

Figure 4.9 Effects of silk fibroin concentration on spinning performance of the process.

4.2.2 Effect of applied voltage

The applied voltage is a very important parameter with regard to the formation of jets in electrospinning systems because a high voltage is used to create an electrically charged jet of a polymer solution [10, 13]. For evaluating the effect of the applied voltage on the electrospinning process, silk fibroin solutions with the concentration 8, 10 and 12 wt% were electrospun at a voltage between 30 kV and 60 kV. SEM micrographs of the obtained fibre and their diameter distributions at the different applied voltages are shown in Figure 4.10, 4.11 and 4.12, respectively.

In this electrospinning system, when the silk fibroin solution was charged with an electric voltage higher than 26 kV, a number of jets were generated from the surface of the spinning electrode. The results show that increasing the applied voltage produced an effect on the fibre diameter, but the concentration of silk fibroin solution apparently has more effect on the fibre diameter than the applied voltage. With an increase in the applied voltage from 30 kV to 60 kV, the average fibre diameter was decreased from 487 nm to 393 nm for 8 wt% of silk solution, from 651 nm to 513 nm for 10 wt% of silk fibroin solution and from 940 nm to 710 nm for 12 wt% of silk fibroin solution, respectively.

However, the spinning performance of electrospinning process was influenced by the applied voltage and polymer concentration. The spinning performance of the process changed from 0.038 g/min/m to 0.787 g/min/m with silk fibroin concentration of 8 wt%, from 0.154 g/min/m to 1.194 g/min/m with silk fibroin concentration of 10 wt% and from 0.246 g/min/m to 1.487 g/min/m with silk fibroin concentration of 12 wt%, when the applied voltage was increased from 30 kV to 60 kV (Fig. 4.13 (b)).

As the electric field is the main driving force initiating the formation of Taylor cones and jets from the surface of the solution, increasing the electric voltage increases the electrostatic force on the polymer jet, which favours more elongation of the jet and the formation of smaller fibres. On the other hand, the electric field also functions to overcome the frictional forces that act within the moving polymer solution and to accelerate filament movement toward the collector electrode. It is easier to generate solution jets at higher applied voltage in a polymer solution charged by a stronger electric field because a larger amount of solution is removed from the surface of the solution, thereby improving the spinning performance of the process [7, 10, 12].

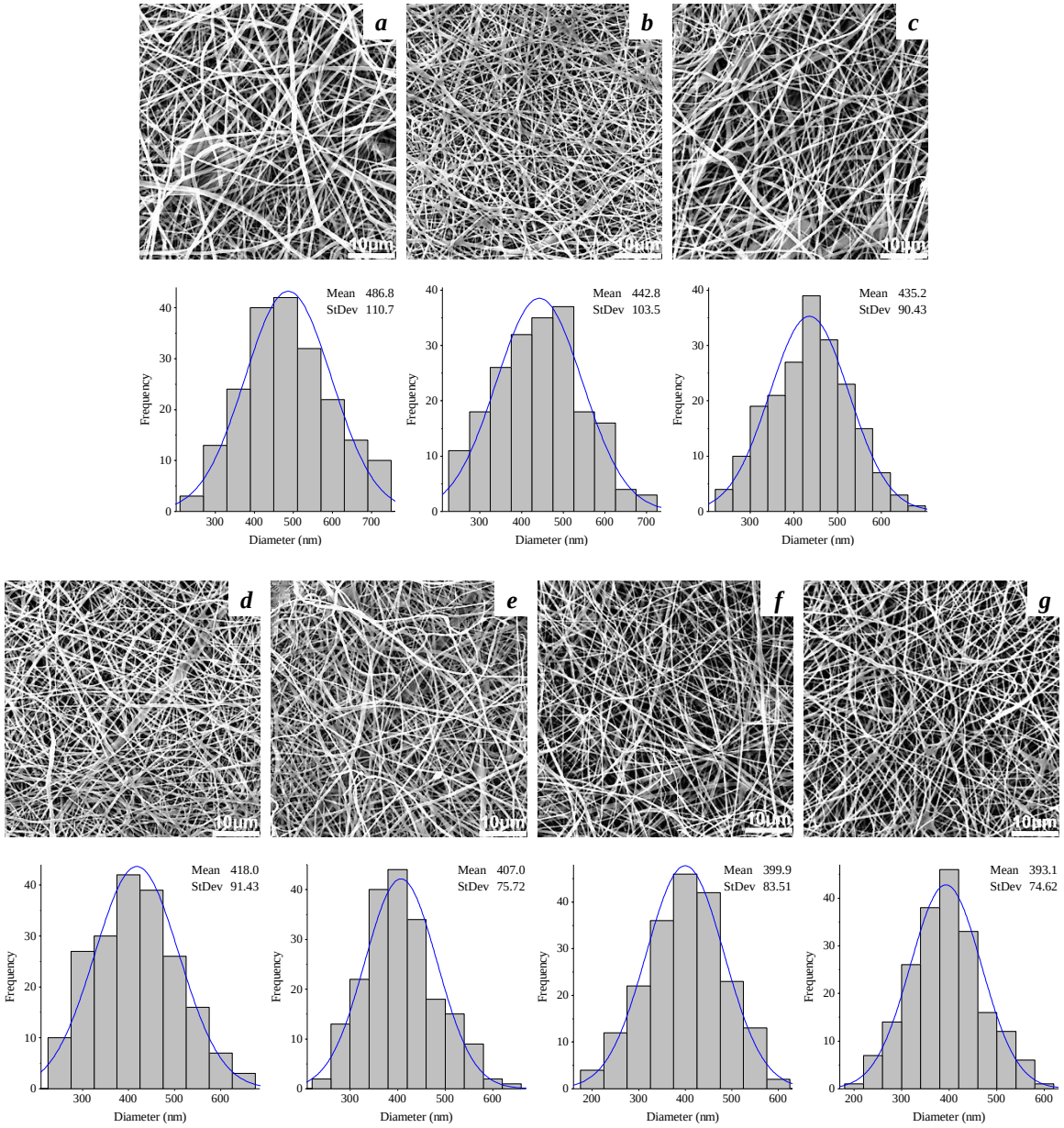

Figure 4.10 SEM micrographs and diameter distribution of electrospun fibres prepared by needleless electrospinning from silk fibroin 8 wt% at various applied voltage (a) 30 kV, (b) 35 kV, (c) 40 kV, (d) 45 kV, (e) 50 kV, (f) 55 kV, (g) 60 kV (SEM magnification 5 kx).

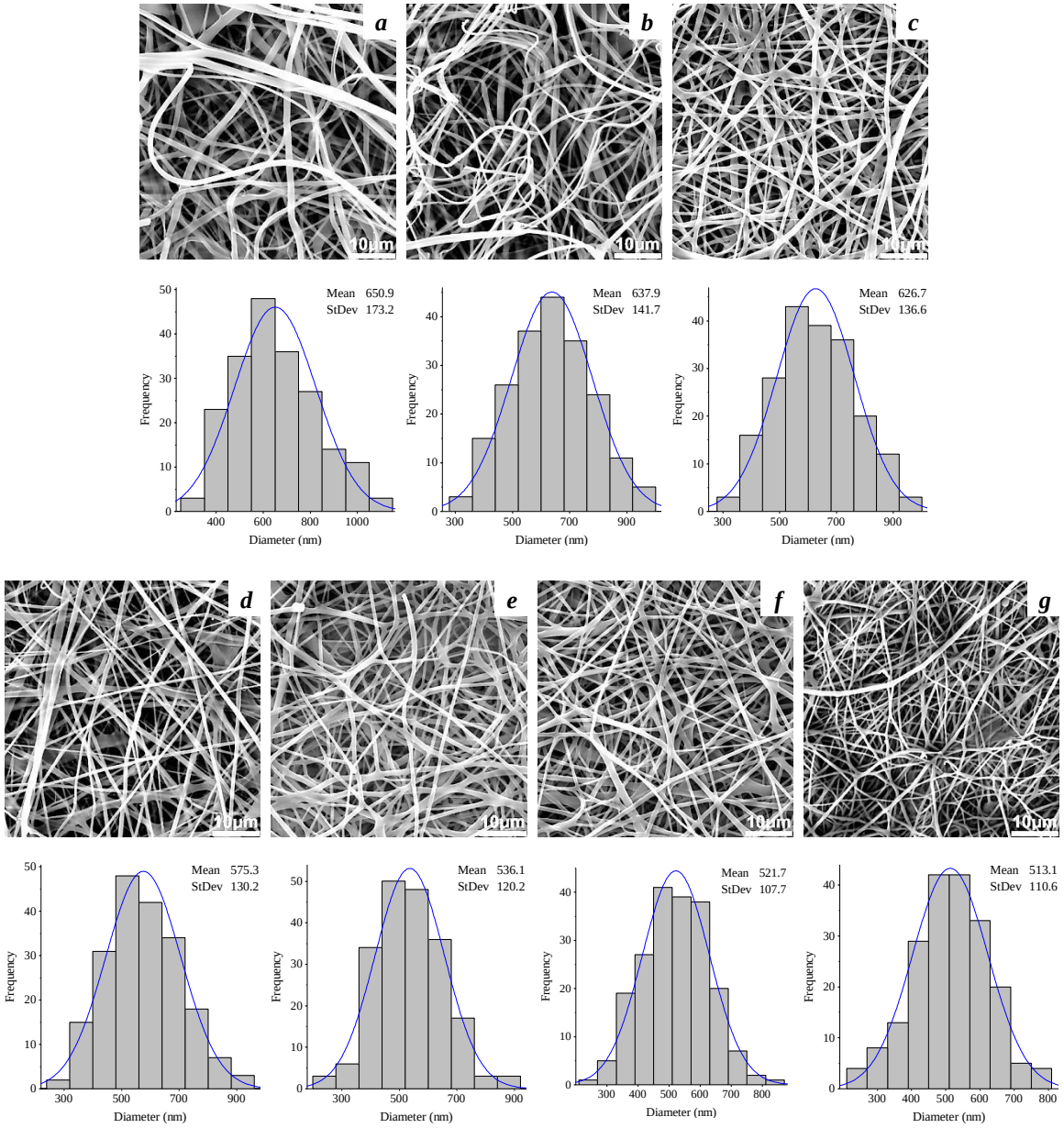

Figure 4.11 SEM micrographs and diameter distribution of electrospun fibres prepared by needleless electrospinning from silk fibroin 10 wt% at various applied voltage (a) 30 kV, (b) 35 kV, (c) 40 kV, (d) 45 kV, (e) 50 kV, (f) 55 kV and (g) 60 kV (SEM magnification 5 kx).

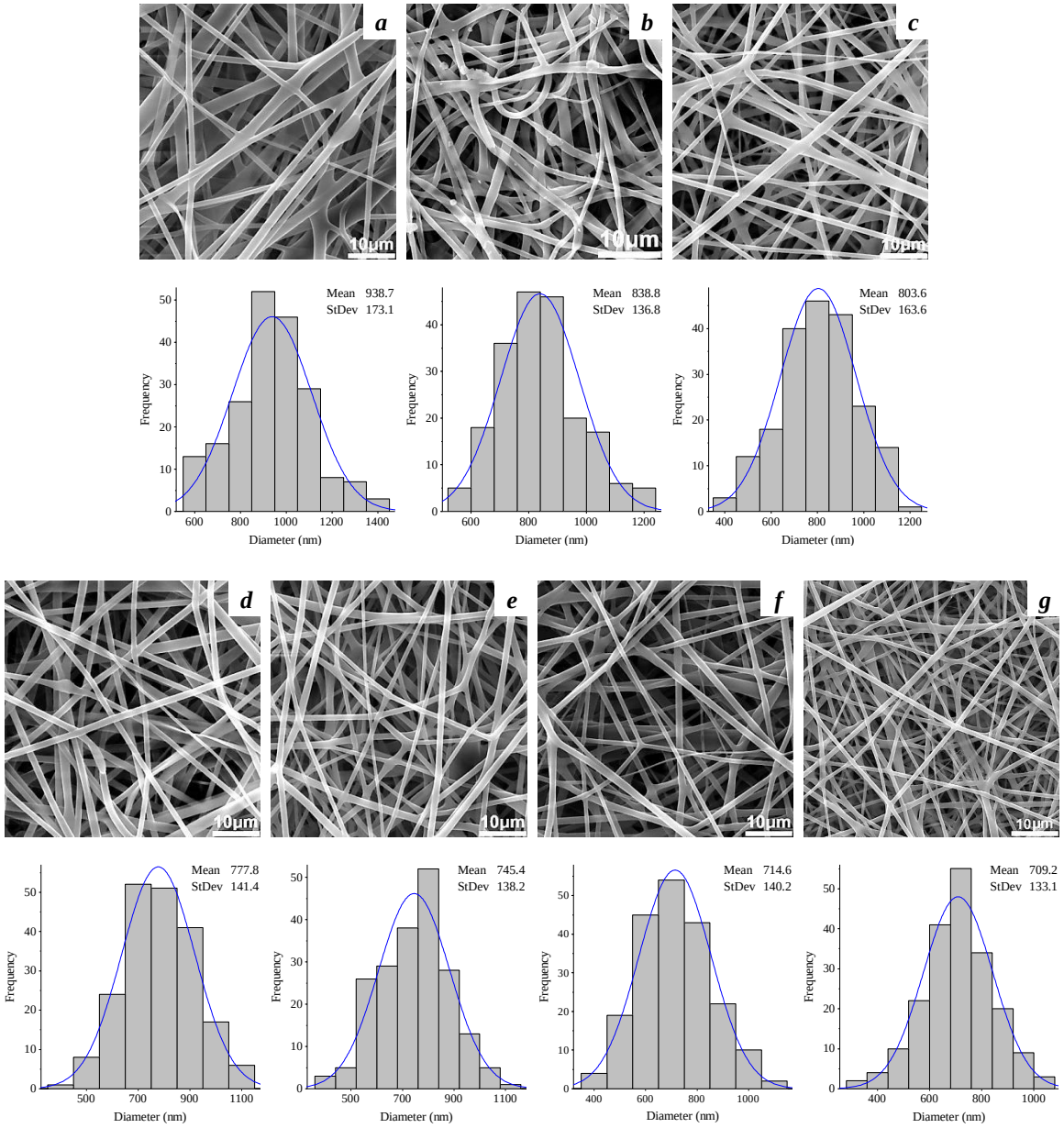

Figure 4.12 SEM micrographs and diameter distribution of electrospun fibres prepared by needleless electrospinning from silk fibroin 12 wt% at various applied voltage (a) 30 kV, (b) 35 kV, (c) 40 kV, (d) 45 kV, (e) 50 kV, (f) 55 kV and (g) 60 kV (SEM magnification 5 kx).

Table 4.2 Effect of applied voltage on average fibre diameter and spinning performances of the process.

Concentration (wt%)	Applied voltage (kV)	Fibre diameter (nm)		Spinning performance (g/min/m)	
		Average	StDev	Average	StDev
8	30	486.80	110.71	0.0379	0.0057
	35	442.75	103.54	0.0502	0.0054
	40	435.18	90.43	0.1096	0.0106
	45	417.98	91.43	0.2230	0.0215
	50	408.98	74.02	0.5037	0.0276
	55	399.86	83.51	0.7211	0.0416
	60	393.14	74.62	0.7874	0.0368
10	30	650.93	173.23	0.1542	0.0254
	35	637.86	141.65	0.2741	0.0214
	40	626.69	136.61	0.4595	0.0516
	45	575.26	130.24	0.7148	0.0772
	50	536.11	120.19	0.8309	0.0292
	55	521.68	107.71	0.9259	0.0584
	60	513.07	110.59	1.1940	0.1048
12	30	939.69	175.61	0.2463	0.0377
	35	838.81	136.82	0.4429	0.0397
	40	803.61	163.62	0.7232	0.0356
	45	777.84	141.37	0.9518	0.0457
	50	745.41	138.22	1.1510	0.0649
	55	714.57	140.24	1.3082	0.0585
	60	709.93	131.09	1.7176	0.0755

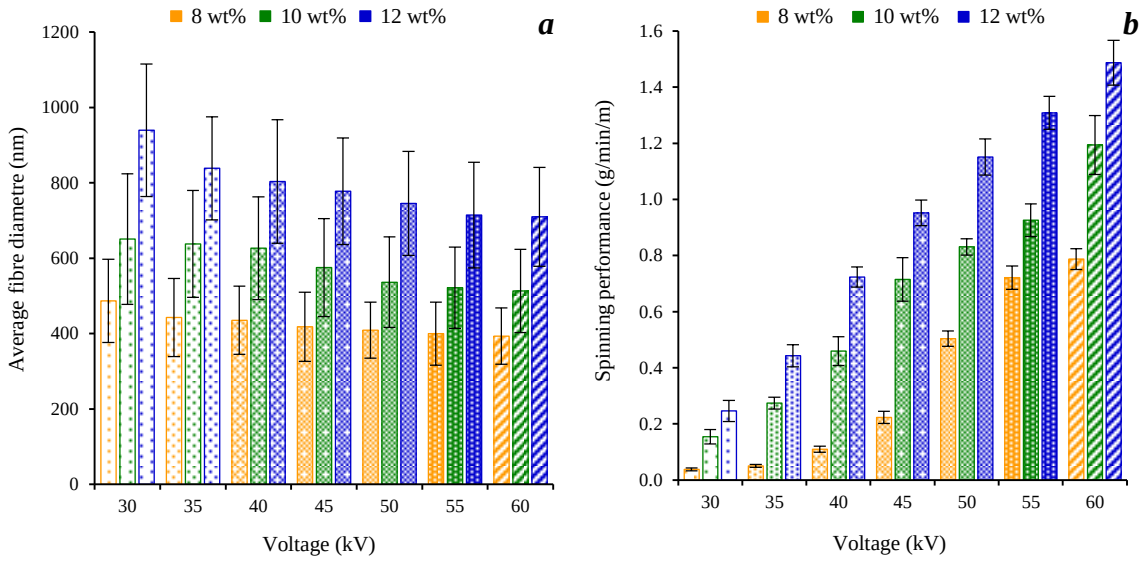

Figure 4.13 Effects of applied voltage on (a) average fibre diameter and (b) spinning performance of the process.

4.2.3 Effect of distance between electrodes

To study the effect of spinning distance on the morphology of the obtained electrospun fibres and the spinning performance of the process. Spinning solutions with a concentration of 8, 10 and 12 wt% were electrospun at a high voltage of 60 kV. Electrospinning was carried out at a distance of 100, 125 and 150 mm. SEM micrographs of the resulting fibres and their distributions at the different spinning distance are shown in Figures 4.14, 4.15 and 4.16, respectively.

The results show that an increase in a spinning distance had a less significant effect on the average fibre diameter but produces an influence on the spinning performance of electrospinning process. An increase in the distance from 100 mm to 150 mm, the average fibre diameter was decreased from 393 nm to 343 nm with silk fibroin concentration of 8 wt%, from 513 nm to 491 nm with silk fibroin concentration of 10 wt% and from 710 nm to 647 nm with silk fibroin concentration of 12 wt%. The performance of electrospinning process changed from 0.787 g/min/m to 0.295 g/min/m (about 38% reduction) with silk fibroin concentration of 8 wt%, from 1.172 g/min/m to 0.383 g/min/m with silk fibroin concentration of 10 wt% and from 1.487 g/min/m to 0.695 g/min/m with silk fibroin concentration of 12 wt% when the distance was increased (see Fig. 4.17).

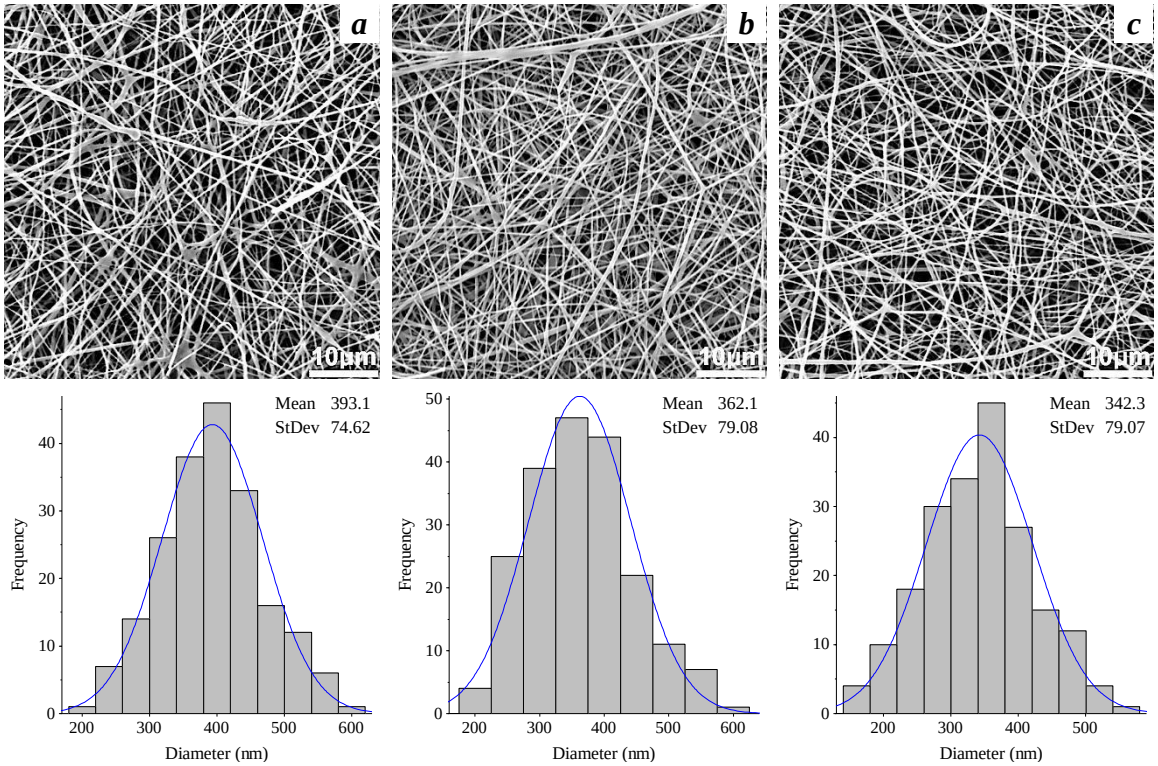

Figure 4.14 SEM micrographs and diameter distribution of electrospun fibres prepared by needleless electrospinning from silk fibroin 8 wt% at different spinning distance. (a) 100 mm; b) 125 mm; c) 150 mm (SEM magnification 5 kx).

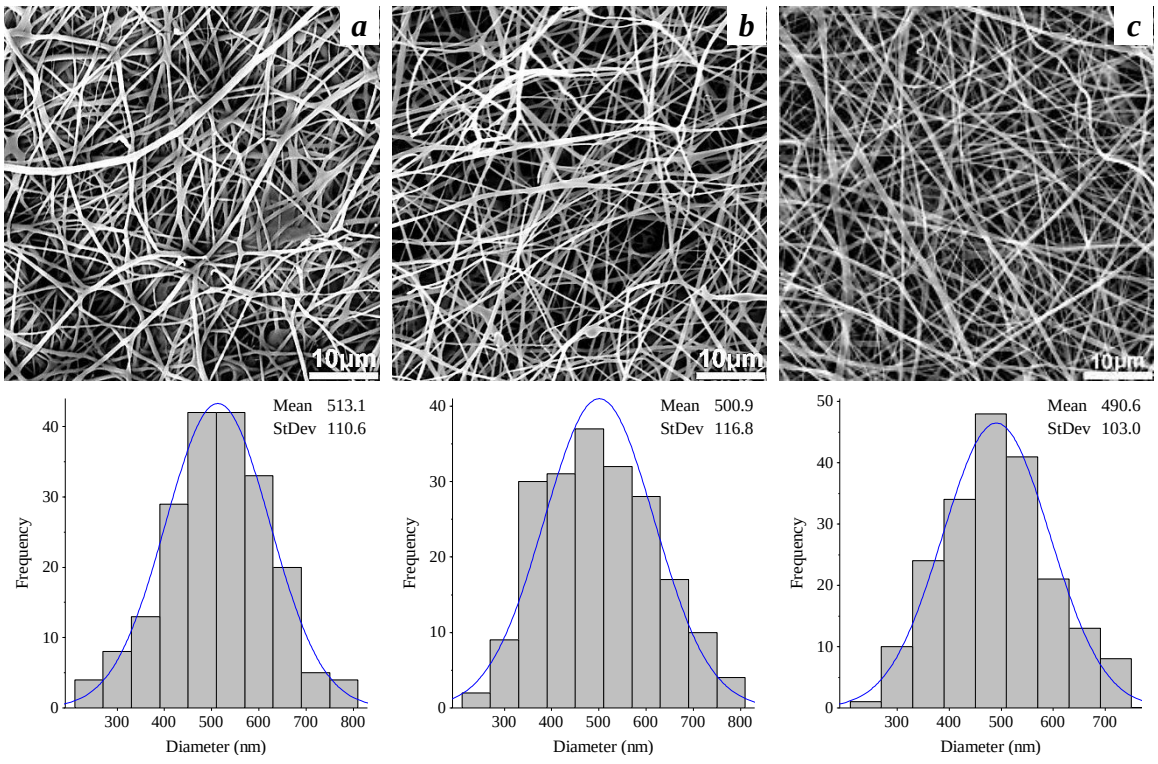

Figure 4.15 SEM micrographs and diameter distribution of electrospun fibres prepared by needleless electrospinning from silk fibroin 10 wt% at different spinning distance. (a) 100 mm; b) 125 mm; c) 150 mm (SEM magnification 5 kx).

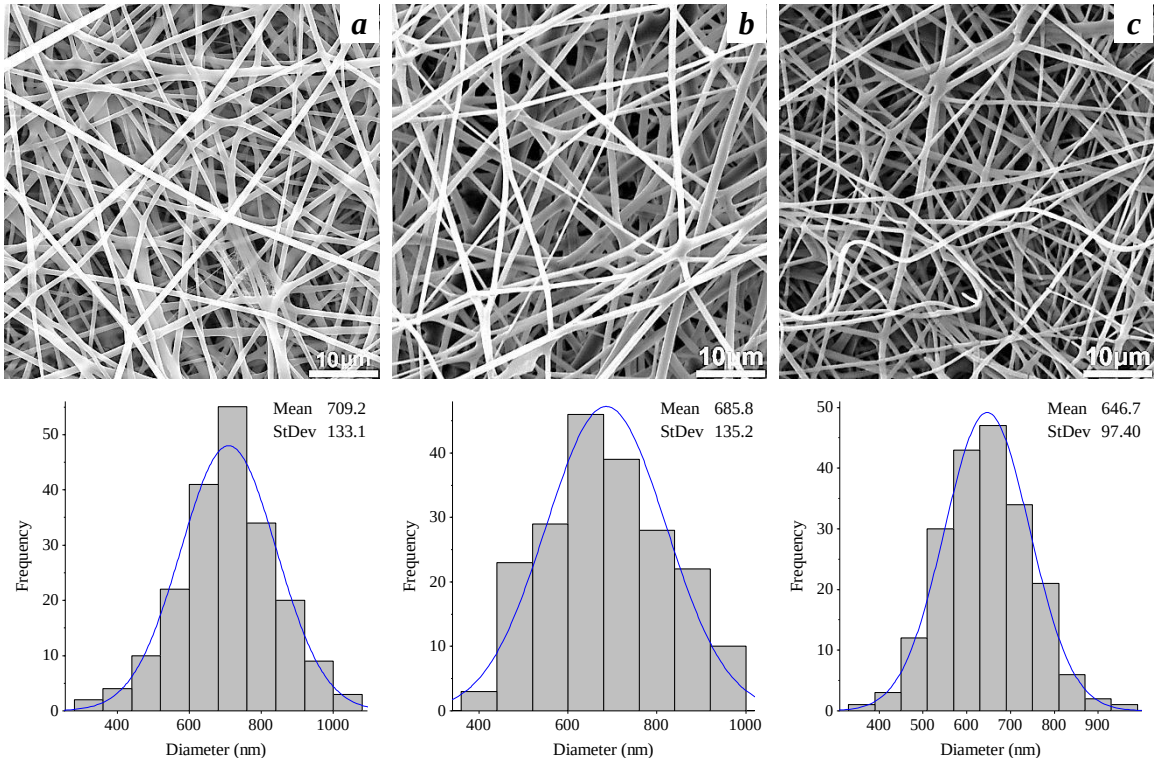

Figure 4.16 SEM micrographs and diameter distribution of electrospun fibres prepared by needleless electrospinning from silk fibroin 12 wt% at different spinning distance. (a) 100 mm; b) 125 mm; c) 150 mm (SEM magnification 5 kx).

The distance between the spinneret and the collector is a key factor in determining the morphology of fibres and the spinning performance that are produced. It is suggested that increasing the distance has the same effect as decreasing the applied voltage and this will cause a decrease in the field strength. Since the electric field is the main driving force to initiate the formation of jets from the surface of solution, decreasing the electric voltage will decrease the electrostatic force on the polymer jet, which results in a decrease of the spinning performance of process. In other circumstances, increasing the distance results in a decrease in the average fibre diameter. As mentioned earlier, jet elongation and thinning only happens while the jet is in flight and still a fluid. This elongation occurs owing to charge repulsion between ions in the solution combined with a net pull towards the collector. While in flight, the polymer solution solidifies as the solvent is evaporated from the surface, forming polymer fibres. Therefore, increasing the spinning distance will increase the time for thinning to occur and provided the polymer is not yet solid, the fibre diameter will be reduced [52].

Table 4.3 Effect of spinning distance on average fibre diameter and spinning performance of the process.

Concentration (wt%)	Distance (mm)	Fibre diameter (nm)		Spinning performance (g/min/m)	
		Average	StDev	Average	StDev
8	100	393.14	74.62	0.7874	0.0368
	125	362.08	79.08	0.5151	0.0250
	150	342.28	79.07	0.2950	0.0158
10	100	513.07	110.59	1.1719	0.0718
	125	500.85	116.82	0.6812	0.0543
	150	490.58	102.98	0.3832	0.0213
12	100	709.93	131.09	1.4870	0.0797
	125	685.83	135.19	1.0783	0.0750
	150	646.68	97.40	0.6953	0.0749

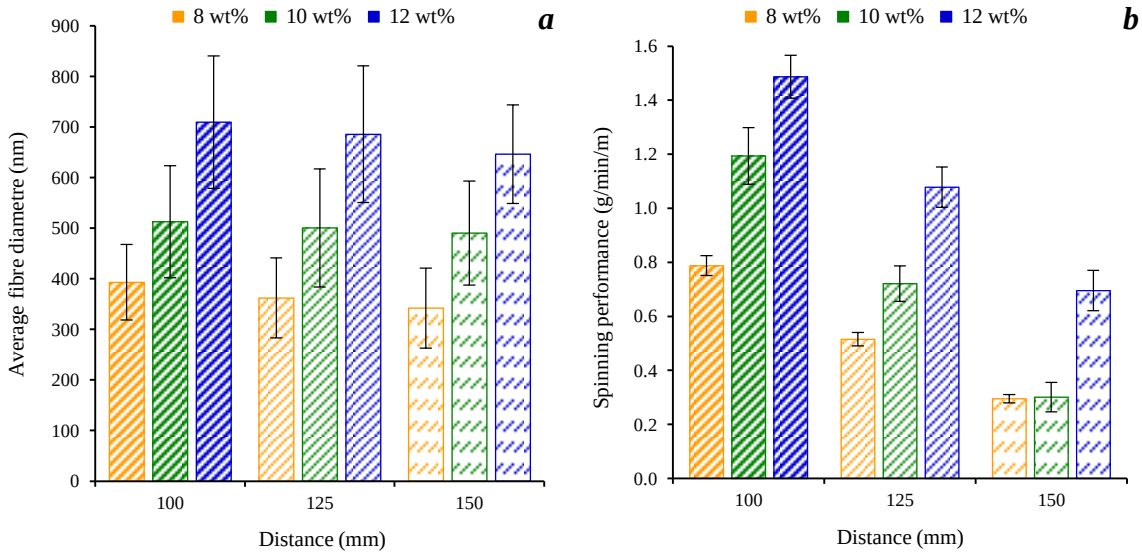

Figure 4.17 Effects of spinning distance on (a) average fibre diameter and (b) spinning performance of the process

4.3 Structure analysis of silk fibroin scaffolds

4.3.1 Secondary molecular structure of silk fibroin

The secondary structure of regenerated silk fibroin materials could be random coils (silk I) and β-sheet (silk II). Depending on processing conditions, one conformation could prevail over the others. As it is well known, prevalently amorphous silk fibroin materials (silk I) can be converted into more stable crystalline ones by physical or chemical treatments that are able to promote the crystallization by random coil to β-sheet conformational transition. The most common method used to change the secondary structure is the treatment with organic solvents like alcohols. Dipping a regenerated silk fibroin material into ethanol is highly effective in the crystallization of silk fibroin from a random coil conformation to a β-sheet conformation [58-59].

FTIR spectroscopy is a useful method to investigate the conformational changes of the secondary structure of silk fibroin. In order to examine the conformation of the electrospun fibre sheets, FTIR spectroscopy was performed on the electrospun and solvent treated fibre sheet. Figure 4.18 shows FTIR spectrum of (a) degummed silk fibres, (b) untreated silk electrospun fibres, (c) a fibre sheet after treatment with 100% ethanol and (d) a fibre sheet after treatment and soaking in distilled water for 2 days.

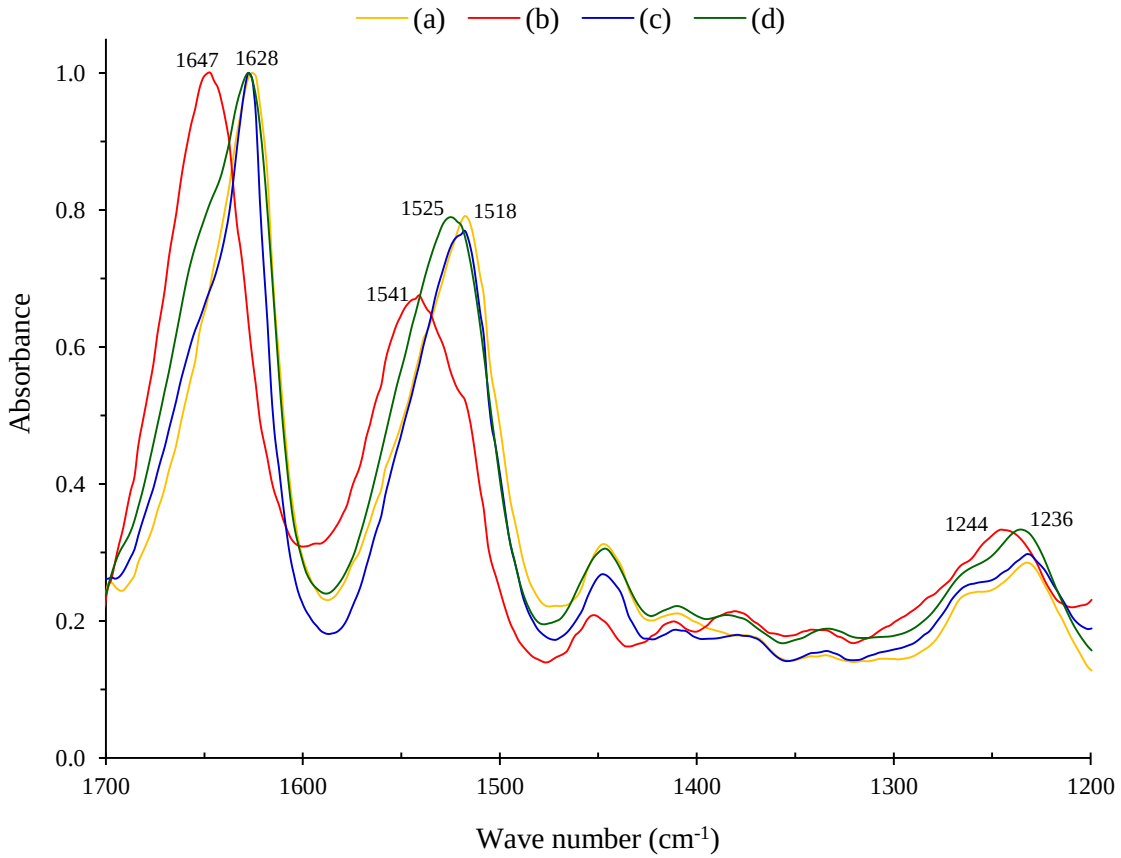

Figure 4.18 FTIR Spectra of degummed silk fibres and silk fibroin electrospun sheets.

Due to the presence of amide groups in silk protein, the IR spectral region within 1700-1200 cm^{-1} is assigned to the peptide backbone of amide I (C=O stretching, 1700-1600 cm^{-1}), amide II (N-H bending, 1600-1500 cm^{-1}) and amide III (C-N stretching,

1400-1200 cm^{-1}) absorption, which have been commonly used for the analysis of different secondary structures of silk fibroin. The β-sheet conformation of silk fibroin is characterized by absorption peaks around 1630-1625 cm^{-1} and 1520-1530 cm^{-1}. Random coil conformation is characterized absorption peaks around 1650-1645 cm^{-1} and 1540-1550 cm^{-1} [81].

The characteristic absorption bands of degummed silk fibres are found in the regions of 1628 cm^{-1} (amide I), 1518 cm^{-1} (amide II) and 1232 cm^{-1} (amide III), which are the characteristic absorption peaks of β-sheet conformation. The untreated electrospun fibre sheet was characterized by the absorption bands at 1647 cm^{-1} (amide I), 1541 cm^{-1} (amide II) and 1246 cm^{-1} (amide III), which can be attributed to the random coil conformation of electrospun silk fibroin. It is assumed that owning to the rapid evaporation of formic acid during the electrospinning process, there are not enough times for the crystallization of the silk fibroin chains. Because of the large molecular weight of silk fibroin, the conformation transition takes places on the minute scale. Therefore rapid evaporation of the solvent during the electrospinning leads to collection of the fibres with a random coil conformation [82].

As shown in Figure 4.18, FTIR spectra of the fibre sheet were shifted to 1628 cm^{-1} (amide I), 1518 cm^{-1} (amide II) and 1232 cm^{-1} (amide III) after treatment with 100 % ethanol, assigned to the β-sheet conformation of silk fibroin. This indicates that the post-treatment of silk electrospun fibre sheet with ethanol will change the structural conformation of the sheet from random coil conformation to β-sheet conformation, which increases the crystallinity and diminishes the water solubility of fibre sheet. It was hypothesized that the silk macromolecules could rearrange to change the crystal structures due to the changes in the hydrogen bonding caused by ethanol. The crystallization mechanism has been proposed that alcohols attract the water from silk fibroin molecules due to their polar character and this promotes the aggregation of hydrophobic amino acids such as alanine and glycine. Since these amino acids are the main components of crystalline regions, the alcohols may induce the β-sheet crystallization of silk fibroin, so-called solvent-induced crystallization [34, 82].

In addition, the spectra of the treated fibre sheet after immersed in distilled water for 2 days also shows absorption bands [1628 cm^{-1} (amide I), 1525 cm^{-1} (amide II) and 1236 cm^{-1} (amide III)] at same wavelengths as degummed silk fibres. No significant spectral changes were observed, indicating that a conformation of the treated fibre sheet remains unchanged after treated with distilled water.

4.3.2 Morphology of silk fibroin electrospun fibres after post-treatment

SEM micrographs of silk fibroin electrospun fibres after post-treatment with ethanol at various concentrations are shown in Figures 4.19. Compared with a non-treated electrospun fibres, morphologies of all treated fibre sheets were significantly changed. The diameters of treated electrospun fibres increased in comparison with non-treated relevant electrospun fibres (see Fig 4.19 and Fig 4.20). This was probably due to the swelling of the silk fibroin electrospun fibres by ethanol during treatment.

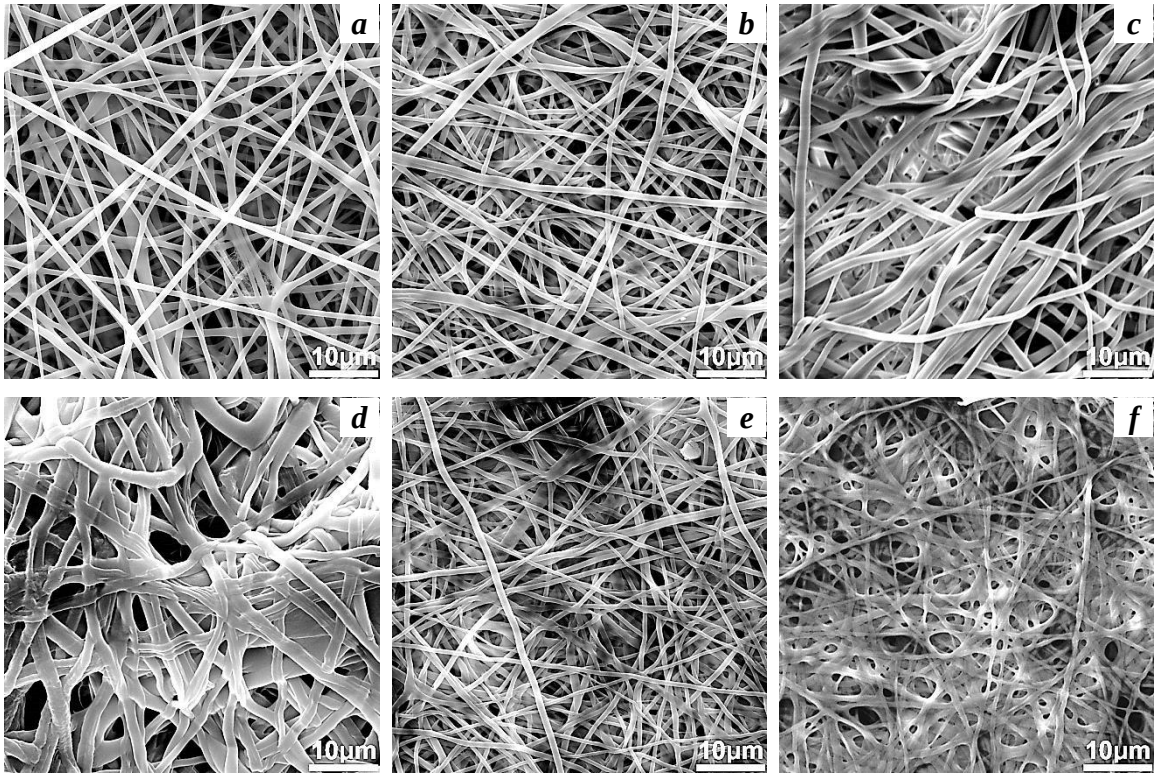

Figure 4.19 SEM micrographs of silk fibroin electrospun fibres (a) non-treated fibres, (b) electrospun fibres after treatment with 100% ethanol, (c) electrospun fibres after treatment with 80% ethanol, (d) electrospun fibres after treatment with 60% ethanol, (e) electrospun fibres after treatment with 100% ethanol and soaking in distilled water for 2 days, (f) non-treated fibres after soaked in water, (SEM magnification 5 kx).

The diameters of silk fibroin electrospun fibres after treatment with 100% ethanol and 80% ethanol aqueous solution were slightly increased. On the other hand, the diameters of electrospun fibres after treatment with 60% ethanol aqueous solution experienced greater change and most of the fibres were swollen and connected to each other. In fact, a presence of water (in ethanol solution) is thought to favor swelling of the electrospun fibre and penetration of ethanol, leading to β-sheet crystallization on drying. However, when the water content is too high, the water molecules bind to the hydrophilic groups in the silk fibroin chains and partially dissolve the silk fibroin fibre in water [84-84].

Furthermore, the spectra of the fibre sheets after treatment with 80% and 60% ethanol aqueous solution also show absorption bands at same wavelengths [1628 cm^{-1} (amide I), 1518 cm^{-1} (amide II) and 1232 cm^{-1} (amide III)] as degummed silk fibres and the electrospun fibres after post-treatment with 100% ethanol (Fig 4.21). No significant spectral changes were observed. In addition, the non-treated electrospun fibres sheet was found to shrink and dissolve after being soaked in deionized water. As shown in Figure 4.19 (f), the nanofibres were obviously swollen and bonded with each other. However, the treated nanofibrous scaffolds after being soaked in deionized water for 2 days still maintained good morphologies (Fig 4.19 (e)).

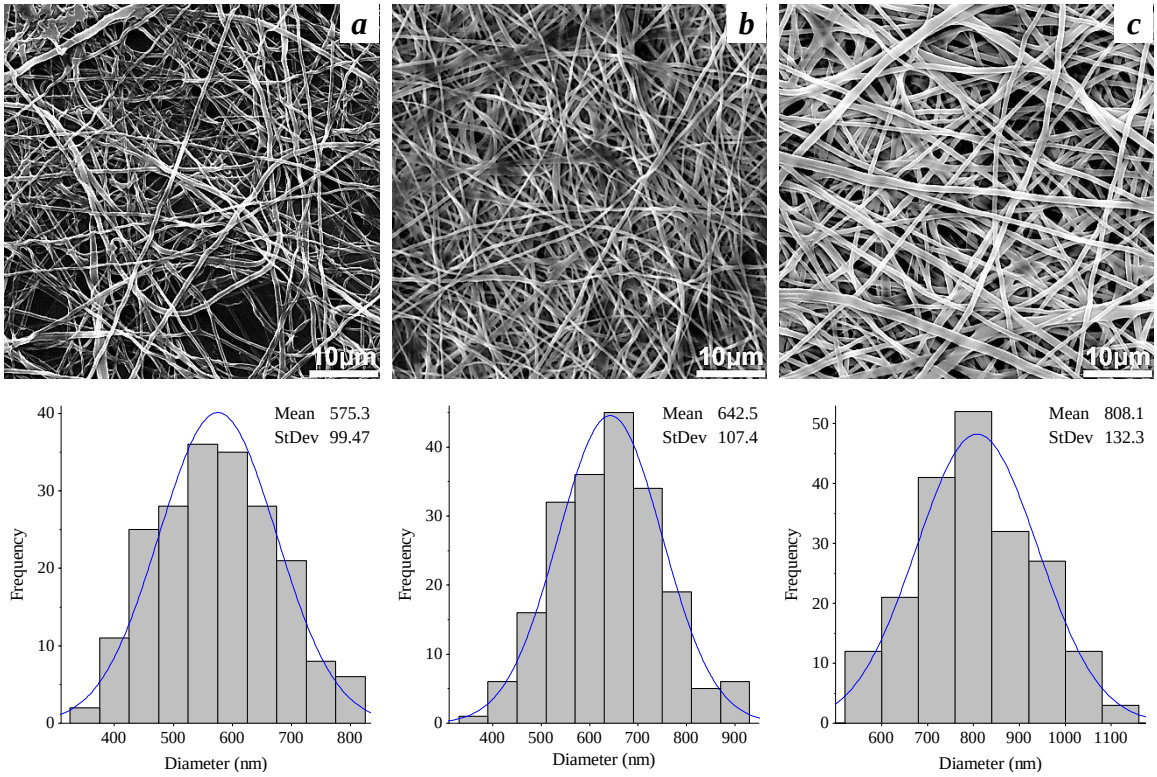

Figure 4.20 SEM micrographs and diameter distribution of silk fibroin electrospun fibres after treatment with 100% ethanol. (a) 8 wt%; (b) 10 wt%; (c) 12 wt%. (SEM magnification 5 kx).

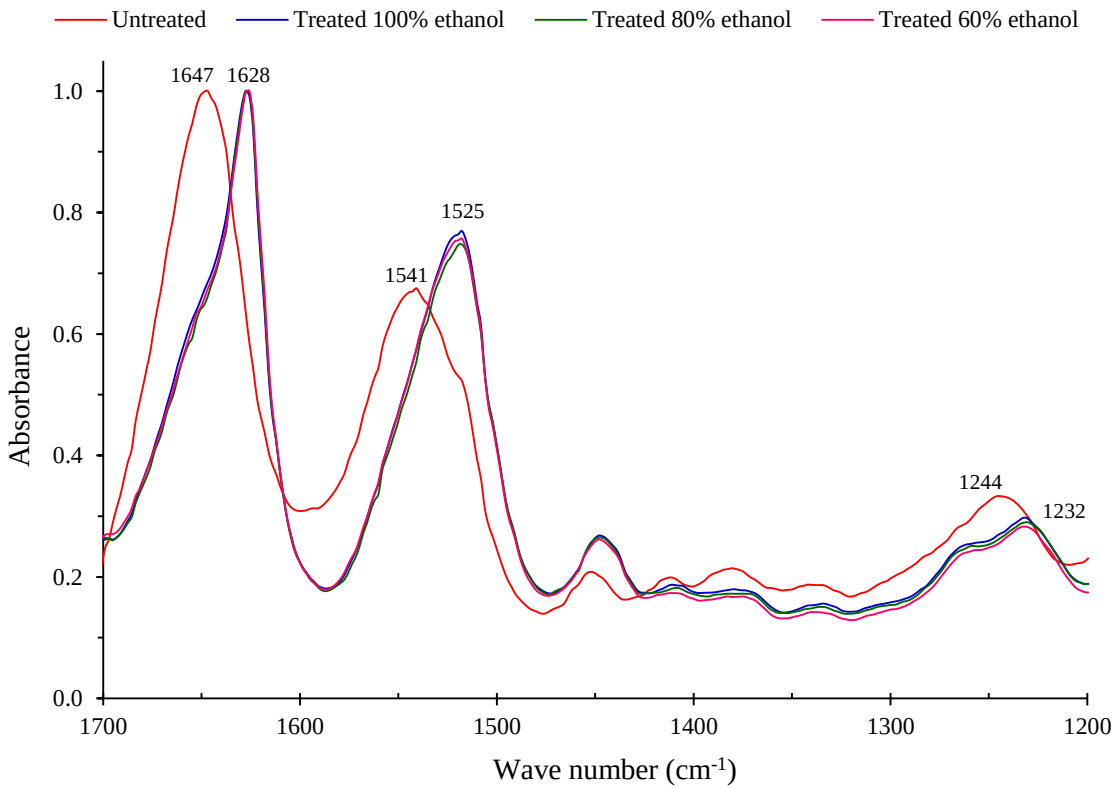

Figure 4.21 FTIR Spectra of silk fibroin electrospun sheets after treatment with ethanol at various concentrations.

4.4 Effect of polycaprolactone on the needleless electrospinning of silk fibroin

4.4.1 Effect of blend ratio of silk fibroin and polycaprolactone on properties of the spinning solution

The properties of silk fibroin/polycaprolactone blend solution including conductivity, surface tension and viscosity at various weight ratios are shown in Figures 4.22, 4.23 4.24 and 4.25, respectively. The results show that the variation of weight ratio of polycaprolactone in the blend solution had a significant effect on properties of the blend solutions.

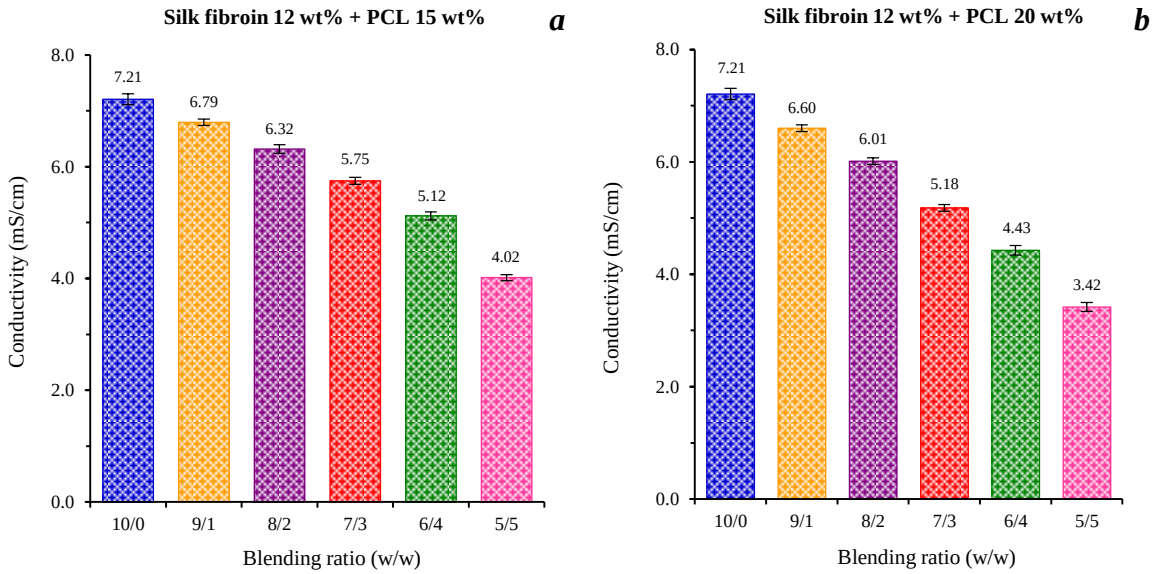

Figure 4.22 Effect of blend ratio of silk fibroin and polycaprolactone on conductivity [blending ratio 10/0 (w/w) means pure silk fibroin solution].

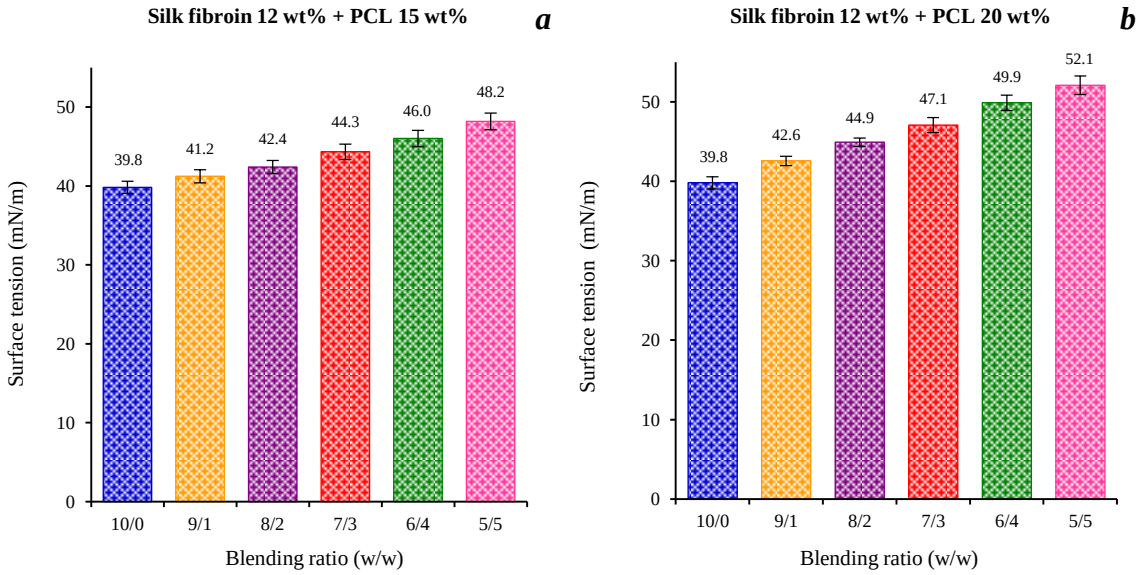

Figure 4.23 Effect of blend ratio of silk fibroin and polycaprolactone on surface tension [blending ratio 10/0 (w/w) means pure silk fibroin solution].

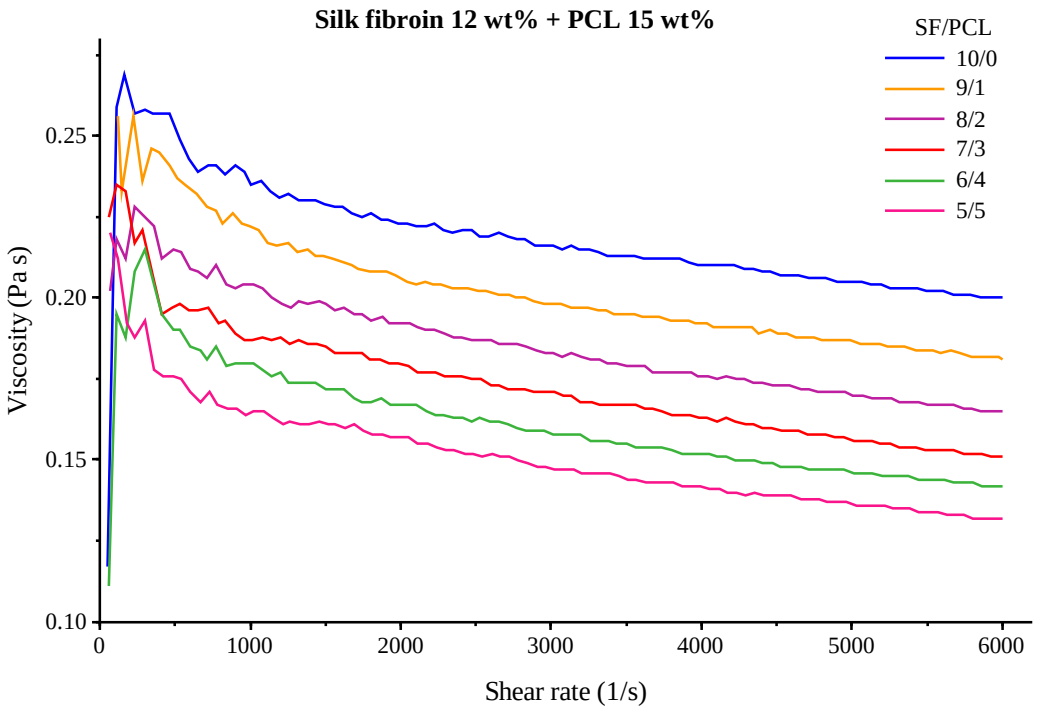

Figure 4.24 Rheological behaviour of silk fibroin (12 wt%) and polycaprolactone (15 wt%) blend solutions at various weight ratios

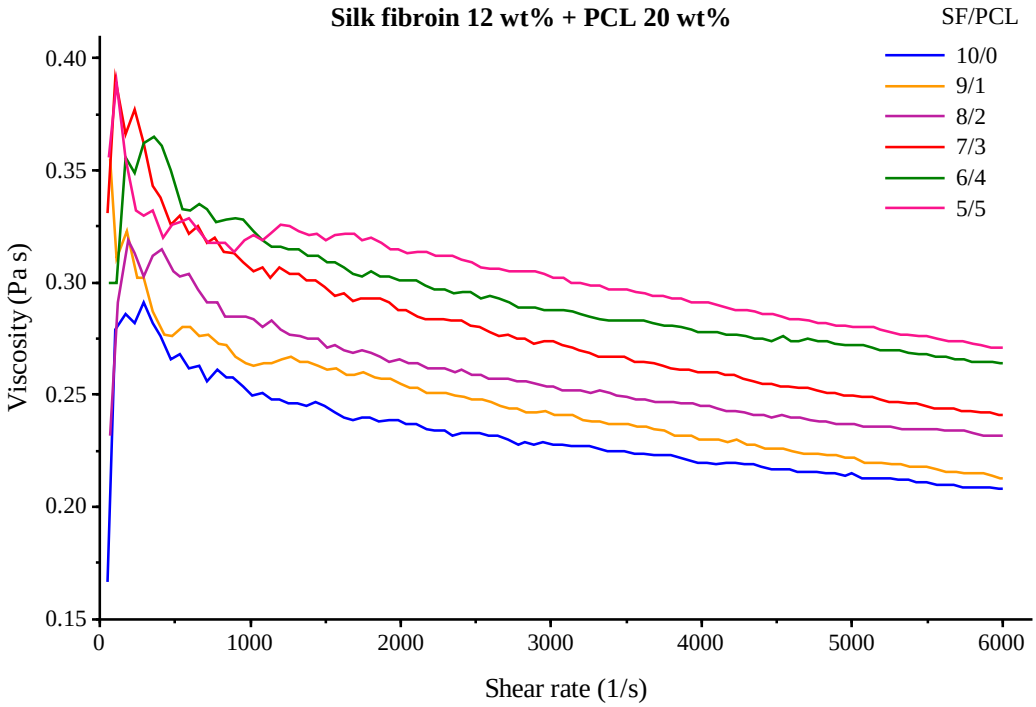

Figure 4.25 Rheological behaviour of silk fibroin (12 wt%) and polycaprolactone (20 wt%) blend solutions at various weight ratios

When silk fibroin solution blends with a solution of 15 wt% polycaprolactone, it is obviously clear that conductivity and viscosity of the blended solution decreased with increasing weight ratio of polycaprolactone, while surface tension of the blended solution was increased. On the other hand, when silk fibroin solution blends

with 20 wt% polycaprolactone solution, conductivity of the blended solutions decreased with increasing polycaprolactone content, while surface tension and viscosity of the solution was increased. It seems that conductivity and surface tension of the blended solutions are affected by a variation of polycaprolactone content in the solution, while viscosity of the blended solutions is depending on the concentration of polycaprolactone solution.

In an electrospinning process, spinning parameters of the process were the same for all the solution. It can assume that conductivity and surface tension of the blended solutions are responsible for significant differences in a fibre morphology and a spinning performance of the process.

4.4.2 Morphology of silk fibroin/polycaprolactone blend electrospun fibres

SEM micrographs and diameter distribution of the electrospun fibre composed of silk fibroin and polycaprolactone at various weight ratios and different concentration of polycaprolactone solution are shown in Figures 4.26 and 4.27, respectively. The results show that under the same concentration of silk solution and electrospinning conditions, the fibre diameter and diameter distribution of the obtained electrospun fibres decreased with both concentration of polycaprolactone in accordance with an increase in the weight ratio of polycaprolactone in a spinning solution. However, the diameters of the electrospun fibres obtained from the 15 wt% polycaprolactone solution were smaller than those obtained from the 20 wt% polycaprolactone solution. This is probably due to the viscosity of 20 wt% polycaprolactone solution is higher than 15 wt% polycaprolactone solution. Thus, at higher viscosity, the diameter of the blend electrospun fibre is greater.

When the weight ratio of blend solution increased from 9/1 to 5/5, the average fibre diameter decreased from 691 nm to 340 nm, respectively, in the polycaprolactone 15 wt% and from 701 nm to 383 nm, respectively, in the polycaprolactone 20 wt%. In particular, pure silk fibroin electrospun fibres had larger diameters and showed greater variation in fibre diameter when compared to silk fibroin/polycaprolactone electrospun fibres, which is attributed to differences in properties of spinning solution. This was presumably due to the dielectric constant of the polycaprolactone solution in this solvent system. Generally, the dielectric constant of a solvent has a significant influence on electrospinning; a solution with a greater dielectric property reduces the diameter of the resultant electrospun fibre and improves uniformity. The bending instability of the electrospinning jet also increases with higher dielectric constant. This may also facilitate the reduction of the fibre diameter due to the increased jet path [53]. In addition, Luo at el [85] described the influence of dielectric constant of solvent systems on an electrospinning of polycaprolactone solutions. They observed that the dielectric constant of the solvent showed a dominant influence on the diameters of the polycaprolactone electrospun fibres. When dissolved polycaprolactone in the solvent with dielectric constants was ~19 and above (at 20 ^{O}C), diameters of polycaprolactone electrospun fibre in the nanometer range were achieved [85] (see Fig. 4.28).

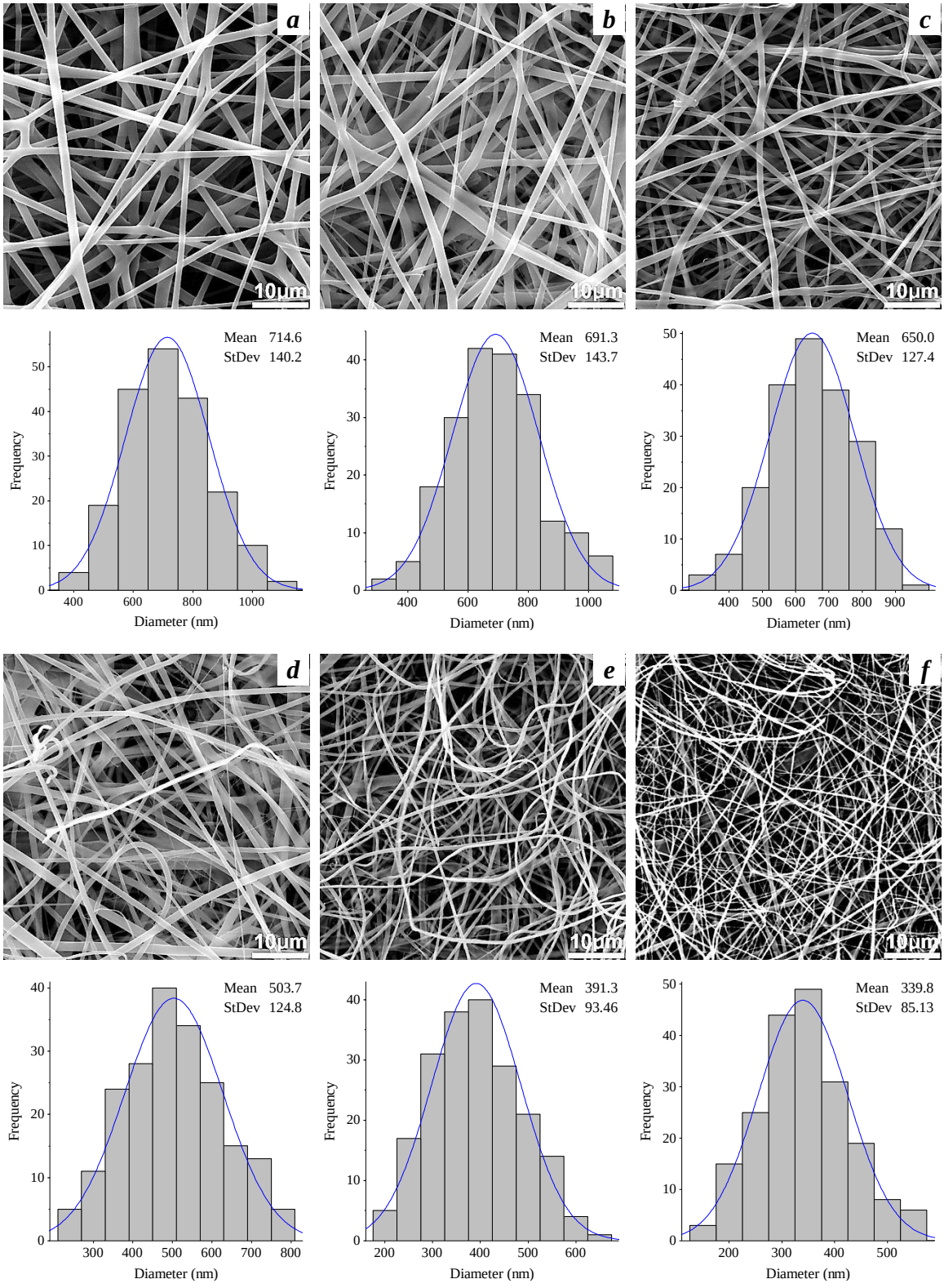

Figure 4.26 SEM micrographs and diameter distribution of electrospun fibres produced by needleless electrospinning with SF 12 wt% and PCL 15 wt% at various weight ratios. a) 10/0, b) 9/1, c) 8/2, d) 7/3, e) 6/4, f) 5/5, (SEM magnification 5 kx).

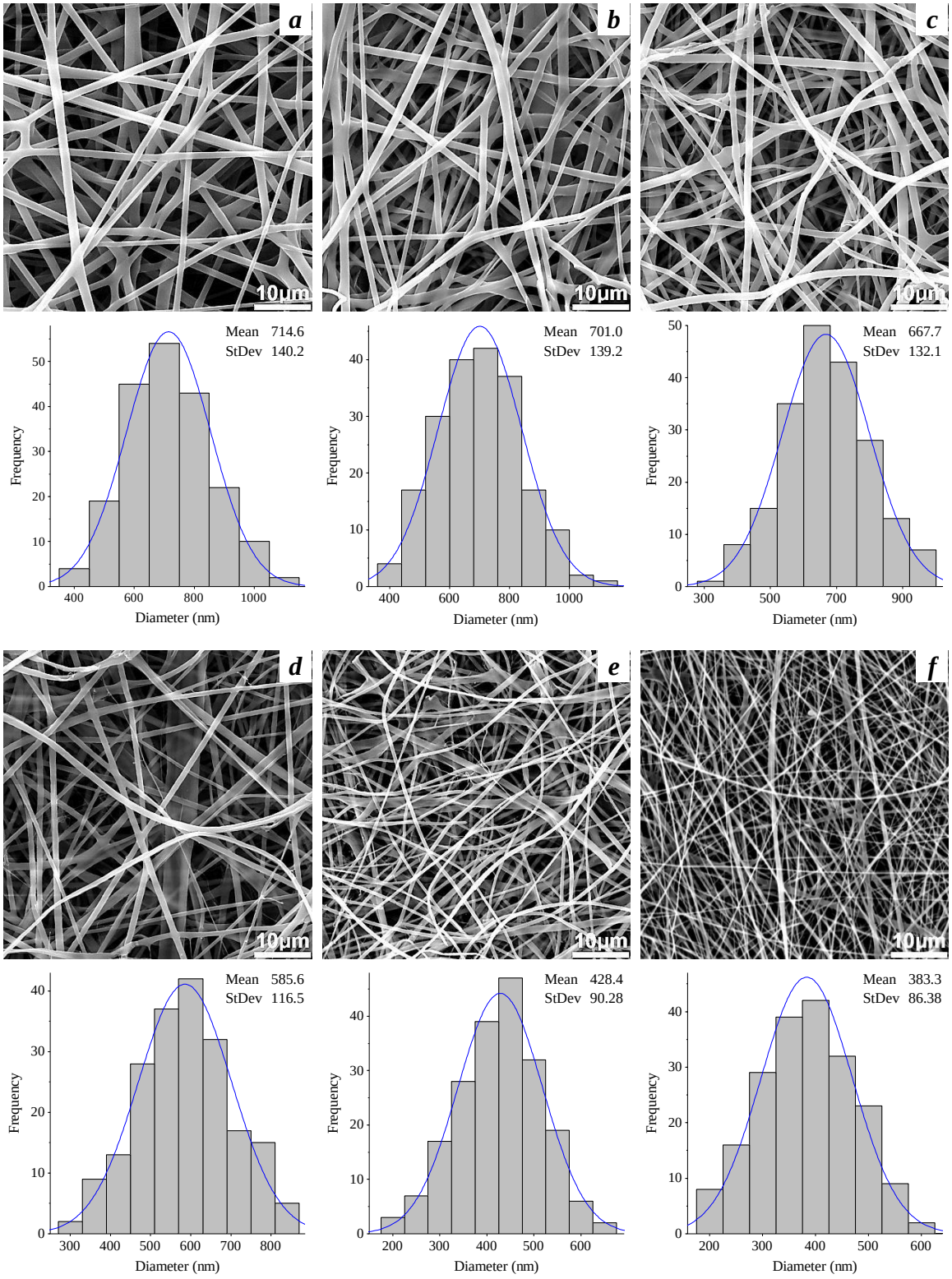

Figure 4.27 SEM micrographs and diameter distribution of electrospun fibres produced by needleless electrospinning with SF 12 wt% and PCL 20 wt% at various weight ratios. a) 10/0, b) 9/1, c) 8/2, d) 7/3, e) 6/4, f) 5/5, (SEM magnification 5 kx)

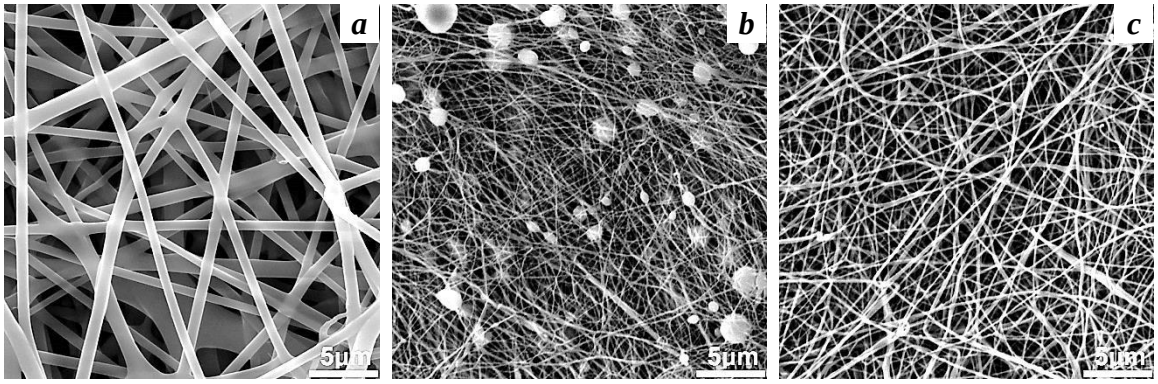

Figure 4.28 SEM micrographs of electrospun fibres produced by (a) silk fibroin 12 wt%, (b) PCL 15 wt% in formic acid and (c) PCL 20 wt% in formic acid (SEM magnification 10 kx).

In these experiments, polycaprolactone was dissolved in formic acid, a solvent with high dielectric constant (ε ~58 at 20 ^{O}C), also resulted in a reduction in electrospun fibre diameter. Therefore, when silk fibroin solution was blended with polycaprolactone solution in this solvent system, the blended solution will has a greater dielectric constant than pure silk fibroin solution (it can assume that pure silk fibroin solution has a lower dielectric constant than polycaprolactone solution due to a presence of calcium chloride in silk fibroin solution). As a result, the fibre diameter of blend nanofibres tends to decrease as the polycaprolactone content in the blend solution increases.

In addition to affecting the diameter of electrospun fibres, the weight ratio of polycaprolactone in the blend solution also influenced the spinning performance. Under the same processing parameters, with the increase in the weight ratio of polycaprolactone in the blend solution, the spinning performance decreased (Fig. 4.29 and Fig. 4.30). When the weight ratio of polycaprolactone in the blend solution increased from 9/1 to 5/5, the spinning performance decreased from 1.104 g/min/m to 0.552 g/min/m, respectively, in the 15 wt% polycaprolactone solution and from 1.009 g/min/m to 0.500 g/min/m, respectively, in the 20 wt% polycaprolactone solution. From the results, it is possible that the addition of polycaprolactone cause an increase in surface tension and a reduction in conductivity of the blended solution. Electrospinning involves stretching of the solution caused by repulsion of the charges at its surface. A reduction in conductivity tends to decrease the charge density at the surface of the jets, which it results in a lower bending instability. As a result, the deposition area of the electrospun fibres is decreased and will also decrease the throughput of electrospinning process [39].

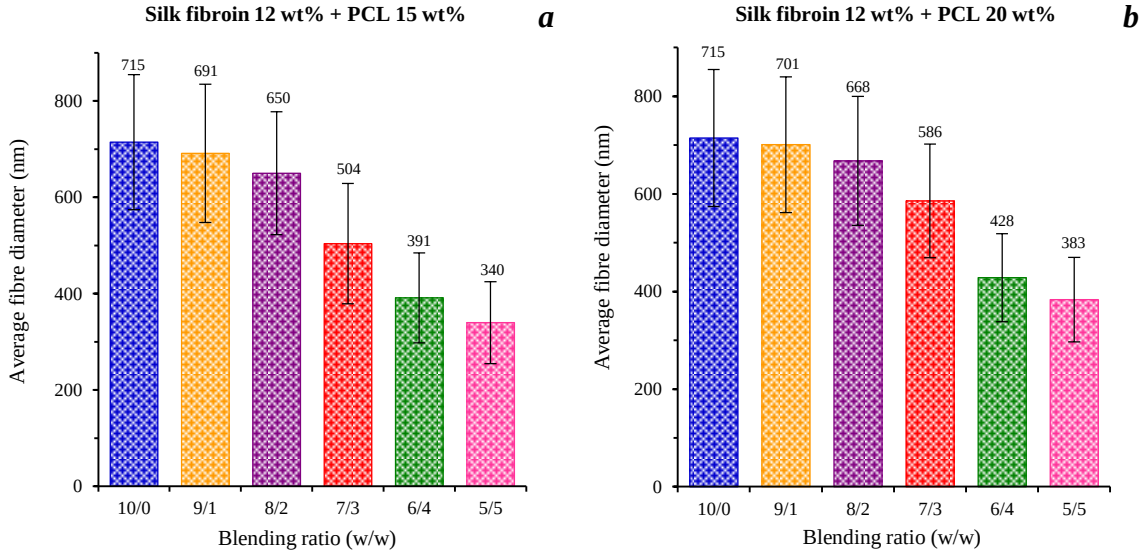

Figure 4.29 Effect of blend ratio of silk fibroin and polycaprolactone on average fibre diameter [blending ratio 10/0 (w/w) means pure silk fibroin solution].

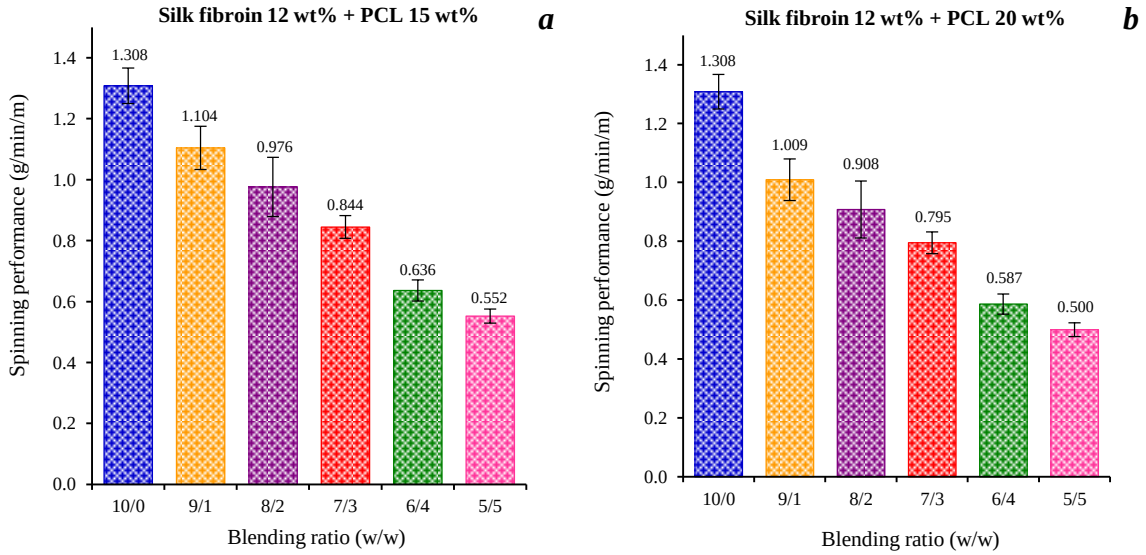

Figure 4.30 Effect of blend ratio of silk fibroin and polycaprolactone on spinning performance of the process [blending ratio 10/0 (w/w) means pure silk fibroin solution].

4.4.3 Effect of blend ratio of silk fibroin and polycaprolactone on physical properties of the blend elctrospun fibres

- Tensile properties

Tensile properties of silk fibroin and silk fibroin/polycaprolactone blend fibre sheets were measured summarized in Table 4.4. From the results, silk fibroin electrospun fibre sheet showed poor tensile properties (typical brittle fracture), the average elongation at break was 5.49 %, and the average tensile strength was 5.5 N. In the case of silk fibroin/polycaprolactone blend fibre sheets, the tensile properties were significantly different, depending on the blend ratios of silk fibroin and polycaprolactone in the blend solution. Considered the effect of the blend ratios on tensile properties of the blend fibre sheets, when the weight ratio of blend solutions (SF/PCL) changed from 9/1 to 5/5, the average elongation at break increased from 7.29% to 19.51%, respectively, in the polycaprolactone 15 wt% and from 8.61% to 22.92%, respectively, in the polycaprolactone 20 wt%. This indicated that the elasticity of silk fibroin electrospun fibres sheet was improved by blending with polycaprolactone. In addition, the increase in the elongation at break of the blend fibre sheets was less significant when the concentration of the polycaprolactone solution increased

Table 4.4 Tensile properties of SF/PCL blend fibre sheets at various blend weight ratios

PCL (wt%)	SF/PCL (w/w)	Force (N)		Elongation (%)		Stress (MPa)	
		Average	StDev	Average	StDev	Average	StDev
15	10/0	5.53	0.31	5.49	0.90	4.60	0.26
	9/1	4.63	0.36	7.29	1.02	4.63	0.36
	8/2	4.27	0.11	8.31	1.04	4.75	0.12
	7/3	3.78	0.23	10.61	1.16	4.84	0.30
	6/4	3.10	0.28	14.12	1.07	5.17	0.47
	5/5	2.51	0.20	19.51	1.59	5.23	0.42
20	10/0	5.53	0.31	5.49	0.90	4.60	0.26
	9/1	5.19	0.22	8.61	1.50	4.72	0.20
	8/2	4.97	0.22	9.58	1.11	4.97	0.22
	7/3	4.34	0.15	11.21	0.91	5.11	0.17
	6/4	3.69	0.21	17.31	1.41	5.26	0.29
	5/5	2.60	0.15	22.92	1.12	5.31	0.31

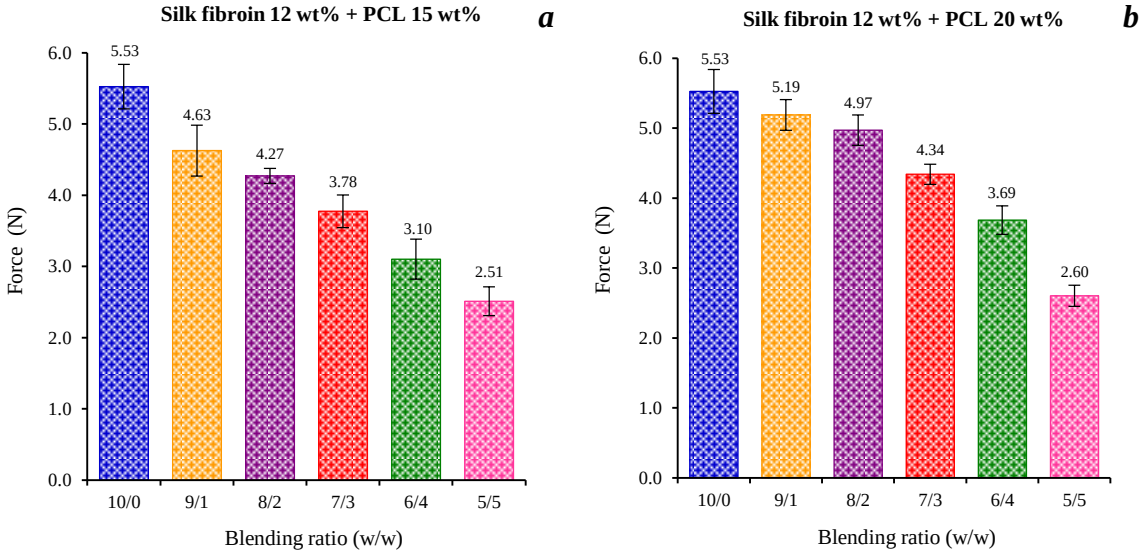

Figure 4.31 Effect of blend ratio of silk fibroin and polycaprolactone on tensile strength of the electrospun fibre sheets [blending ratio 10/0 (w/w) means pure silk fibroin solution].

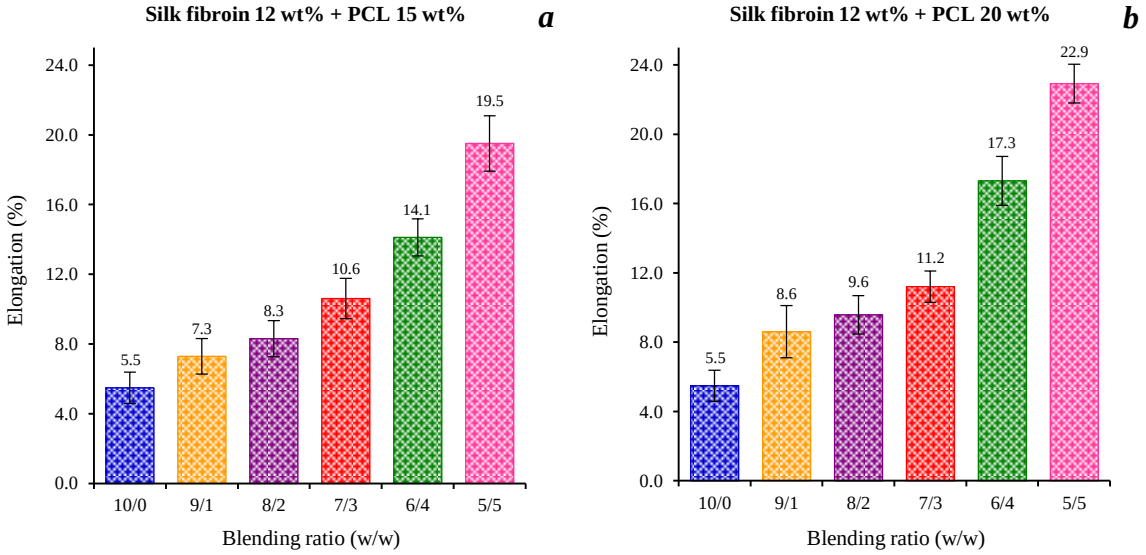

Figure 4.32 Effects of blend ratios of silk fibroin and polycaprolactone on elongation at break of the electrospun fibre sheets [blending ratio 10/0 (w/w) means pure silk fibroin solution].

- Hydrophilicity of the electrospun fibre sheets

Hydrophilicity is an important parameter for determining the biocompatibility of polymeric materials. This is because cells mostly have a much higher affinity on hydrophilic surface as compared to hydrophobic surface [86]. The water contact angle of silk fibroin and silk fibroin/polycaprolactone fibre sheets with different weight ratios was shown in Figure 4.33. The pure silk fibroin fibre sheet showed a water contact angle around 42.1^{O}, indicating that the silk fibres sheet possessed good

hydrophilicity. When the weight ratio of blend solution (SF/PCL) changed from 9/1 to 5/5, the water contact angles of the fibre sheets increased from 51.3^{O} to 81.7^{O}, respectively, in the polycaprolactone 15 wt% and from 55.9^{O} to 85.6^{O}, respectively, in the polycaprolactone 20 wt%.

Even though, silk fibroin is mostly composed of hydrophobic amino acids (glycine and alanine) and serine, its structural characteristic provides some hydrophilicity, resulting in a lower contact angle as compared to the blend fibre sheet and pure polycaprolactone (119^{O}). Assuming same morphological structures, the contact angle strongly depends on the hydrophilicity of the material. The increase in contact angle was likely due to the increase of hydrophobicity of the silk fibroin/polycaprolactone fibre sheets with polycaprolactone content in the blend. However, silk fibroin/polycaprolactone blend fibre sheets still have good compatibility with living cells (more detail in Topic 4.5).

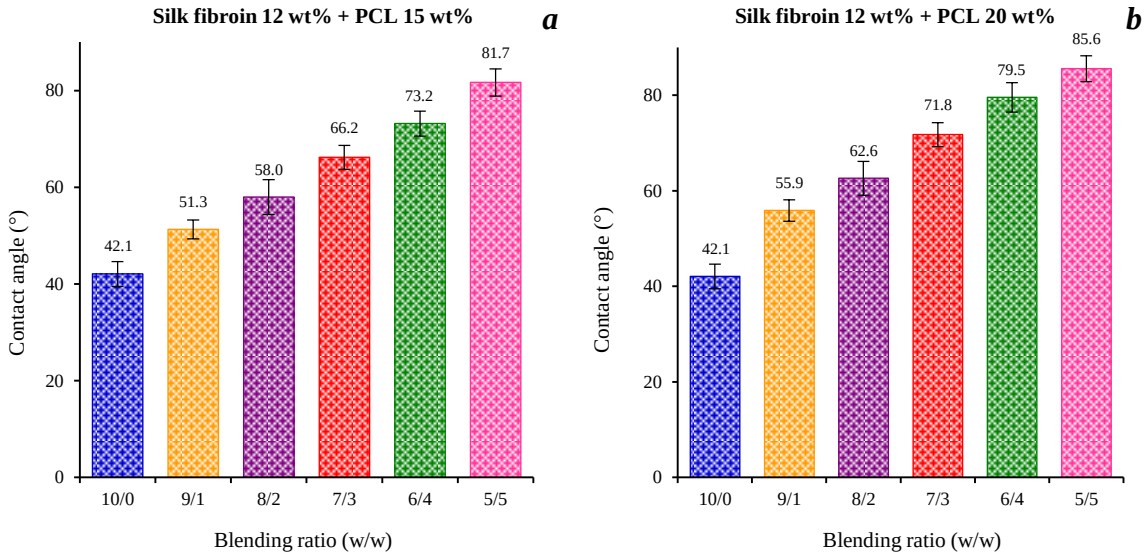

Figure 4.33 Effects of blend ratios of silk fibroin and polycaprolactone on water contact angle of the blend electrospun fibre sheets [blending ratio 10/0 (w/w) means pure silk fibroin solution].

4.5 *In vitro* test results of electrospun fibre sheets from silk fibroin and its blend with polycaprolactone

4.5.1 In vitro tests with 3T3 mouse fibroblasts

- Cell proliferation

Cultivation of 3T3 mouse fibroblasts with silk fibroin and silk fibroin/polycaprolactone blend fibre sheets was evaluated using methods that reflect the response of cells in terms of the adhesion and proliferation rate on the tested materials. Cell viability seeded on silk fibroin and silk fibroin/polycaprolactone blend fibre sheets was measured by MTT test during the time of cultivation in days 1, 3, 7 14 and 21 as shown in Figure 4.34. From the result, it can see that all tested materials support fibroblast proliferation during 3 weeks of cultivation. Cells adhered to the scaffold and proliferated through the surface. The proliferation rate increased after 7 days of cultivation where the absorbance increased. The highest proliferation rate was found between days 7 and 14. Then it was slowed down probably because of the fact that cells had covered almost all the surface of tested scaffolds.

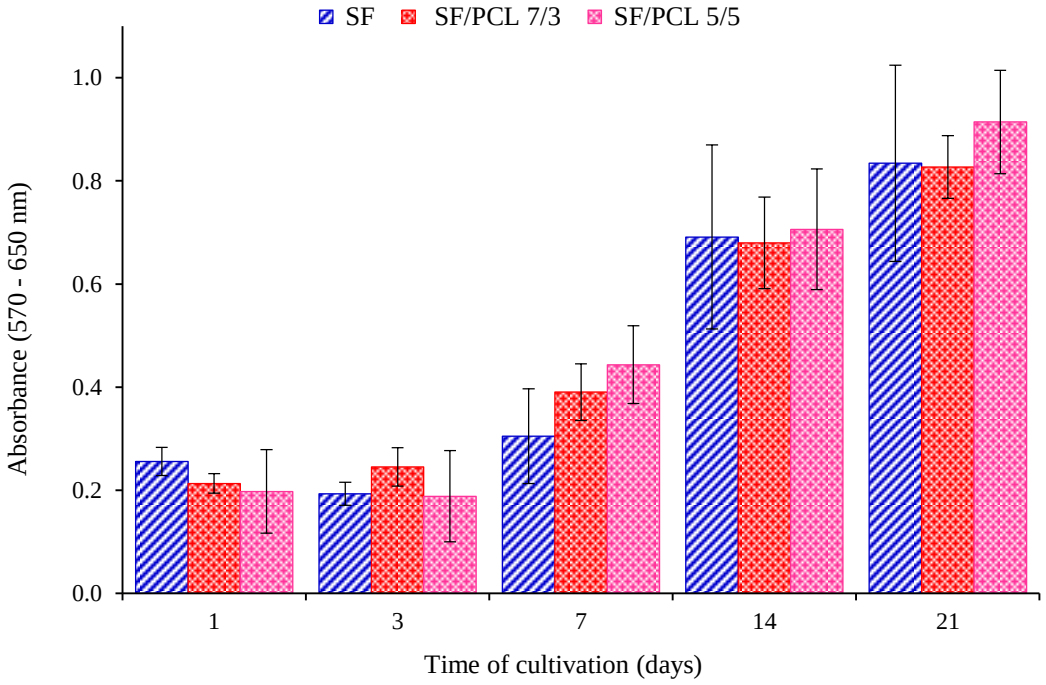

Figure 4.34 Cell viability measured by MTT test after cultivation with 3T3 mouse fibroblasts.

- Fluorescence microscopy analysis

After a period of incubation (1, 3, 7, 14 and 21 days), the fibre sheets were fixed and analyzed by fluorescence microscope. Red cell nuclei were stained by propidium iodide. From the result as shown in Figure 4.35. It can see that during the time of cultivation, cells adhered and proliferated well on the surface of the fibre sheets in all tested materials. Previous results obtained by MTT test was confrimed by microscopic technique. It shown a very good biocompatibility of pure silk fibroin and silk fibroin/ polycaprolactone blend fibre sheets.

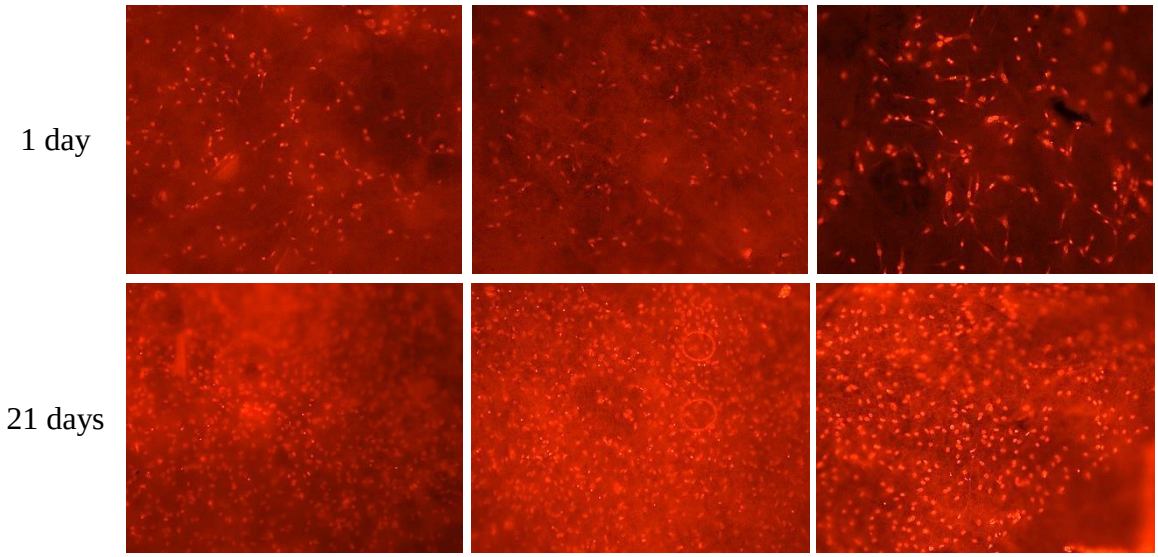

Figure 4.35 Fluorescence microscopy pictures of 3T3 mouse fibroblasts stained with propidium iodide during cell culture (magnification 100 x).

- *SEM analysis*

For electron microscopic analysis, after a period of cultivation the fibre sheets were fixed and dehydrated and analyzed by SEM microscope. The cells adhered on the surface of the scaffolds is depicted in Figure 4.36. The results are in agreement with fluorescence microscopy results. Cells proliferated through the surface of the fibre sheets and in the end of the experiment (after 21 days of cell culture) cells almost completely covered all the surface of the tested specimens. Finally, all tested materials showed very good properties in terms of proliferation rate.

From the result of *In vitro* tests show very good biocompatibility of all tested nanofibrous material. Silk fibroin and silk fibroin/polycaprolactone blend fibre sheets are promising candidates for tissue engineering applications. Further tests for deeper understanding of cellular adhesion as well as overall behaviour of cells on those nanofibrous structures have to be carried out.

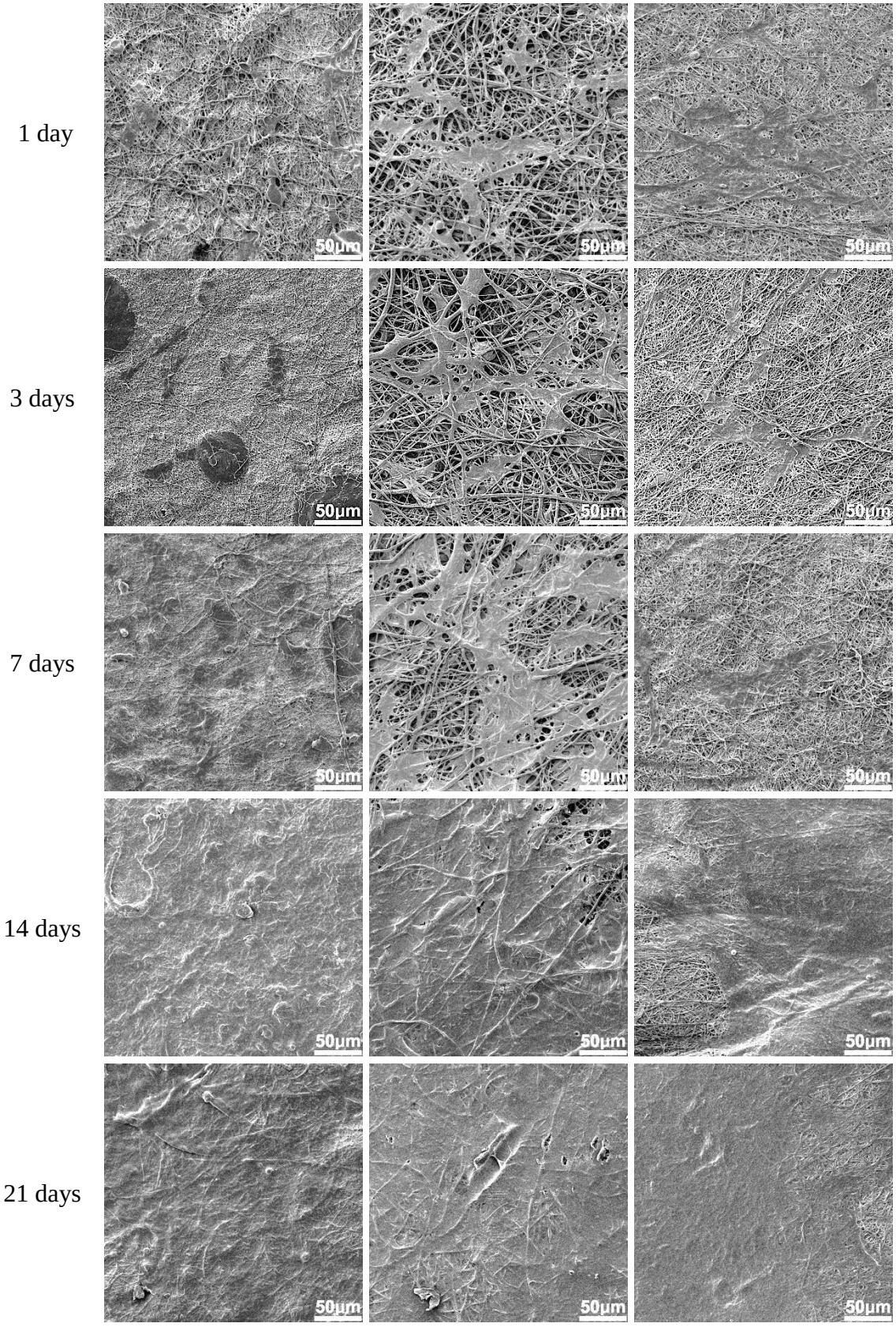

Figure 4.36 SEM micrographs of the fibre sheets after cell cultured with 3T3 mouse fibroblasts (SEM magnification 1 kx).

4.5.2 In vitro tests with normal human dermal fibroblasts (NHDF)

- Cell proliferation

Cell proliferation was measured by MTT test during the time of cultivation in days 1, 3, 7 and 14. The results are shown in Figure 4.37, it can see that all tesdted samples (silk fibroin and silk fibroin/polycaprolactone electrospun fibre sheet) support fibroblast proliferation during 2 weeks of cultivation. Cells adhered to the fibre sheets and proliferated through the surface. From the third day of incubation period, the fibre sheet composed of silk fibroin/polycaprolactone in ratio of 7/3 (w/w) showed the highest cell viability in comparison to the other tested materials. Pure silk fibroin and combination of silk fibroin and polycaprolactone in ratio of 5/5 (w/w) showed similar cell proliferation rate during 2 weeks incubation period.

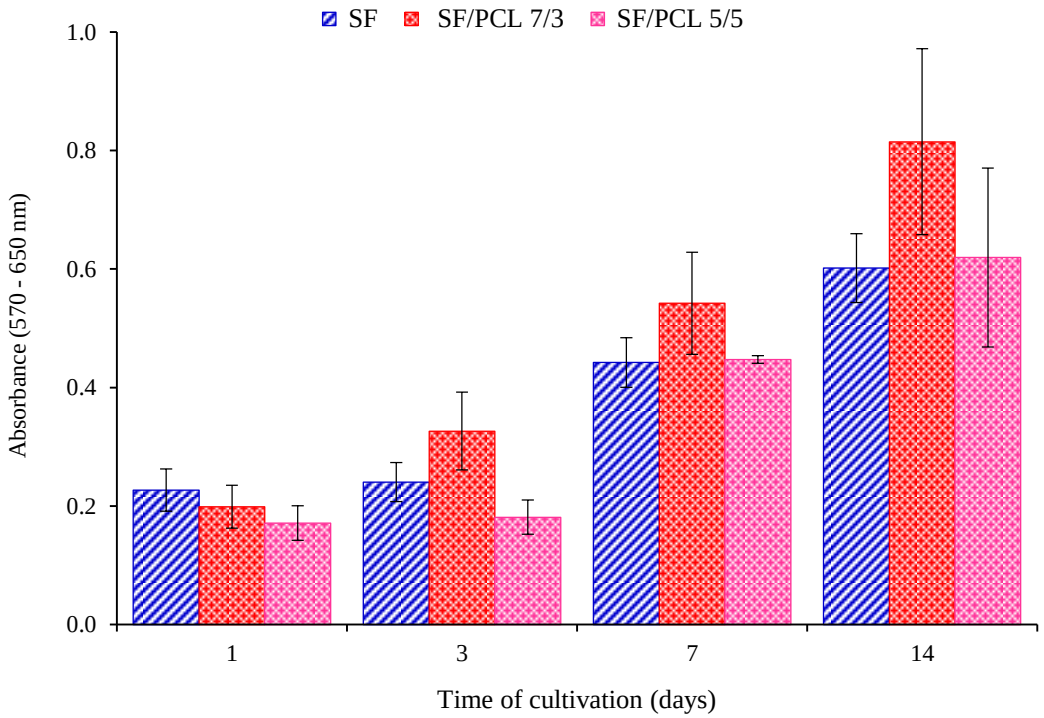

Figure 4.37 Cell viability measured by MTT test after cultivation with normal human dermal fibroblasts.

- Fluorescence microscopy analysis

After a period of incubation, the fibre sheets were fixed and analyzed by fluorescence microscope. Red cell nuclei were stained by propidium iodide. From the result as shoown in Figure 4.38 It can see that during the time of cultivation, cells adhered and proliferated well on the surface of the fibre sheet in all tested materials, but silk fibroin has a high level of autofluorescence therefore it is difficult to distinguish between red cell nuclei and stained fibres when pure silk fibroin or combination of silk fibroin and polycaprolactone is used.

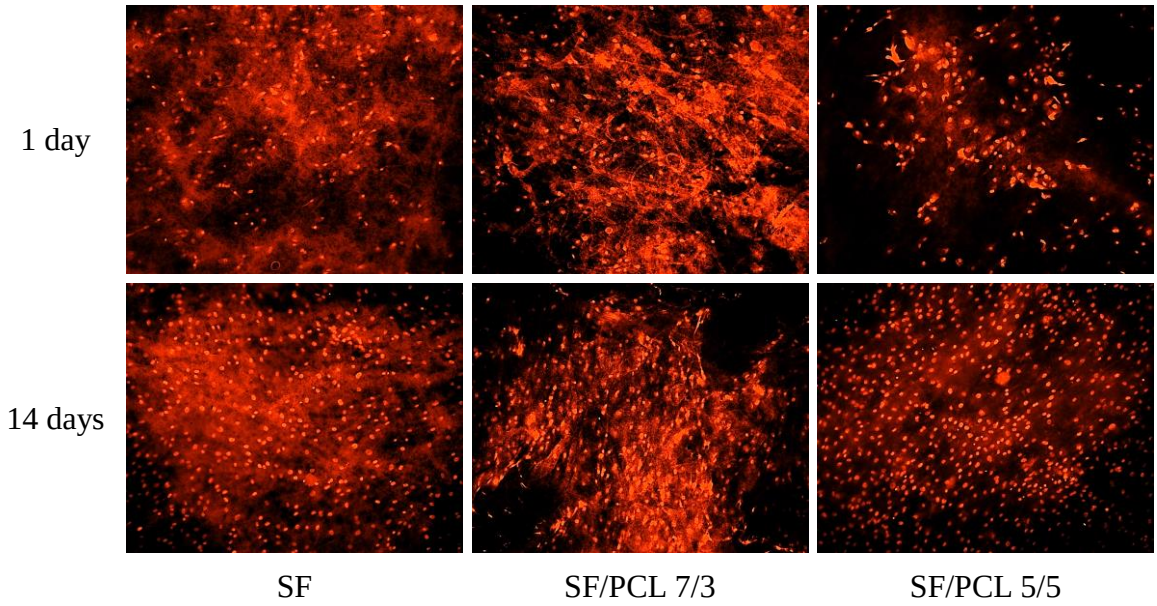

Figure 4.38 Fluorescence microscopy pictures of normal human dermal fibroblasts stained with propidium iodide during cell culture (magnification 100 x).

- *SEM analysis*

For electron microscopic analysis, the fibre sheets were fixed and dehydrated after a period of cultivation, and then analyzed by SEM microscope.The cells adhered on the surface of the fibre sheets that is depicted in Figure 4.39 where the cells are well dispersed onto nanofibrous layers. Cells proliferated through the surface of the fibre sheets and in the end of the experiment (after 14 days of cell culture) cells covered almost all the surface of the fibre sheet, especially on the fibre sheet made from composition of 7/3 (silk fibroin/polycaprolactone). This outcome is in agreement with MTT results where this layer showed the highest value of cell viability. All tested materials showed very good properties for normal human dermal fibroblast spreading through their surface. After 14 days, most of the surface was covered by fibroblasts.

In vitro tests show very good biocompatibility of all tested nanofibrous material with human dermal fibroblasts. The most promising one from the tested materials seems to be the combination of natural polymer (silk fibroin) and synthetic polymer (polycaprolactone) in ration of 7/3. The results were confirmed by viability measurement with MTT test, fluorescence microscopy as well as scanning electrone microscopy. All tested materials showed good adhesion evaluated 1 day after seeding of normal human dermal fibroblasts onto the fibre sheets. During the 2 weeks experiment, the cells proliferated through the surface of the fibre sheets, covered most of the surface.

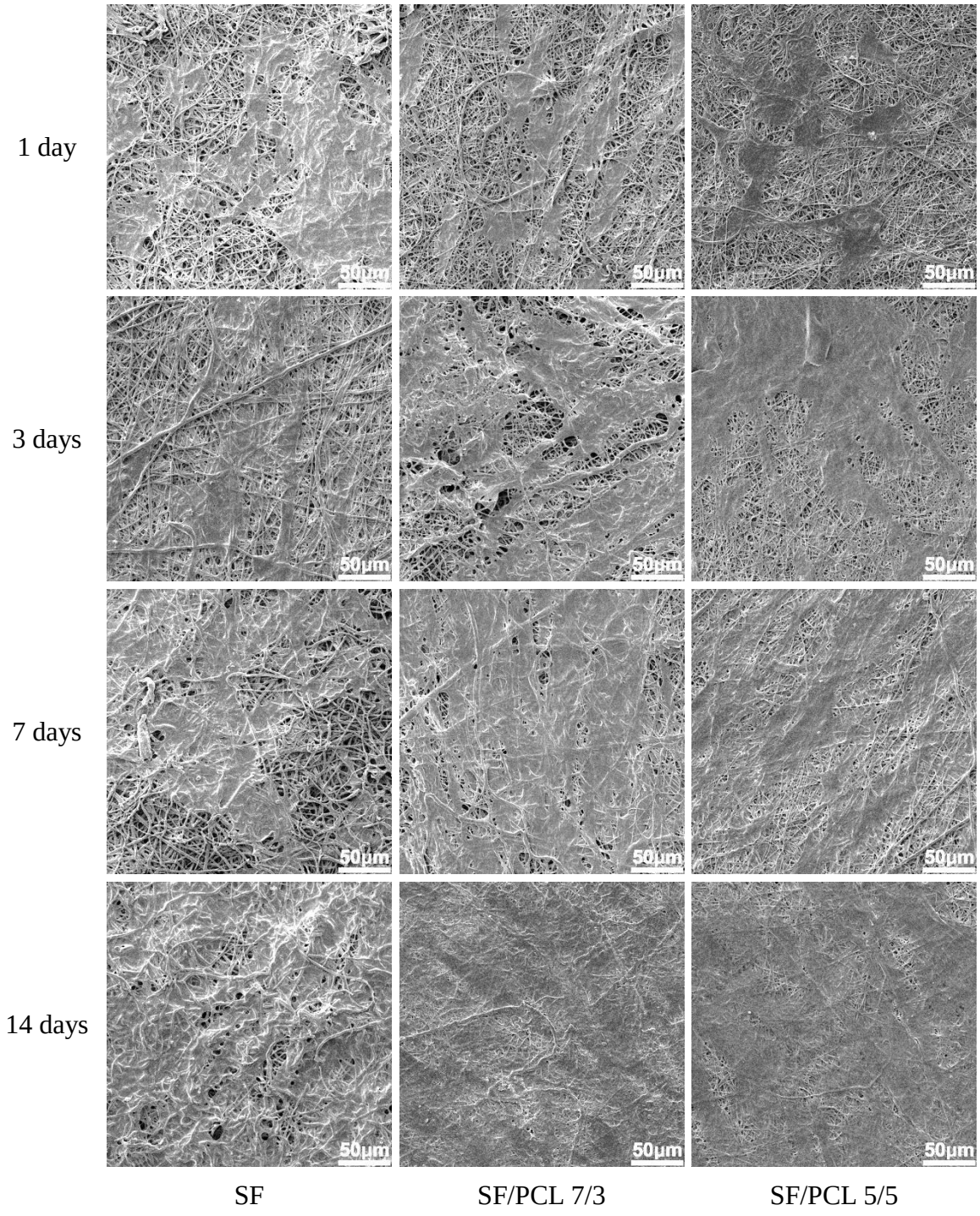

Figure 4.39 SEM micrographs of the fibre sheets after cells cultured with normal human dermal fibroblasts (SEM magnification 1 kx).

4.5.3 In vitro tests with MG 63 osteoblasts

- Cell proliferation

Cell viability seeded on the fibre sheets was measured by MTT test during the time of cultivation in days 1, 3, 7 and 14 shown in Figure 4.40. From the result, it can see that all tested materials support osteoblast proliferation during 2 weeks of cultivation. Cells adhered to the fibre sheet and proliferated through the surface. Silk fibroin electrospun fibre sheet showed the highest proliferation rate at the end of cultivation. This phenomenon could explain silk is a natural polymers that contain aminoacid sequences that promotes cell adhesion and proliferation.

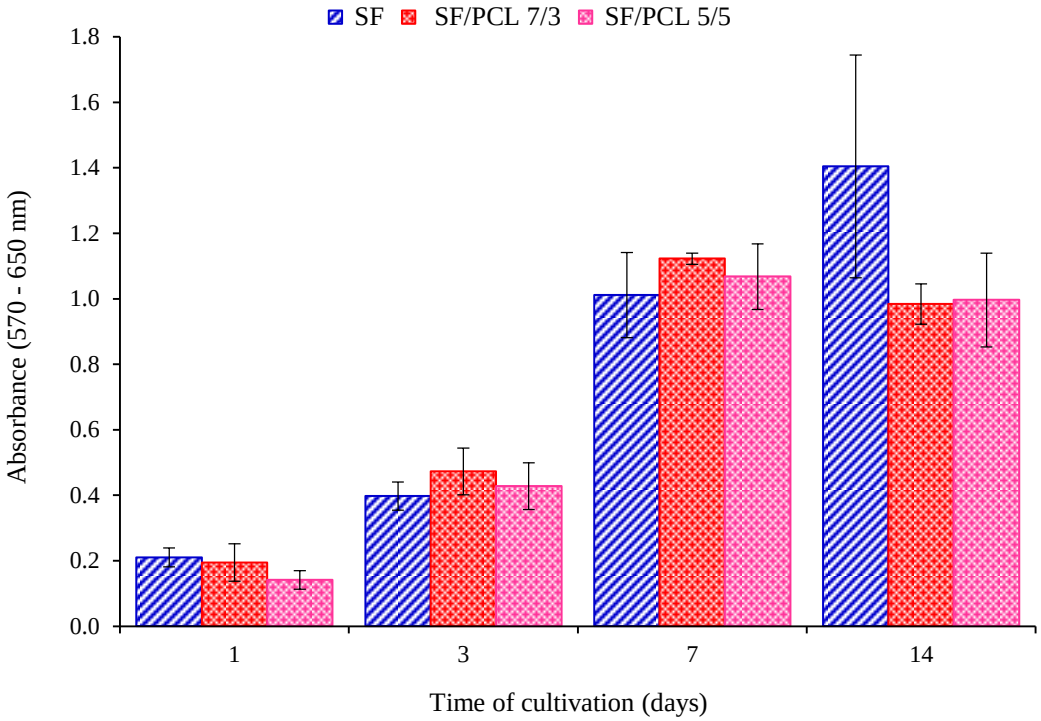

Figure 4.40 Cell viability measured by MTT test after cultivation with MG 63 osteoblasts.

- Fluorescence microscopy analysis

From the result as shown in Figure 4.41. It can see that during the time of cultivation, cells adhered and proliferated well on the surface of the fibre sheets in all tested materials. Fluorescence microscopy pictures confirmed MTT test results that obtained by the previous experiment. It shown a very good biocompatibility of silk fibroin and silk fibroin/polycaprolactone blend fibre sheets with MG 63 osetoblasts.

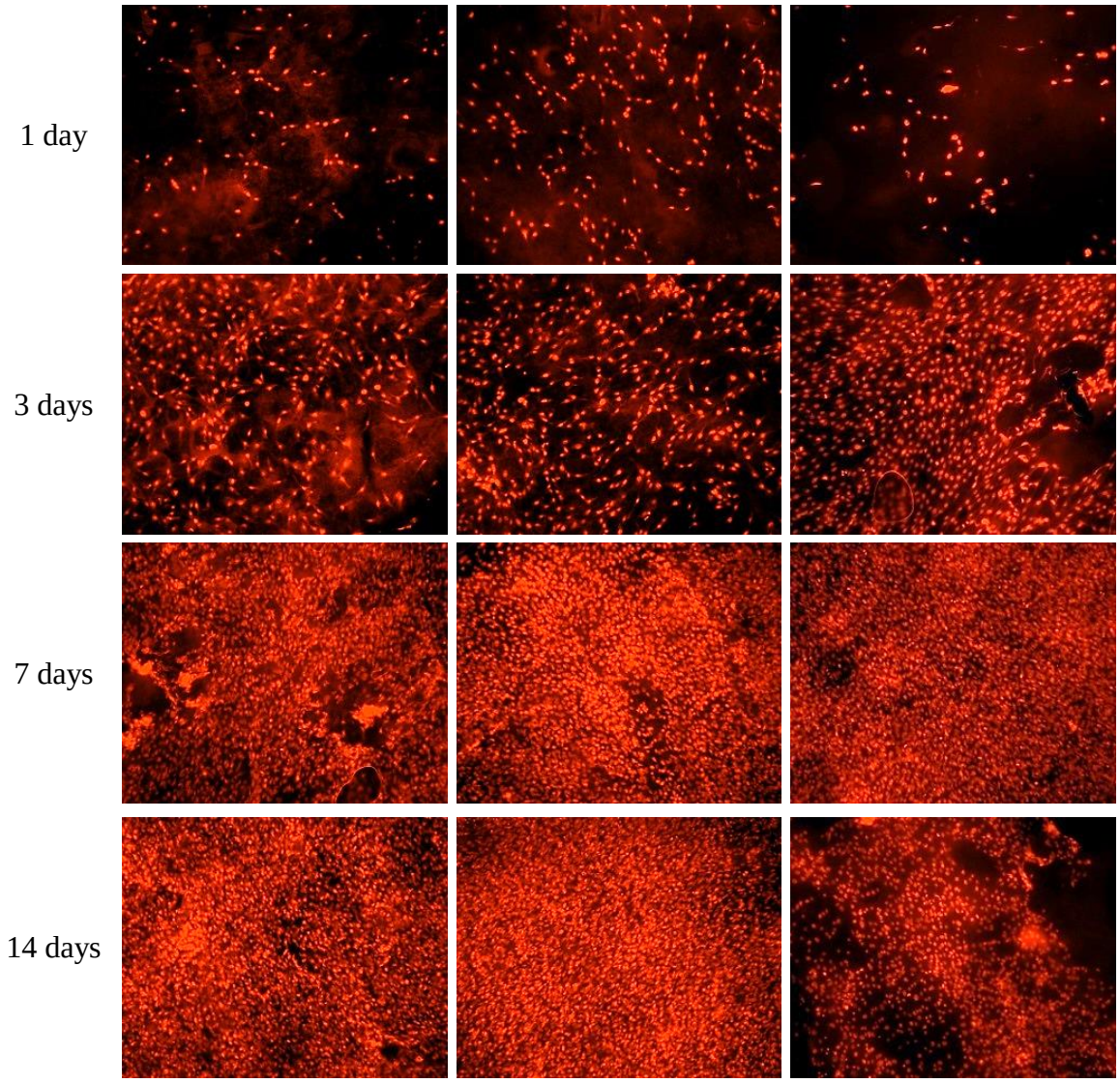

Figure 4.41 Fluorescence microscopy pictures of MG-63 osteoblasts stained with propidium iodide during cell culture (magnification 100 x).

- *SEM analysis*

SEM micrographs from scanning electrone microscopy are in agreement with fluorescence microscopy as well as MTT test. As shown in Figure 4.42, cellular adhesion is depicted and cellular spreading during 2 weeks of cell culture. After a week, the surface was almost covered with cells. Cells in silk fibroin electrospun fibre sheets have different morphology. In the other fibre sheets, cells create a confluent mololayer. But in silk fibroin fibre sheets, single cells can be distinguished. It is possible that not only a single layer is created. This outcome could explain the highest viability measured by MTT test.

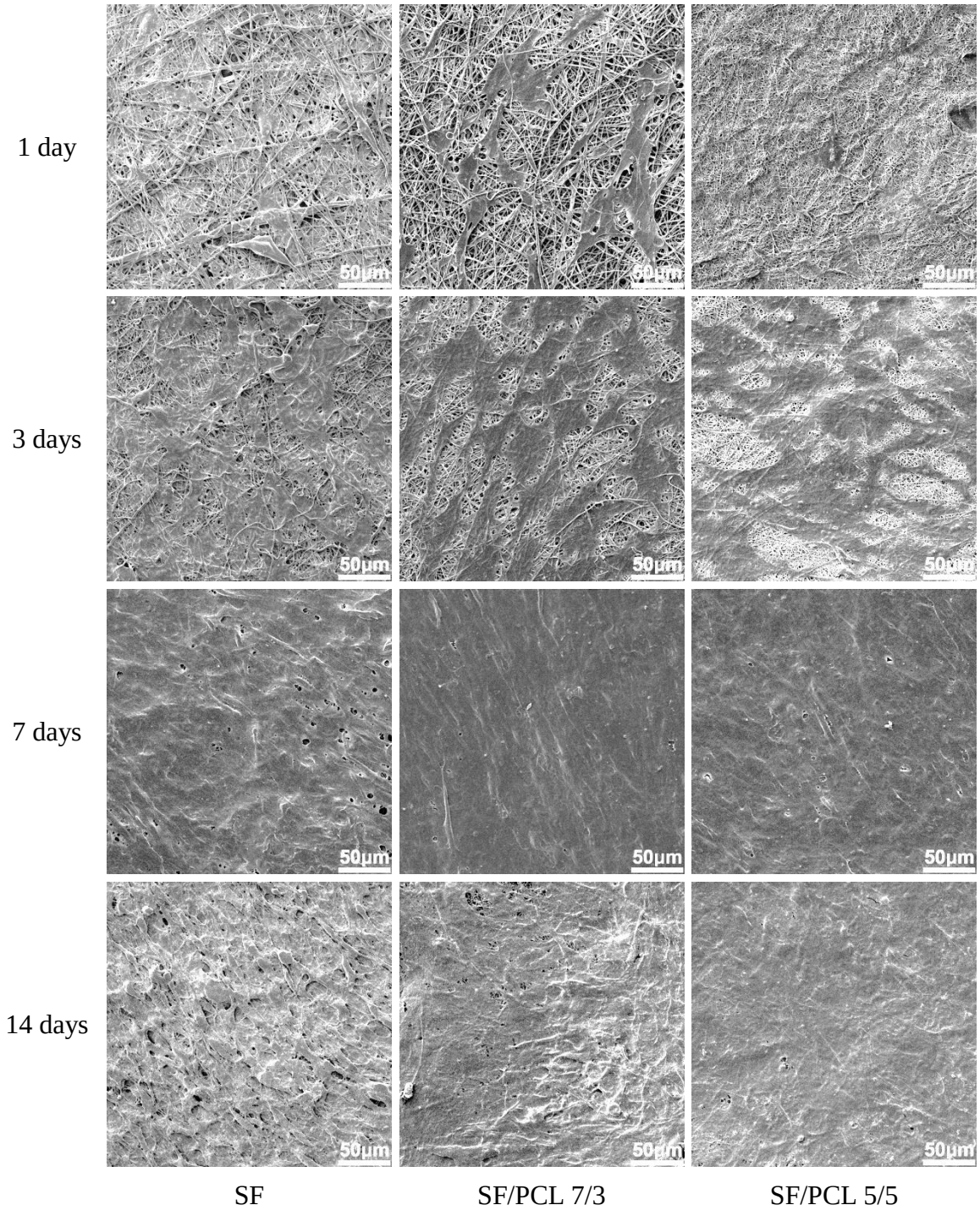

Figure 4.42 SEM micrographs of the fibre sheets after cells cultured with MG-63 osteoblasts (SEM magnification 1 kx).

From *In vitro* tests show very good biocompatibility of all tested nanofibrous material with MG-63 osteoblasts. The most promising one seems to be the pure silk fibroin. The results were confirmed by viability measurement with MTT test, fluorescence microscopy as well as scanning electrone microscopy. All tested materials showed good adhesion evaluated 1 day after seeding of osteoblasts onto the fibre sheets. During the 2 weeks of experiment, the cells proliferate through the surface of the fibre sheets and cover

most of the fibre sheets surface. The highest proliferation rate showed nanofibrous pure silk fibroin probably due to the presence of adhesive sequences in its structure. From the results can conclude that silk fibroin or in combination with polycaprolactone is a good material for bone tissue engineering scaffolds.

4.5.4 In vitro tests with human umbilical vein endothelial cells (HUVEC)

- Cell proliferation

Cell proliferation was measured during the time of cultivation in days 1, 4 and 7 by MTT test. From the results as shown in Figure 4.43, it can see that silk fibroin fibre sheets do not support endothelial cell proliferation during 7 days of cultivation. Cells adhered to the scaffold within the first day but then the proliferation rate was low. Where even lower viability than the first day was measured. After 7 days of incubation period, slight increase in cell viability was observed.

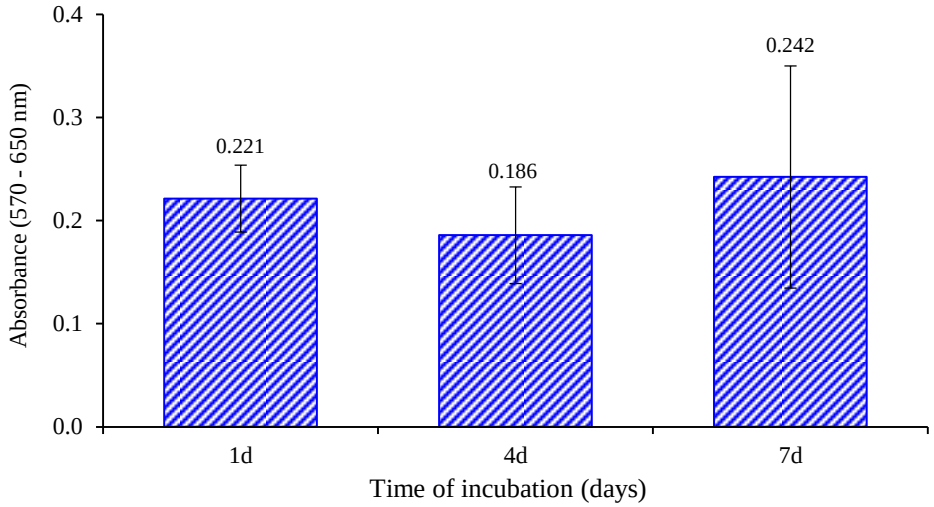

Figure 4.43 Cell viability measured by MTT test after cultivation with human umbilical vein endothelial cells.

- Fluorescence microscopy analysis

From the result as shown in Figure 4.44. It can see that during the time of cultivation (7 days), cells adhered and spared across the surface of the fibre sheets. Previous results obtained by MTT test were confirmed by microscopic technique that the silk fibroin scaffolds do not support endothelial cell proliferation.

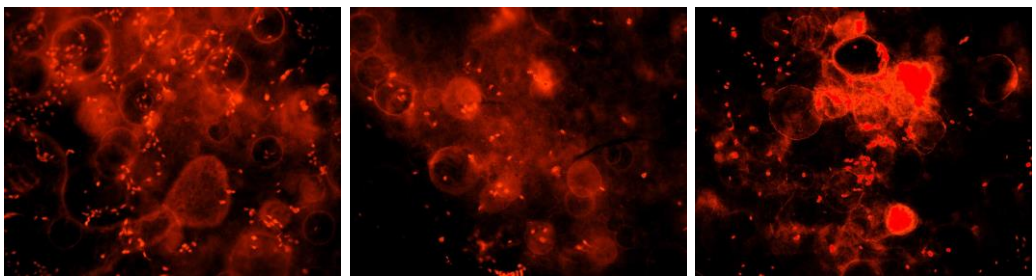

1 day 4 days 7 days

Figure 4.44 Fluorescence microscopy pictures of human umbilical vein endothelial cells stained with propidium iodide during cell culture (magnification 100 x).

- *SEM analysis*

The results showed adequate cellular adhesion as depicted in Figure 4.45 During the culture period, the silk fibroin scaffold has not supported cell proliferation. After 7 days of cultivation, it can still observe just adhered single cells.

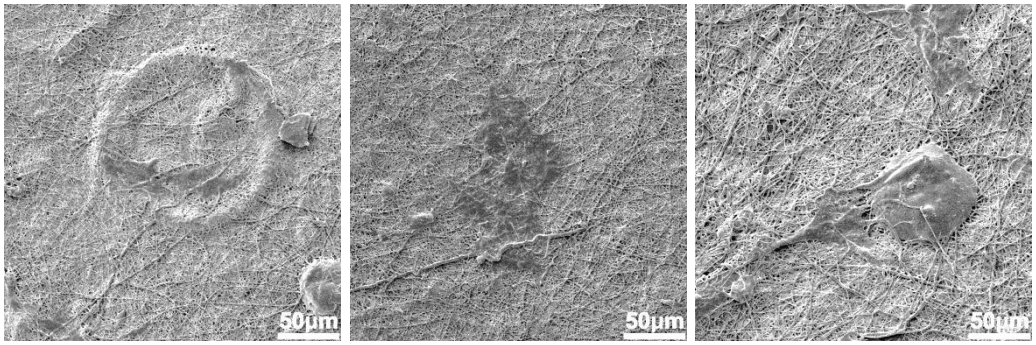

1 day 4 days 7 days

Figure 4.45 SEM micrographs of the silk electrospun fibre sheets after cell cultured with human umbilical vein endothelial cells (SEM magnification 1 kx).

In order to predict a usage of silk electrospun fibres for vascular graft fabrication, human umbilical vein endothelial cells were seed on the scaffold. Silk fibroin was a representative of biological material with hydrophilic properties. The results shown that silk fibroin have not supported cell proliferation. This outcome has to be explained by specific materials properties (crystalinity, hydrophilicity, surface roughness etc.), the assumption of hydrophobicity of materials or its origin (natural or synthetic polymer) have not shown to have a significant effect on endothelial cell proliferation as expected.

4.6 Result from supplementary experiments

4.6.1 Comparison between needle and needleless electrospinning of silk fibroin

- Effect of silk fibroin concentration

Considered the effect of concentration of spinning solution on fibre morphology with the applied voltage of 50 kV, when the silk fibroin concentration increased from 8 wt% to 12 wt%. The SEM micrographs and diameter distribution of the silk fibroin electrospun fibres produced by the needle and roller electrospinning techniques are shown in Figure 4.46 and 4.47, respectively. The results show that under the same electrospinning conditions, the fibre diameter and fibre diameter distribution of the obtained electrospun fibres increased with both systems in accordance with an increase in the silk fibroin concentration. In needle electrospinning, a solution with a low concentration leads to nanofibres with beads because of the low relation of viscosity to surface tension. On the other hand, a solution with a high concentration produces fibres with greater diameters due to the limited deformability of the polymer jet and/or the shorter time needed for the solidification of the more concentrated solution [51, 53]. In the present study, the concentration of the silk solution played an important role in the spinnability of the roller system (as explained in topic 4.2.1).

In addition to affecting the fibre morphology and spinnability, the concentration of the spinning solution also influenced the production rate. The production rate of the silk electrospun fibres from roller electrospinning increased from 0.81 g/h to 2.07 g/h when the concentration increased from 8 wt% to 12 wt%. The increase in the production rate with the needle system was less significant when the concentration of the silk solution increased (see Fig. 4.48).

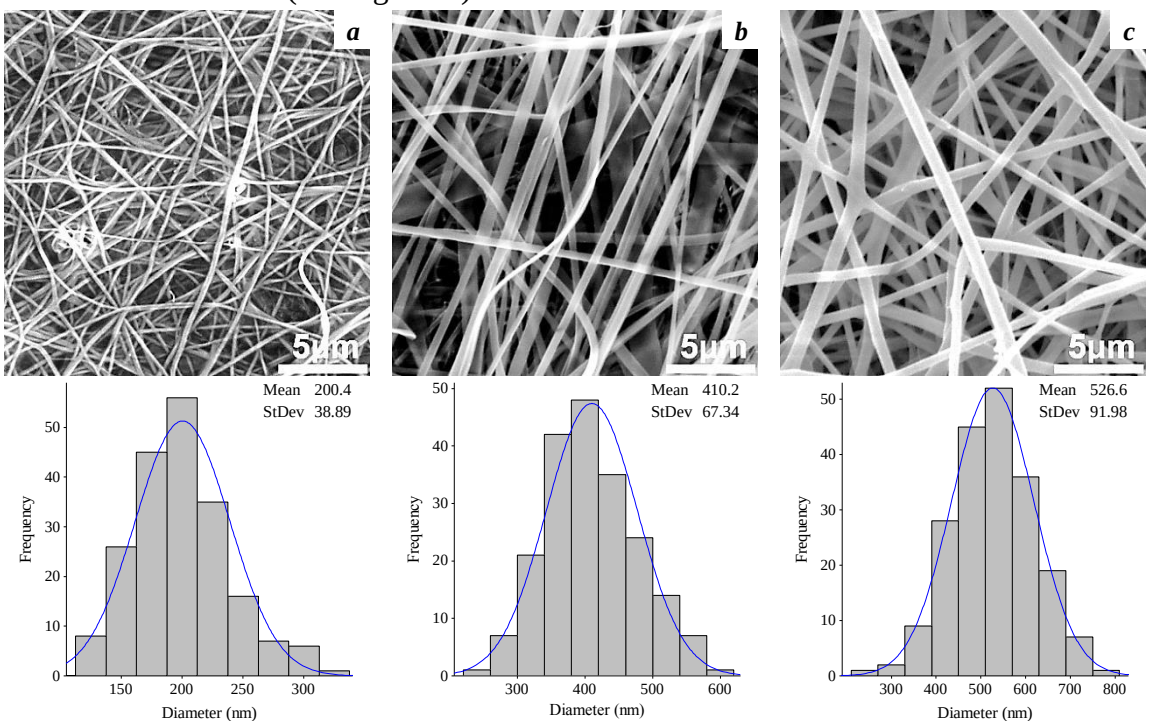

Figure 4.46 SEM micrographs and diameter distribution of electrospun fibres produced by needle electrospinning with silk fibroin solution at various concentrations. a) 8 wt%; b) 10 wt%; c) 12 wt%. (SEM magnification 10 kx)

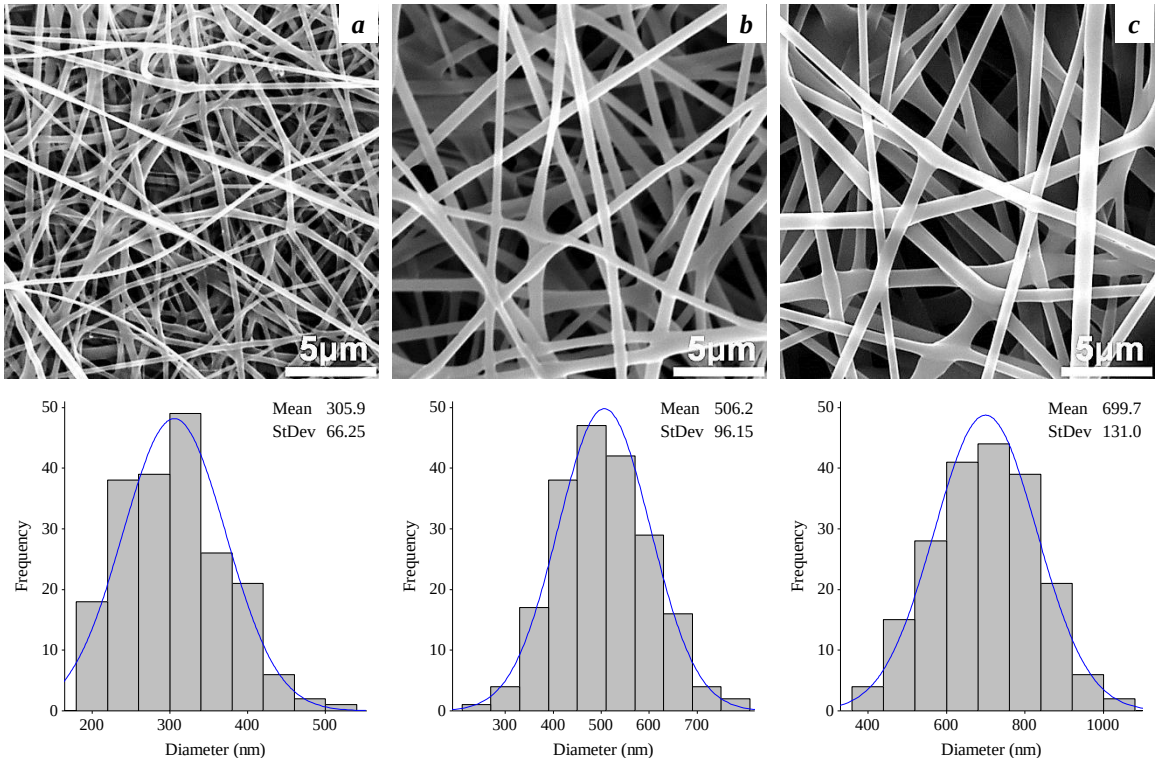

Figure 4.47 SEM micrographs and diameter distribution of electrospun fibres produced by roller electrospinning with silk fibroin solution at various concentrations. a) 8 wt%; b) 10 wt%; c) 12 wt%. (SEM magnification 10 kx)

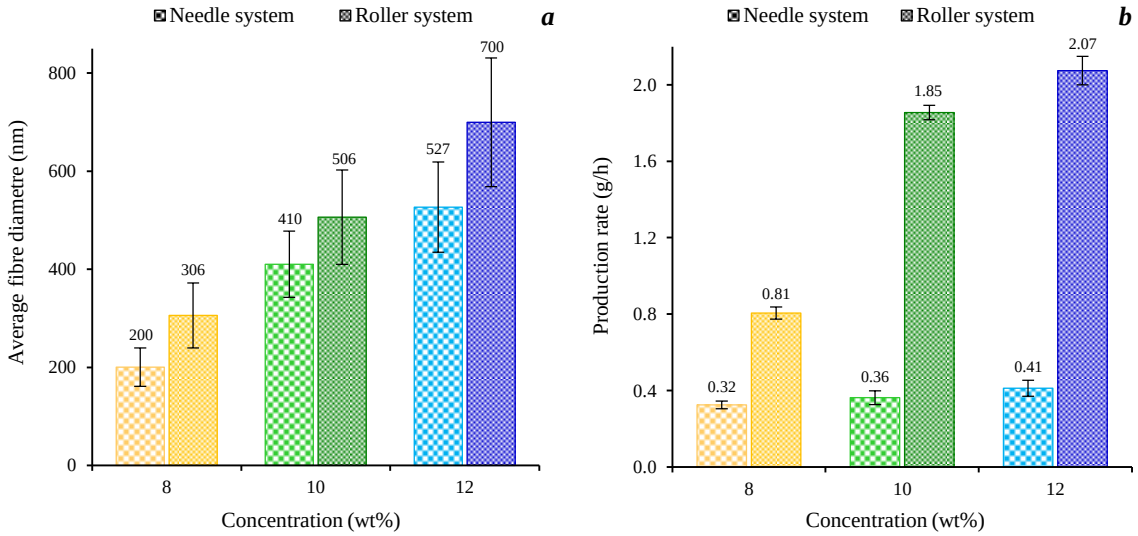

Figure 4.48 Effects of silk fibroin concentration on (a) average fibre diameter and (b) production rate.

- Effect of spinning electrode

The SEM micrographs of the silk fibroin electrospun fibres produced by the needle and roller electrospinning methods are shown in Figure 4.46 and 4.47, respectively. The results show that under the same operating conditions, both electrospinning systems produced uniform fibres. However, the diameters of the silk

electrospun fibres obtained from the needle electrospinning were smaller and the fibre diameter distribution was narrower than those obtained from the roller electrospinning. When the concentration increased from 8 wt% to 12 wt%, the average fibre diameter increased from 200 nm to 527 nm, respectively, in the needle system and from 306 nm to 700 nm, respectively, in the roller system (Fig. 4.48 (a)).

It is possible that the setup of the solution bath, which is normally exposed to air, in the roller electrospinning system may increase the evaporation of solvent from the spinning solution during the spinning process. Thus, the evaporation rate of solvent in the roller system was higher than that in the needle system. The evaporation of solvent from solution can increase the concentration of a solution. As shown in Figure 4.49, more concentrated silk solutions increased the viscosity of the spinning solution, and the viscosity of the spinning solution was significantly higher after electrospinning with the roller system. The concentration of the spinning solution has a dominant effect on the fibre diameter, with higher concentrations generally yielding electrospun fibres with larger average diameters [5, 51, 87]. In addition, Niu et al [7] described the electric field intensity profile of a cylinder-spinning electrode in upward needleless electrospinning that can be used to understand electrospinning behaviours. In a rotating cylinder electrode, they observed that the electric field intensity profile was unevenly distributed along the surface of the cylinder. A high-intensity electric field mainly formed on the cylinder ends and a much lower intensity electric field formed on the middle surface area of the cylinder. Electrospinning occurred in both areas of high-electric field intensity and low-electric field intensity. Furthermore, the diameters of the electrospun fibres produced from the two areas on the roller were very different [7]. As a result, the diameter and diameter distribution of electrospun fibres from a roller system are greater than those from a needle system.

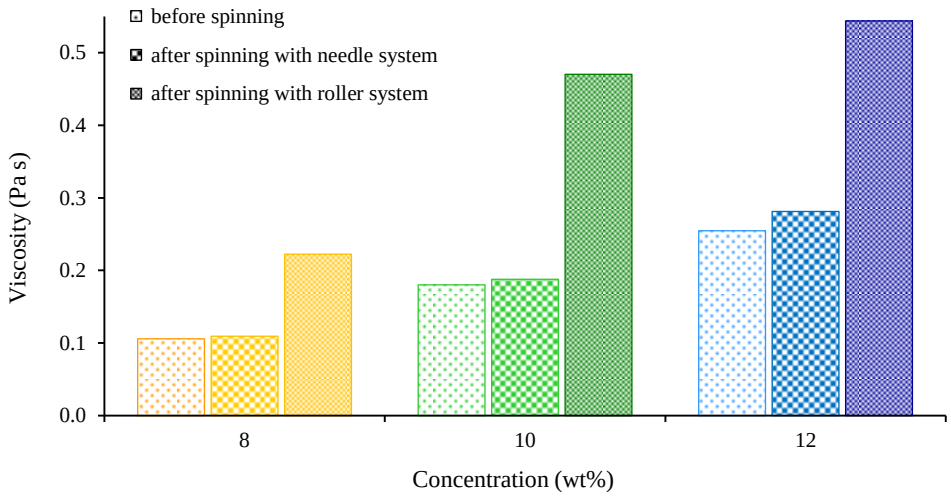

Figure 4.49 Comparison of the viscosity of silk fibroin solution at various concentrations.

The spinning electrode affected the production rate of the electrospinning process, resulting in a higher production rate in the roller than the needle system. For example, using a 12 wt% silk solution and the rotating spinning electrode instead of the needle, the production rate of silk electrospun fibres increased from 0.41 g/h to 2.07 g/h. In contrast to conventional needle electrospinning in which a Taylor cone is

generated and stabilised through constantly feeding the polymer solution through the needle, a number of jets can be simultaneously generated from the layer of solution on the surface of the rotating spinning electrode in the roller electrospinning system. As a result, the productivity of the roller system is much higher than that of the needle system.

- *Effect of applied voltage*

To study the effect of the applied voltage on the morphology of the obtained fibres and the spinning performance, a spinning solution with a concentration of 12 wt% was electrospun at a voltage between 35 kV and 50 kV. SEM micrographs of the resulting fibres and their distributions at the different applied voltages are shown in Figure 4.50 and 4.51, respectively. The applied voltage is a very important parameter with regard to the formation of jets in electrospinning systems because a high voltage is used to create an electrically charged jet of a polymer solution. Using the same polymer solution, the electric voltage required to initiate the spinning process from the roller was higher than that needed to generate fibres from the needle [10, 13].

In the roller electrospinning system, when the silk fibroin solution was charged with an electric voltage higher than 30 kV, a number of jets were generated from the surface of the spinning electrode. Increasing the applied voltage influenced the electrospinning process, with the average fibre diameter decreasing from 811 nm to 700 nm with an increase in the electric voltage from 35 kV to 50 kV, respectively. Furthermore, increasing the applied voltage affected the production rate of the spinning process. The production rate of the silk electrospun fibres from roller electrospinning changed from 0.63 g/h to 2.07 g/h when the applied voltage was increased (Fig. 4.52).

In the present study, the critical voltage required to initiate nanofibres on the needle electrospinning system was lower than on the roller system. The lowest voltage for initiating a jet from the tip of the needle was 6 kV. The average fibre diameter under the operating voltage range is shown in Figure 4.50. Increasing the applied voltage slightly reduced the average fibre diameter. Increasing the applied voltage from 35 kV to 50 kV decreased the average fibre diameter from 626 nm to 527 nm, respectively. Figure 4.52 depicts the effect of the variation in the applied electric fields on the production rate of nanofibres with the needle system. It can be seen that the effect of the applied electric field with the needle system was not as strong as with the roller system. The rate of production with the needle electrospinning system was 0.27 g/h and 0.41 g/h at applied voltages of 35 kV and 50 kV, respectively.

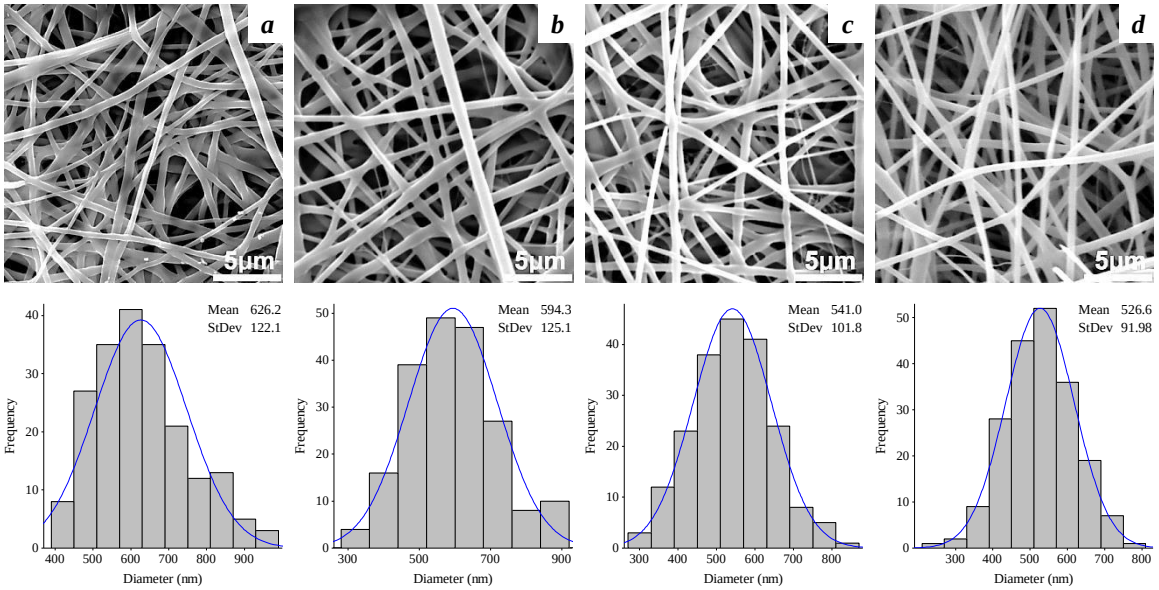

Figure 4.50 SEM micrographs and diameter distribution of electrospun fibres prepared by needle electrospinning from silk fibroin 12 wt% at a) 35 kV, b) 40 kV, c) 45 kV and d) 50 kV. (SEM magnification 10 kx)

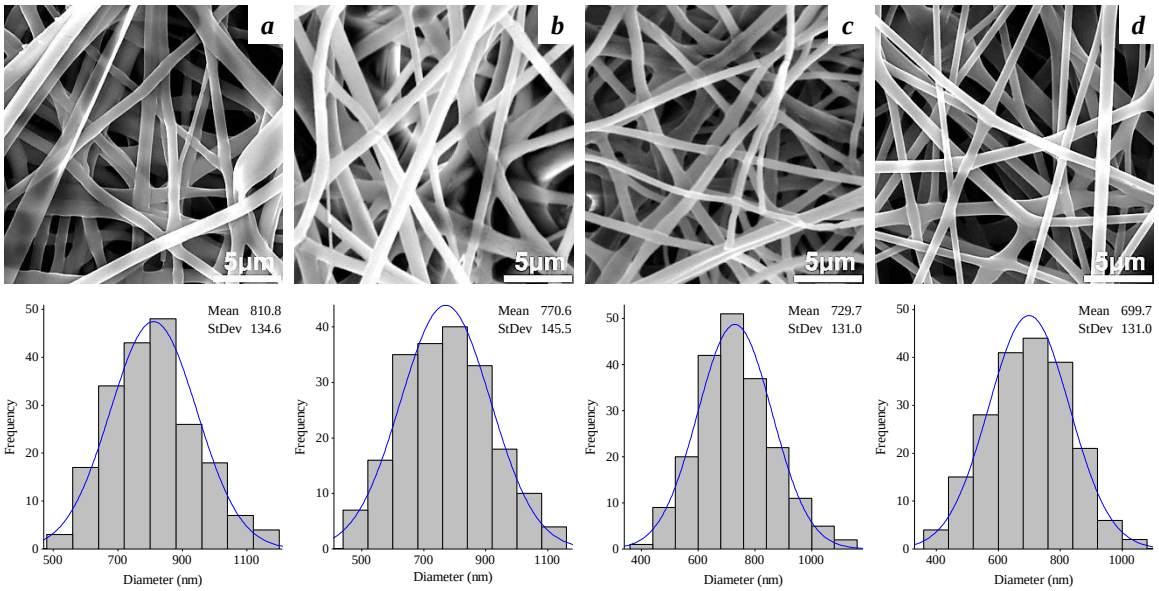

Figure 4.51 SEM micrographs and diameter distribution of electrospun fibres prepared by roller electrospinning from silk fibroin 12 wt% at a) 35 kV, b) 40 kV, c) 45 kV and d) 50 kV. (SEM magnification 10 kx)

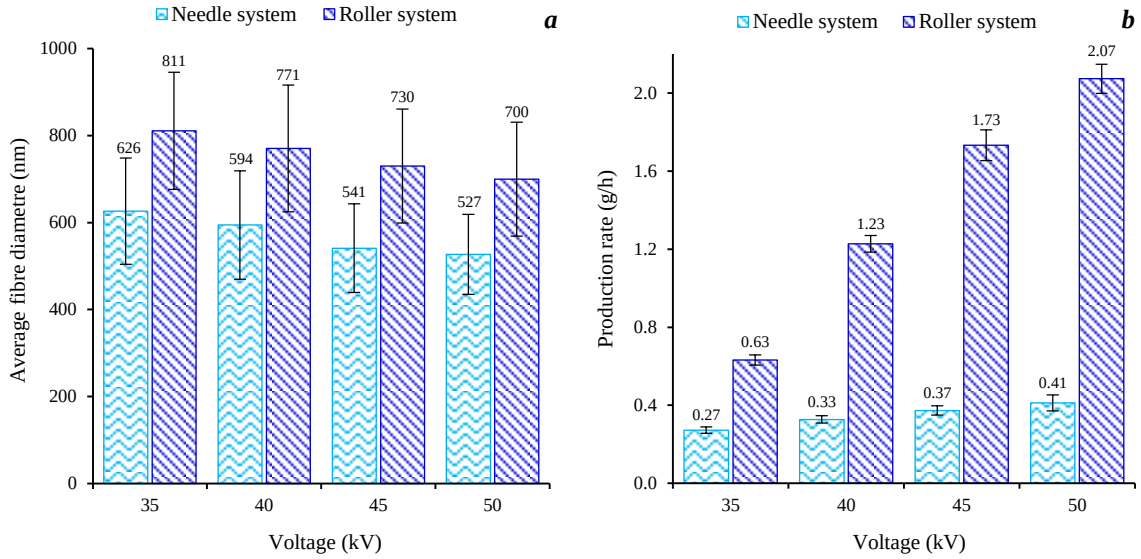

Figure 4.52 Effects of applied voltage on (a) average fibre diameter and (b) production rate (silk fibroin 12 wt%)

4.6.2 Enzyme immobilization on polycaprolactone/silk fibroin blend fibre sheets

- *Morphology of the PCL/SF blend fibre sheets*

The SEM micrograph and diameter distribution of the blend fibres are shown in Figure 4.53. An average fibre diameter of the PCL/SF blend fibre sheet is 348±62 nm and surface density is 6.2 g/m^2.

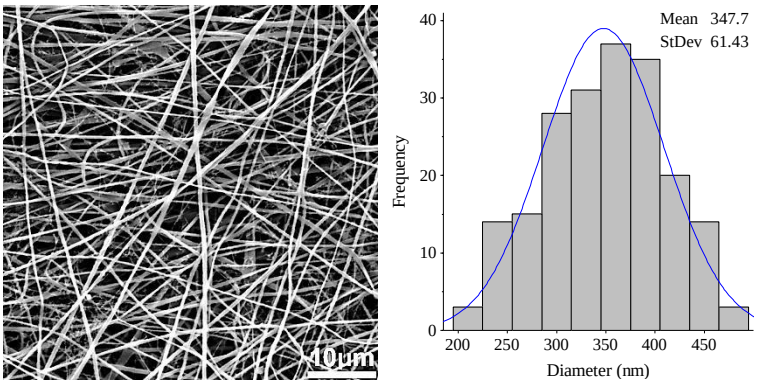

Figure 4.53 SEM micrograph and diameter distribution of PCL/SF electrospun fibres (SEM magnification 5 kx).

- *Effect of parameters on immobilization process*

Table 4.5 shows the relevant results comparing immobilization yields (IY), activity yields (AY) and the final loadings of samples prepared by different modification methods. The results are organized into several sections of partially similar parameters of the immobilization process. This arrangement allowed a specification and a comparison of the parameters influencing the activity of prepared samples.

Table 4.5 Enzyme activity of immobilized laccase on the PCL/SF blend fibre sheet prepared by different modification methods.

Modification method	Immobilization		Crosslinking		IY [%]	AY [%]	Loading [U/g]
	Enzyme solution	Time/ Temperature	Crosslinking agent	Time/ Temperature			
GA (2 h, 20 ^{O}C, pH 7.8, 12.5% v/v)	1 ml Laccase, 1 mg/ml 100 mM acetate buffer pH 4.5	5 h 20 ^{O}C	-	-	21.0 ± 2.7	2.1 ± 0.6	7.7 ± 0.3
GA (2 h, 20 ^{O}C, pH 7.8, 12.5% v/v)	1 ml Laccase,1 mg/ml, 100 mM McIlvaine buffer pH 4.5	5h 20 ^{O}C	-	-	3.0 ± 1.8	0.6 ± 0.2	9.8 ± 1.0
GA (2 h, 20 ^{O}C, pH 7.8, 12.5% v/v)	2 ml Laccase, 2 mg/ml 20 mM McIlvaine buffer pH 3.0	5 h 20 ^{O}C	-	-	6.7 ± 1.1	0.6 ± 0.16	14.4 ± 2.8
GA (2 h, 20 ^{O}C, pH 7.8, 12.5% v/v)	2 ml Laccase, 2 mg/ml 50 mM McIlvaine buffer pH 3.0	5 h 20 ^{O}C	-	-	3.6 ± 1.5	0.1 ± 0.06	6.2 ± 0.6
GA (2 h, 30 ^{O}C, pH 7.8, 12.5% v/v)- HMD (3 h, 30 ^{O}C, DIW, 0.1 M) - GA (2 h, 30 ^{O}C, pH 7.8, 12.5% v/v)	1 ml Laccase, 1 mg/ml, 20 mM acetate buffer pH 4.5	5 h 20 ^{O}C	-	-	7.5 ± 0.9	5.3 ± 1.4	35.6 ± 6.4
GA (2 h, 30 ^{O}C, pH 7.8, 12.5% v/v)- HMD (3 h, 30 ^{O}C, DIW, 0.1 M)- GA (2 h, 30 ^{O}C, pH 7.8, 12.5% v/v)	1 ml Laccase, 1 mg/ml 50 mM acetate buffer pH 6.0	5 h 20 ^{O}C	-	-	9.1 ± 1.2	0.7 ± 0.06	12.2 ± 2.5

Table 4.5 Enzyme activity of immobilized laccase on the PCL/SF blend fibre sheet prepared by different modification methods.

Modification method	Immobilization		Crosslinking		IY [%]	AY [%]	Loading [U/g]
	Enzyme solution	Time/ Temperature	Crosslinking agent	Time/ Temperature			
GA (2 h, 30 ^{O}C, pH 7.8, 12.5% v/v)-HMD (3 h, 30 ^{O}C, DIW, 0.1 M) -GA (2 h, 30 ^{O}C, pH 7.8, 12.5% v/v)	2 ml Laccase, 2 mg/ml 50 mM McIlvaine buffer pH 3.0	5 h 20 ^{O}C	-	-	9.3 ± 1.4	1.1 ± 0.2	13.2 ± 6.1
GA (2 h, 30 ^{O}C, pH 7.8, 12.5% v/v)-HMD (3 h, 30 ^{O}C, DIW, 0.1 M)-GA (2 h, 30 ^{O}C, pH 7.8, 12.5% v/v)	1 ml Laccase, 2 mg/ml 50 mM McIlvaine buffer pH 3.0	5 h 20 ^{O}C	-	-	16.9 ± 2.5	4.7 ± 1.3	80.2 ± 5.4
GA (2 h, 30 ^{O}C, pH 7.8, 12.5% v/v)-HMD (3 h, 30 ^{O}C, DIW, 0.1 M) -GA (2 h, 30 ^{O}C, pH 7.8, 12.5% v/v)	1 ml Laccase, 2 mg/ml 50 mM McIlvaine buffer pH 4.5	5 h 20 ^{O}C	-	-	10.5 ± 1.6	0.8 ± 0.12	19.8 ± 2.2
GA (2 h, 30 ^{O}C, pH 7.8, 12.5% v/v)-HMD (3 h, 30 ^{O}C, DIW, 0.1 M)-GA (2 h, 30 ^{O}C, pH 7.8, 12.5% v/v)	1 ml Laccase, 2 mg/ml 50 mM McIlvaine buffer pH 6.0	5 h 20 ^{O}C	-	-	2.8 ± 0.8	0.1 ± 0.01	12.5 ± 4.7
GA (2 h, 30 ^{O}C, pH 7.8, 12.5% v/v)-HMD (3 h, 30 ^{O}C, DIW, 0.1 M)-GA (2 h, 30 ^{O}C, pH 7.8, 12.5% v/v)	1 ml Laccase, 2 mg/ml 50 mM McIlvaine buffer pH 7.8	5 h 20 ^{O}C	-	-	0	0	0
GA (2 h, 20 ^{O}C, DIW, 12.5% v/v)-BSA (3 h, 20 ^{O}C, DIW, 1 mg/ml)-GA (2 h, 20 ^{O}C, DIW, 12.5% v/v)	1 ml Laccase, 2 mg/ml 50 mM McIlvaine buffer pH 3.0	5 h 20 ^{O}C	-	-	15.2 ± 2.0	4.4 ± 1.3	65.8 ± 10.9
GA (2 h, 20 ^{O}C, DIW, 12.5% v/v)-BSA (3 h, 20 ^{O}C, DIW, 1 mg/ml)-GA (2 h, 20 ^{O}C, DIW, 12.5% v/v)	1 ml Laccase, 2 mg/ml 50 mM McIlvaine buffer pH 4.5	5 h 20 ^{O}C	-	-	14.8 ± 1.5	6.5 ± 2.3	21.6 ± 11

Table 4.5 Enzyme activity of immobilized laccase on the PCL/SF blend fibre sheet prepared by different modification methods.

Modification method	Immobilization		Crosslinking		IY [%]	AY [%]	Loading [U/g]
	Enzyme solution	Time/ Temperature	Crosslinking agent	Time/ Temperature			
GA (2 h, 20 ^{O}C, DIW, 12.5% v/v)-BSA (3 h, 20 ^{O}C, DIW, 1 mg/ml)-GA (2 h, 20 ^{O}C, DIW, 12.5% v/v)	1 ml Laccase, 2 mg/ml 50 mM McIlvaine buffer pH 6.0	5 h 20 ^{O}C	-	-	15.6 ± 6.2	5.2 ± 2.8	16.4 ± 4.4
GA (2 h, 20 ^{O}C, DIW, 12.5% v/v)-BSA (3 h, 20 ^{O}C, DIW,1 mg/ml)-GA (2 h, 20 ^{O}C, DIW, 12.5% v/v)	1ml Laccase, 2 mg/ml 50 mM McIlvaine buffer pH 7.8	5h 20 ^{O}C	-	-	19.8 ± 2.5	3.9 ± 0.9	13.8 ± 1.6
GA (2 h, 20 ^{O}C, DIW, 12.5% v/v)-BSA (3 h, 20 ^{O}C, DIW, 1 mg/ml)-GA (2 h, 20 ^{O}C, DIW, 12.5% v/v)	1ml Laccase, 2 mg/ml 50 mM McIlvaine buffer pH 3.0	5 h 20 ^{O}C	GA (0.5% v/v)	2h, 20 ^{O}C	26.8 ± 3.6	5.3 ± 1.3	55.2 ± 4.8
GA (2 h, 20 ^{O}C, DIW, 12.5% v/v)-BSA(3 h, 20 ^{O}C, DIW, 1 mg/ml) -GA (2 h, 20 ^{O}C, DIW, 12.5% v/v)	0.5 ml Laccase, 2 mg/ml 50 mM McIlvaine buffer pH 3.0	5 h 20 ^{O}C	-	-	18.5 ± 2.6	6.2 ± 1.9	75.5 ± 5.9
GA (2 h, 20 ^{O}C, DIW, 12.5% v/v)-BSA (3 h, 20 ^{O}C, DIW, 1 mg/ml)-GA (2 h, 20 ^{O}C, DIW, 12.5% v/v)	0.5 ml Laccase, 2 mg/ml 50 mM McIlvaine buffer pH 3.0	20 h 4 ^{O}C	-	-	23.6 ± 4.8	10.2 ± 2.1	156.6 ± 12.4
GA (2 h, 20 ^{O}C, DIW, 12.5% v/v)-BSA (3 h, 20 ^{O}C, DIW, 1 mg/ml)-GA (2 h, 20 ^{O}C, DIW, 12.5% v/v)	0.5 ml Laccase, 2 mg/ml 50 mM McIlvaine buffer pH 4.4	20 h 4 ^{O}C	-	-	26.2 ± 1.9	3.9 ± 0.4	38.0 ± 5.7

Table 4.5 Enzyme activity of immobilized laccase on the PCL/SF blend fibre sheet prepared by different modification methods.

Modification method	Immobilization		Crosslinking		IY [%]	AY [%]	Loading [U/g]
	Enzyme solution	Time/ Temperature	Crosslinking agent	Time/ Temperature			
GA (2 h, 20 ^{O}C, DIW, 12.5% v/v)-BSA (3 h, 20 ^{O}C, DIW, 5 mg/ml)-GA (2 h, 20 ^{O}C, DIW, 12.5% v/v)	0.5 ml Laccase, 2 mg/ml 50 mM McIlvaine buffer pH 3.0	20 h 4 ^{O}C	-	-	21.7 ± 5.1	9.4 ± 1.6	121.2 ± 13.6
GA (2 h, 20 ^{O}C, DIW, 12.5% v/v)-BSA (3 h, 20 ^{O}C, DIW,5 mg/ml)-GA (2 h, 20 ^{O}C, DIW, 12.5% v/v)	0.5 ml Laccase, 2 mg/ml 50 mM McIlvaine buffer pH 4.4	20 h 4 ^{O}C	-	-	0	0	0
GA (2 h, 20 ^{O}C, DIW, 12.5% v/v)-BSA (3 h, 20 ^{O}C, DIW, 5 mg/ml)-GA (2 h, 20 ^{O}C, DIW, 12.5% v/v)	1 ml Laccase, 2 mg/ml 50 mM McIlvaine buffer pH 3.0 + 500 µg PEG	20 h 4 ^{O}C	-	-	36.4 ± 4.8	2.6 ± 1.2	166 ± 10.4
GA (2 h, 20 ^{O}C, DIW, 12.5% v/v)-BSA (3 h, 20 ^{O}C, DIW, 5 mg/ml)-GA (2 h, 20 ^{O}C, DIW, 12.5% v/v)	1 ml Laccase, 2 mg/ml 50 mM McIlvaine buffer pH 3.0 + 500 µg PEG	20 h 4 ^{O}C	GA (0.5% v/v)	2h 20 ^{O}C	46.8 ± 10.3	4.9 ± 1.0	94,8 ± 8.7
GA (2 h, 20 ^{O}C, DIW, 12.5% v/v)-BSA (3 h, 20 ^{O}C, DIW, 5 mg/ml)-GA (2 h, 20 ^{O}C, DIW, 12.5% v/v)	1 ml Laccase, 2 mg/ml 50 mM McIlvaine buffer pH 3.0	20 h 4 ^{O}C	-	-	18.9 ± 1.6	3.3 ± 0.06	104.8 ± 12.9
GA (2 h, 20 OC, DIW, 12.5% v/v)-BSA (3 h, 20 OC, DIW, 5 mg/ml)-GA (2 h, 20 OC, DIW, 12.5% v/v)	1 ml Laccase, 2 mg/ml 50 mM McIlvaine buffer pH 3.0	20 h 4 ^{O}C	GA (0.5% v/v)	2h 20 OC	21.6 ± 5.3	1.2 ± 0.07	70.6 ± 8

Table 4.5 Enzyme activity of immobilized laccase on the PCL/SF blend fibre sheet prepared by different modification methods.

Modification method	Immobilization		Crosslinking		IY [%]	AY [%]	Loading [U/g]
	Enzyme solution	Time/ Temperature	Crosslinking agent	Time/ Temperature			
GA (2 h, 20 ^{O}C , pH 7.8, 12.5% v/v)-BSA (3 h, 20 ^{O}C, pH 7.8, 5 mg/ml)-GA (2 h, 20 ^{O}C, pH 7.8, 12.5% v/v)	1 ml Laccase, 2 mg/ml 50 mM McIlvaine buffer pH 3.0	20 h 4 ^{O}C	-	-	19.4 ± 4.2	1.9 ± 0.06	43.9 ± 6.1
GA (2 h, 20 ^{O}C, pH 7.8, 12.5% v/v) - BSA (3 h, 20 ^{O}C , pH 7.8, 5 mg/ml)-GA (2 h, 20 ^{O}C, pH 7.8, 12.5% v/v)	1 ml Laccase, 2 mg/ml 50 mM McIlvaine buffer pH 3.0	20 h 4 ^{O}C	GA (0.5% v/v)	2 h 20 ^{O}C	23.9 ± 1.9	0.98 ± 0.07	22.8 ± 2.6
GA (2 h, 20 ^{O}C, DIW, 12.5% v/v) - BSA (3 h, 20 ^{O}C, DIW, 5 mg/ml) - GA (2 h, 20 ^{O}C, DIW, 12.5% v/v)	1 ml Laccase, 2 mg/ml 100 mM McIlvaine buffer pH 3.0	20 h 4 ^{O}C	-	-	38.4 ± 3.7	0.23 ± 0.09	16.4 ± 4.8
GA(2 h, 20 ^{O}C, DIW, 12.5% v/v)-BSA (3 h, 20 ^{O}C, DIW, 1 mg/ml)-GA (2 h, 20 ^{O}C, DIW, 12.5% v/v)	0.5 ml Laccase, 2 mg/ml 20 mM McIlvaine buffer pH 3.0	20 h 4 ^{O}C	-	-	4.3 ± 1.1	91 ± 3.6	244.8 ± 20.5
GA(2 h, 20 ^{O}C, DIW, 12.5% v/v)-BSA (3 h, 20 ^{O}C, DIW, 1 mg/ml)-GA (2 h, 20 ^{O}C, DIW, 12.5% v/v)	0.5 ml Laccase, 2 mg/ml 20 mM McIlvaine buffer pH 3.0	20 h 4 ^{O}C	GA (1% v/v)	2 h 20 ^{O}C	76.2 ± 6.2	0.1 ± 0.03	38.8 ± 6.4
GA (2 h, 20 OC, DIW, 12.5% v/v)-HMD (3 h, 20 OC, DIW, 0.1 M)-GA (2 h, 20 OC, DIW, 12.5% v/v)	0.5 ml Laccase, 2 mg/ml 20 mM McIlvaine buffer pH 3.0	20 h 4 ^{O}C	GA (5% v/v)	2 h 20 OC	68.2 ± 5.3	0.14 ± 0.05	18.5 ± 2.6

Table 4.5 Enzyme activity of immobilized laccase on the PCL/SF blend fibre sheet prepared by different modification methods.

Modification method	Immobilization		Crosslinking		IY [%]	AY [%]	Loading [U/g]
	Enzyme solution	Time/ Temperature	Crosslinking agent	Time/ Temperature			
GA (2 h, 20 ^{O}C, DIW, 12.5% v/v)-HMD (3 h, 20 ^{O}C, DIW, 0.1 M)-GA (2 h, 20 ^{O}C, DIW, 12.5% v/v)	0.5 ml Laccase, 2 mg/ml 20 mM McIlvaine buffer pH 3.0	20 h 4 ^{O}C	GA (10% v/v)	2 h 20 ^{O}C	74.4 ± 8.1	0.11 ± 0.02	25.0 ± 1.3
GA (2 h, 20 ^{O}C, DIW, 12.5% v/v)-BSA(3 h, 20 ^{O}C, DIW, 1 mg/ml)-GA (2 h, 20 ^{O}C, DIW, 12.5% v/v)	0.5 ml Laccase, 2 mg/ml 20 mM McIlvaine buffer pH 3.0	20 h 4 ^{O}C	GA (10% v/v)	2 h 20 ^{O}C	44.6 ± 3.1	0.13 ± 0.04	21.4 ± 4.3
GA (2 h, 20 ^{O}C, milli-Q, 12.5% v/v)-BSA (14 h, 20 ^{O}C, milli-Q, 1 mg/ml)-GA (2 h, 20 ^{O}C, milli-Q, 12.5% v/v)	0.5 ml Laccase, 2 mg/ml 20 mM McIlvaine buffer pH 3.0	20 h 4 ^{O}C	-	-	25.1 ± 6.7	4.3 ± 1.2	95.0 ± 8.4

Remark

- GA : Glutaraldehyde
- BSA : Bovine serum albumin
- HMD: Hexamethylenediamine
- DIW : Deionized water
- Milli-Q : Ultrapure water

Effect of time and temperature on immobilization process: The best results were achieved when the laccase was immobilized for 20 hours at 4 ^{O}C. This is probably due to the reaction of enzyme, laccase needed a gradual reaction with the modified matrix to form an active conformation obtaining an accessible active site. Moreover, this might be the reason why an additional crosslinker inactivated most of the enzyme immobilized for 20 hours by binding to amine groups in the active sites. Samples where the laccase was immobilized only for 5 hours at 20 ^{O}C did not show such remarkable inactivation compared to the similar samples without the additional crosslinker.

Effect of the modification method: Three hours for modification via glutaraldehyde and four hours for bovine serum albumin or hexamethylenediamine spacing under alkaline pH ~ 8.0 and 40 ^{O}C were used in a study by Da Silva et al. [74]. Silva et al. [75] also used alkaline solution (pH 9.5) for introducing of glutaraldehyde and hexamethylenediamine during 2 hours and 4 hours reactions. However, longer time for each modification step other than described in Table 4.5 did not show any improvement in activity of the immobilized laccase. Using distilled water for glutaraldehyde and bovine serum albumin or hexamethylenediamine solutions was eventually more efficient than a citrate-phosphate buffer with pH 7.8 that was supposed to ensure more stable Schiff base. During the first trials bovine serum albumin appeared to be a better modification compound compared to hexamethylendiamine, therefore hexamethylenediamine was excluded from subsequent experiments with SF/PCL blend fibre sheets.

Effect of the laccase concentration and volume of the mixture: The molar concentration and pH played a very important role in enzyme immobilization. The optimal pH was 3.0 and the most preferable concentration was 20 mM. The best results were achieved when using laccase solution with the concentration of 2 mg/ml in 20 mM McIlvaine buffer with pH 3.0. The lowest volume acceptable for the nanofibrous samples was 500 µl which appeared to be the most efficient amount of the enzyme solution with the highest achieved activity after immobilization.

Effect of supporting chemicals and crosslinking agent: The influence of polyethylene glycol on immobilization efficiency is unclear. However, it was observed that polyethylene glycol increased viscosity of the laccase solution and positively influenced its solubility with lower marks of the enzyme sedimentation on the bottom of a vial. In case of all samples, the additional crosslinking agent had a negative influence on the immobilization efficiency.

From the obtained result, the polycaprolactone/silk fibroin blend fibre sheet showed to be a promising material for enzyme immobilization for its sufficient mechanical stabilities and affinity to the enzyme. After long immobilization periods, it tended to degrade and partially break down into small filaments, especially when stored at low pH. This fact might affect the storage stability of the immobilized enzyme. In case of several samples, the loading exceeded 100 U/g of the support, which was a very promising result. The highest achieved loading of the immobilized laccase was more than 240 U/g, which is a reasonable result with regard to the considerable amount of impurities or inactive protein

in the stock laccase. The best immobilization procedure included a modification via GA-BSA-GA and the 20 hours for the laccase attachment at pH 3.0 and 4 ^{O}C.

- Degradation of bisphenol A and 17α-ethinyl estradiol

Figure 4.54 shows the decrease in concentration of bisphenol A (BPA) and Figure 4.55 shows the degradation of 17α-ethinyl estradiol (EE2) in the micropollutant mixture after incubation with different amount of the laccase from *Trametes versicolor*. The degradation was more rapid with growing amount of laccase expressed by its activity in units.

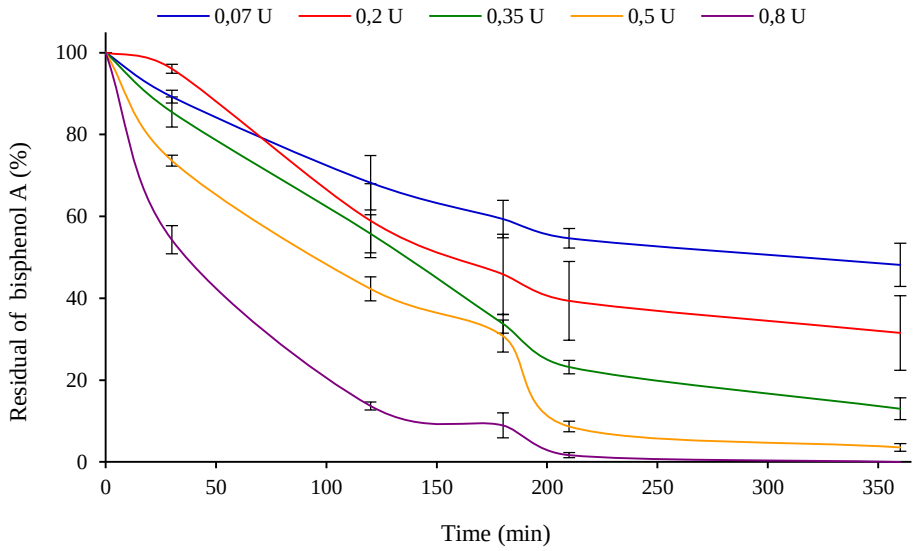

Figure 4.54 Degradation of bisphenol A by different amounts of laccase from *Trametes versicolor*

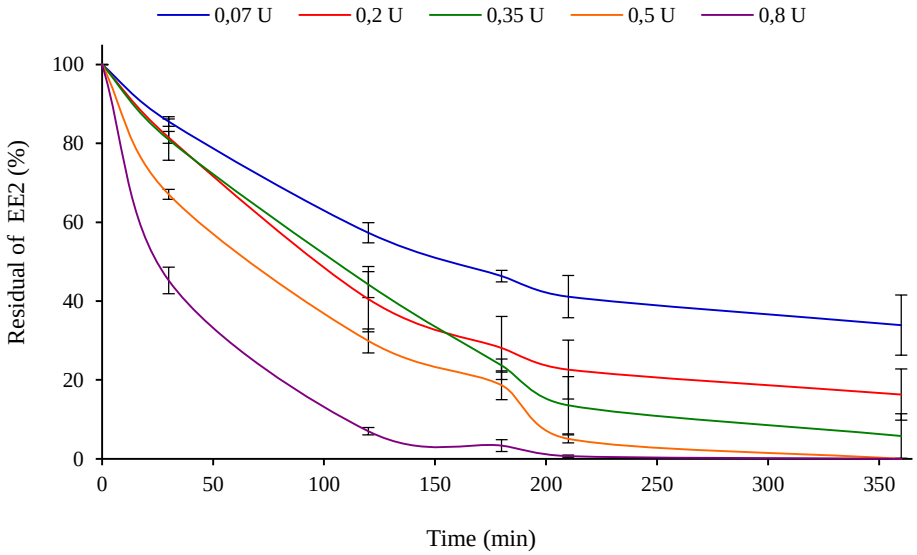

Figure 4.55 Degradation of 17α-ethinyl estradiol by different amounts of laccase from *Trametes versicolor*

The degradation of bisphenol A and 17α-ethinyl estradiol by the immobilized laccase on PCL/SF blend fibre sheets are shown in Figure 4.56 and 4.57, respectively. The immobilized laccase blend fibre sheets were able to degrade around 80% of bisphenol A and 97% of 17α-ethinyl estradiol after 4 hours, which was a better result, compared to the free laccase with 0.07 U. The experiment was repeated the next day after an incubation in ultrapure water at 4 ^{O}C overnight. Even during the second usage, they consumed 75% of bisphenol A and 86% of 17α-ethinyl estradiol. After the second usage, the blend fibre sheets showed marks of mechanical damage during the long time process. Their edges were gradually losing small filaments so it was impossible to recover the original mass of the samples for the second measurement.

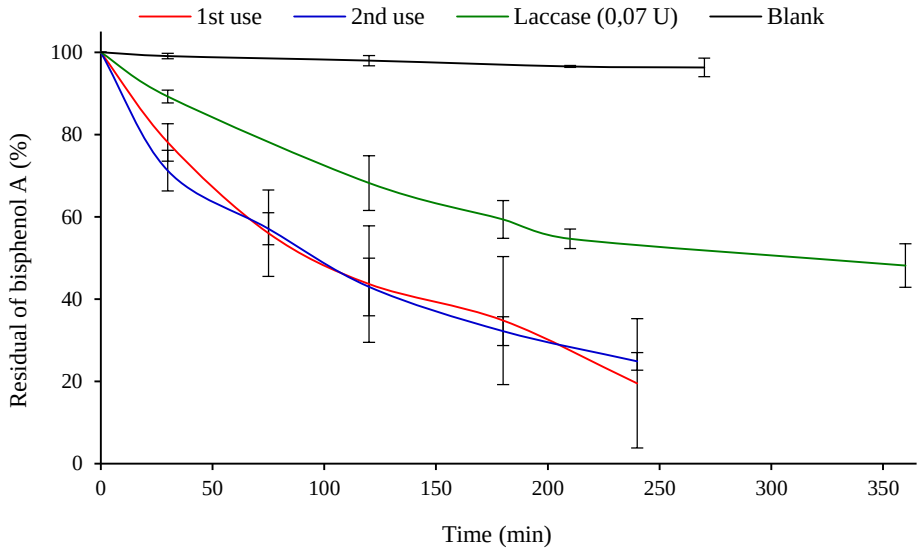

Figure 4.56 Degradation of bisphenol A by the immobilized laccase on PCL/SF blends fibre sheets.

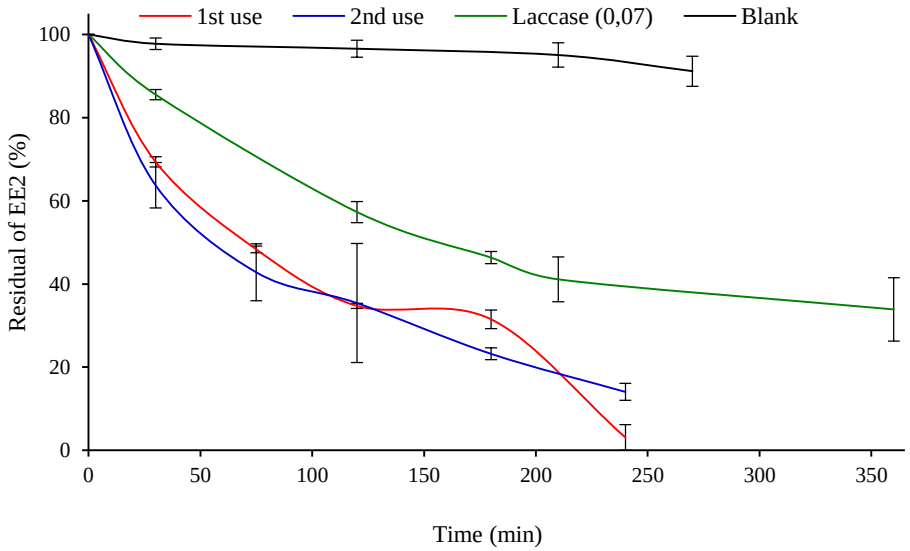

Figure 4.57 Degradation of 17α-ethinyl estradiol by the immobilized laccase on PCL/SF blend fibre sheets.

The result shown that a dagradation of bisphenol A and 17α-ethinyl estradiol by the immobilized laccase on the blend fibre sheets was faster than degradation by the free laccase. This finding was not expected because the free laccase had an advantage against the immobilized enzyme. This advantage was its solubility in the micropollutant mixture offering the laccase to constantly catalyze the degradation in the whole volume of the liquid. On the other hand; the immobilized laccase was attached to the square matrix with the diameter of only 1 cm and this piece of textile was haphazardly floating in the 3 ml of the liquid. The higher catalytic effectiveness of the modified nanofibres might be explained by an increased stability of the immobilized laccase at 40 ^{O}C and constant shaking of 120 rpm compared to the free enzyme which could have lost its activity at these conditions. In some cases, the degradation curve had different shape because of a point where the concentration of the micropollutants increased although it generally showed decreasing tendency. This phenomenon was probably caused by a sampling error.

5. Conclusion

The research studied a fabrication of silk nanofibres with a needleless electrospinning method, concentrating on the effect of the processing parameters on the morphology of the obtained fibres and the spinning performance of the electrospinning process. Biocompatibility of the electrospun fibre sheets was evaluated by *In vitro* testing with living cells.

In these works, a new method for a preparation of a silk fibroin solution by dissolving degummed silk fibre in a mixture of formic acid and calcium chloride is being used instead of a ternary solvent system of $CaCl_2/C_2H_5OH/H_2O$. The use of formic acid-calcium chloride as the solvent for silk fibroin dissolution has an advantage of being simple in an operation when compared to the ternary solvent system. The solvent system consists of formic acid and calcium chloride can directly dissolve silk fibroin at room temperature. The weight ratio of 1:0.25 (w/w) of silk fibres to calcium chloride seems to be a suitable ratio for dissolution of silk fibroin in formic acid.

In an electrospinning process of silk fibroin with formic acid-calcium chloride solvent system, the concentration of the silk solution played an important role in the spinnability of the needleless electrospinning system. The silk electrospun fibres had diameter ranging from 100 nm to 2400 nm when the concentration of silk fibroin increased from 6 wt% to 14 wt%. Concentrations of silk fibroin in the range of 8 wt% to 12 wt% seem to be a suitable concentration for a preparation of silk fibroin nanofibres with the needleless electrospinning. Furthermore, increasing the concentration of the silk fibroin solution improved the spinning ability and the spinning performance of the electrospinning process. An increase in the applied voltage also enhancing the spinning performance of the process, however, an increase in the applied voltage had a little effect on a reduction of diameter of silk fibroin electrospun fibres. On the other hand, the variation of spinning distance in the spinning process was affected the spinning performance. The spinning performance of the process was decreased when the spinning distance was increased.

Compared to a needle electrospinning of silk fibroin in a same the solvent system, the diameter of the electrospun fibres produced with the needle system was smaller and the fibres had a narrower distribution than those obtained with the needleless system. Furthermore, the applied voltage required to initiate the spinning process from the needleless system was higher than that needed to generate fibres from the needle. However, the spinning performance of the needleless electrospinning was much higher than that of the needle electrospinning. In addition, the difference in solvent system for silk fibroin dissolution also influenced the diameters of the obtained fibre. Under the same operating conditions, although, the diameters of the silk electrospun fibres obtained from formic acid-calcium chloride solvent system were greater than those obtained from the ternary solvent system, the processing duration of silk electrospun fibres with this solvent system is much shorter than that of the ternary solvent system. Thus, dissolution of silk fibroin in formic acid and calcium chloride could be potentially employed in a preparation of spinning solution for a large-scale production of silk nanofibres with a needleless electrospinning method.

Even though silk fibroin nanofibres were successfully fabricated with the needleless electrospinning, pure silk electrospun fibres sheet is fragile (low elasticity) in the dry state, which is a disadvantage and would be unsuitable for practical use. Mechanical properties of silk electrospun fibre sheet can improve by blending with synthetic polymers such as polycaprolactone. The blend fibre of silk fibroin and polycaprolactone can also prepare with needleless electrospinning in a same condition and the elasticity of the blend fibre sheet depending on the blend ratios of silk fibroin and polycaprolactone in the solution. An increase in the weight ratio of polycaprolactone in the blend solution increasing the elongation at break of the blend fibres. However, increasing the polycaprolactone content in the blend solution reduced the average fibre diameter and the spinning performance of the process. Moreover, the hydrophilicity of the blend fibre sheet also decreased when increasing the polycaprolactone content, but the blend fibre sheets still have a compatibility with living cell.

The results from *in vitro* tests with living cells show very good biocompatibility of silk fibroin and silk fibroin/polycaprolactone blend fibre sheet. The fibre sheets were able to promote adhesion, spreading and proliferation of 3T3 mouse fibroblasts, normal human dermal fibroblasts and MG 63 osetoblasts. All tested fibre sheets showed good adhesion evaluated 1 day after seeding onto the fibre sheets. During the 2 weeks of experiment, the cells proliferate through the surface of the fibre sheets and cover most of the fibre sheets surface. On the other hand, puer silk fibroin electrospun fibre sheets do not support human umbilical vein endothelial cells proliferation. Endothelial cells adhered on the fibre sheet within the first day but the proliferation was low. After 7 days of incubation period, slight increase in cell viability was observed. It can assume that the silk fibroin electrospun fibre sheet and its blends with polycaprolactone are promising material for the biomedical applications such as wound dressing and bone tissue engineering.

In addition, these works also studied feasibility in enzyme immobilization on the blend fibre sheet. Laccase from *Trametes versicolor* was immobilized on the blend PCL/SF (8/2) nanofibre sheets by covalent attachment method. The appropriate immobilization procedure included a modification via GA-BSA-GA and the 20 hours for the laccase attachment at temperature 4 ^{O}C and pH 3.0. From the obtained result, the PCL/SF blend fibre sheets showed to be a promising material for enzyme immobilization for its sufficient mechanical stabilities and affinity to the enzyme. Several samples, the loading exceeded 100 U/g of the support. Moreover, the PCL/SF blend fibre sheets with the immobilized laccase were more efficient in the degradation of endocrine disrupting chemicals (bisphenol A and 17α-ethinyl estradiol) than approximately same amount of the free laccase. It can suggest that the blend nanofibres could be applied as a component of established water filtering systems for a treatment of effluents coming from facilities known for their high production of endocrine disrupting chemicals in the wastewater.

6. References

1. R.M. Nerem and A. Sambanis, “From Biology to Biological Substitutes”, *Tissue Engineering,* Vol. 1 (2007), pp. 3-13.
2. J.J. Stankus, L.Soletti and K. Fujimoto, “Fabrication of Cell Microintegrated Blood Vessel Constructs Through Electrohydrodynamic Atomization”, *Biomaterials,* Vol. 28 (2007), pp. 2738-2746.
3. N. Amiralian, M. Nouri and M. Haghighat Kish, “Effects of Some Electrospinning Parameters on Morphology of Natural Silk-Based Nanofibers”, *Journal of Applied Polymer Science,* Vol. 113 (2009), pp. 226-234.
4. T. Lin and X.Wang, *Needleless Electrospinning of Nanofibers - Technology and Applications,* Pan Stanford Publishing Pte. Ltd. ISBN-13 : 978-981-4316-84-2 (eBook), 2014.
5. H. Niu, X. Wang and T. Lin, “Needleless Electrospinning : Developments and Performances”, *Nanofibers - Production, Properties and Functional Applications,* InTech, ISBN 978-953-307-420-7, pp. 17-36, 2011.
6. D. Lukáš, A. Sarkar, L. Martinová, K. Vodsedálková, D. Lubasová, J. Chaloupek, P. Pokorný, P. Mikeš, J. Chvojka and M. Komárek, “Physical Principles of Electrospinning (Electrospinning as a Nano-Scale Technology of The Twenty-First Century)”, *Textile Progress,* Vol. 41 (2009), Issue 2, pp. 59-140.
7. H. Niu, T. Lin, and X. Wang, “Needleless Electrospinning I. A Comparison of Cylinder and Disk Nozzles”, *Journal of Applied Polymer Science,* Vol. 114 (2009), Issue 6, pp. 3524-3530.
8. A. L. Yarin and E. Zussman, “Upward Needleless Electrospinning of Multiple Nanofibers”, *Polymer,* Vol. 45 (2004), Issue 9, pp. 2977-2980.
9. O. Jirsak, et al., *A Method of Nanofibers Production from a Polymer Solution Using Electrostatic Spinning and a Device for Carrying Out the Method,* in *EP1673493*. 2005: Czech Republic.
10. X. Wang, H. Niu, T. Lin, and X. Wang, “Needleless Electrospinning of Nanofibers with a Conical Wire Coil”, *Polymer Engineering and Science,* Vol. 49 (2009), No. 8, pp. 1582-1586.
11. O. Jirsak, P. Sysel, F. Sanetrnik, J. Hruza, and J. Chaloupek, “Polyamic Acid Nanofibers Produced by Needleless Electrospinning”, *Journal of Nanomaterials,* Vol. 2012 (2012).
12. C. Huang, H. Niu, J. Wu, Q. Ke, X. Mo and T. Lin, “Needleless Electrospinning of Polystyrene Fibers with an Oriented Surface Line Texture”, *Journal of Nanomaterials,* Vol. 2012 (2012)
13. X. Wang, H. Niu, X.Wang and T. Lin, “Needleless Electrospinning of Uniform Nanofibers Using Spiral Coil Spinnerets”, *Journal of Nanomaterials,* Vol. 2012 (2012).
14. F.Cengiz and O. Jirsak, “The Effect of Salt on the Roller Electrospinning of Polyurethane Nanofibers”, *Fibers and Polymers,* Vol. 10 (2009), No. 2, pp. 177-184, ISSN 1229-9197.

15. A. Matsumoto, H.J. Kim, I.Y. Tsai, X. Wang, P. Cebe and D.L. Kaplan, “Silk”, *Handbook of Fiber Chemistry*, CRC Press Taylor & Francis Group, pp. 383-404, ISBN 0-8247-2565-4, 2007.
16. C. Vepari, D.L. Kaplan, “Silk as a Biomaterial”, *Progress in Polymer Science*, Vol. 32 (2007), pp. 991-1007.
17. B-M. Min, G. Lee, SH. Kim, YS. Nam, TS. Lee and WH. Park, “Electrospinning of Silk Fibroin Nanofibers and Its Effect on the Adhesion and Spreading of Normal Human Keratinocytes and Fibroblasts *In vitro*”, *Biomaterials*, Vol. 25 (2004), pp. 1289-1297.
18. N. Amiralian, M. Nouri, M.H. Kish, An Experimental Study on Electrospinning of Silk Fibroin, http://www.docstoc.com/docs/26292086. Accessed: 2011-05-02.
19. N. Minoura, M. Tsukada and M.Nagura, “Fine-Structure and Oxygen Permeability of Silk Fibroin Membrane Treated with Methanol”. *Polymer*, Vol. 31 (1990), Issue 2, pp. 265-269,
20. Y. Wang, H.J. Kim, G.V. Novakovic and D.L. Kaplan, “Stem Cell-Based Tissue Engineering with Silk Biomaterials”, *Biomaterials*, Vol. 27 (2006), pp. 6064-6082.
21. B.M. Min, L. Jeong, K.Y. Lee and W.H. Park, “Regenerated Silk Fibroin Nanofibers: Water Vapor-Induced Structural Changes and Their Effects on the Behavior of Normal Human Cells”. *Macromolecular Bioscience*, Vol. 6 (2006), pp. 285-292.
22. C. Prommuaka, W. De-Eknamkulb and A. Shotipruka, “Extraction of Flavonoids and Carotenoids from Thai Silk Waste and Antioxidant Activity of Extracts”, *Separation and Purification Technology*, Vol. 62 (2008), Issue 2, pp. 444-448.
23. D. Naskar , R. R. Barua , A. K. Ghosh and S. C. Kundu, “Introduction to Silk Biomaterials”, *Silk Biomaterials for Tissue Engineering and Regenerative Medicine*, Woodhead Publishing Series in Biomaterials: Number 74, pp. 3-40, ISBN 978-0-85709-706-4 (online), 2014.
24. K. Murugesh Babu, “Introduction to Silk and Sericulture”, *Silk: Processing, Properties and Applications*, Woodhead Publishing Series in Textiles: Number 149, pp. 1-32, ISSN 2042-0811 (online), 2013.
25. N.V. Padaki, B. Das1 and A. Basu, “Advances in Understanding the Properties of Silk”, *Advances in Silk Science and Technology*, Woodhead Publishing Series in Textiles: Number 163, pp.3-16, ISBN 978-1-78242-324-9 (online), 2015.
26. A.A. Trevisan, M. Hart, V.Yuste, A. Hjoellund, D. Galle and O. Bergman, “ Cocoon Silk: A Natural Architecture ”.
27. K. Murugesh Babu, “Structural Aspects of Silk”, *Silk: Processing, Properties and Applications*, Woodhead Publishing Series in Textiles: Number 149, pp. 56-83, ISSN 2042-0811 (online), 2013.
28. M. N. Padamwar and A. P. Pawar “Silk Sericin and Its Applications”. *Journal of Scientific & Industrial Research*, Vol. 63, pp. 323-329, 2004.
30. L.G.Wade, *Organic Chemistry six edition*, Pearson Education, Inc., pp.1190, ISBN 0-13-147871-0, 2006.

31. S. Nakamura, J. Magoshi, Y. Magoshi, "Thermal Properties of Silk Proteins in Silkworms", *Silk Polymers-Materials Science and Biotechnology*, American Chemical Society, pp. 211-221, ISBN13: 9780841227439, 1994.
32. W.E. Morton and J.W.S. Hearle, *Physical Properties of Textile Fibres fourth edition*, The Textile Institute, Woodhead Publishing in Textiles, 2008.
33. W. Abdel-Naby and B.D. Lawrence, " Processing of Silk Biomaterials", *Advances in Silk Science and Technology*, Woodhead Publishing Series in Textiles: Number 163, pp. 171-183, ISBN 978-1-78242-324-9 (online), 2015.
34. B. D. Lawrence, "Processing of *Bombyx mori* Silk for Biomedical Applications", *Silk Biomaterials for Tissue Engineering and Regenerative Medicine*, Woodhead Publishing Series in Biomaterials: Number 74, pp. 78-98, ISBN 978-0-85709-706-4 (online), 2014.
35. K. Murugesh Babu, "Developments in the Processing and Applications of Silk", *Silk: Processing, Properties and Applications*, Woodhead Publishing Series in Textiles: Number 149, pp. 140-155, ISSN 2042-0811 (online), 2013.
36. T. Asakura, H. Yoshimizu, M. Kakizaki, "An ESR Study of Spin-Labeled Silk Fibroin Membranes and Spin-Labeled Glucose-Oxidase Immobilized in Silk Fibrion Membranes", *Biotechnology and Bioengineering*, Vol. 35 (1990), Issue 5, pp. 511-517
37. W.S. Muller, L.A. Samuelson, S.A. Fossey, D. L. Kaplan, "Formation and Characterization of Langmuir silk films", *Langmuir*, Vol. 9 (1993), pp. 1857-1861.
38. J. H. Wendorff, S. Agarwal and A. Greiner, *Electrospinning Materials, Processing, and Applications*, Wiley-VCH Verlag & Co. KGaA, Germany, ePDF ISBN: 978-3-527-64773-6, 2012.
39. L. Wang and A. J. Ryan, "Introduction to Electrospinning", *Electrospinning for Tissue Regeneration*, Woodhead Publishing Limited, pp.3-33, ISBN 978-0-85709-291-5 (online), 2011.
40. G. Larsen, R. Velarde-Ortiz, K. Minchow, A. Barrero and I. G. Loscertales, "A Method for Making Inorganic and Hybrid (Organic/Inorganic) Fibers and Vesicles with Diameters in the Submicrometer and Micrometer Range via Sol-Gel Chemistry and Electrically Forced Liquid Jets", *Journal of the American Chemical Society*, Vol. 125 (2003), Issue 5, pp. 1154-1155.
41. D. Li and Y. Xia, "Direct Fabrication of Composite and Ceramic Hollow Nanofibers by Electrospinning", *Nano Letters*, Vol. 4 (2004), Issue 5, pp. 933-938.
42. D. Li, J.T. Mccann and Y. Xia, "Use of Electrospinning to Directly Fabricate Hollow Nanofibers with Functionalized Inner and Outer Surfaces", *Small*, Vol. 1 (2005), Issue 1, pp. 83-86.
43. Z. Sun, E. Zussman, A. L. Yarin, J. H. Wendorff and A. Greiner, "Compound Core-Shell Polymer Nanofibers by Co-Electrospinning", *Advanced Materials*, Vol. 15 (2003), Issue 22, pp. 1929-1932.
44. M. Wang, J.H. Yu, D. L. Kaplan and G. C. Rutledge, "Production of Submicron Diameter Silk Fibers under Benign Processing Conditions by Two-Fluid Electrospinning", *Macromolecules*, Vol. 39 (2006), Issue 3, pp. 1102-1107.

45. J. H. Yu, S. V. Fridrikh and G. C. Rutledge, “Production of Submicrometer Diameter Fibers by Two-Fluid Electrospinning”, *Advanced Materials*, Vol. 16 (2004), Issue 17, pp. 1562-1566.
46. Y. Z. Zhang, Z. M. Huang, X. J. Xu, C. T. Lim and S. Ramakrishna, “Preparation of Core-Shell Structured PCL-r-Gelatin Bi-Component Nanofibers by Coaxial Electrospinning”, *Chemistry of Materials*, Vol. 16 (2004), Issue 18, pp. 3406-3409.
47. B. Ding, E. Kimura, T. Sato, S. Fujita and S. Shiratori, “Fabrication of Blend Biodegradable Nanofibrous Nonwoven Mats via Multi-Jet Electrospinning”, *Polymer*, Vol. 45 (2004), Issue 6, pp. 1895-1902.
48. P. Gupta and G. L. Wilkes, “Some Investigations on the Fiber Formation by Utilizing a Side-by-Side Bicomponent Electrospinning Approach”, *Polymer*, Vol. 44 (2003), Issue 20, pp. 6353-6359.
49. G. Kim, Y. S. Cho and W. D. Kim, “Stability Analysis for Multi Jets Electrospinning Process Modified with a Cylindrical Electrode”, *European Polymer Journal*, Vol. 42 (2006), Issue 9, pp. 2031-2038.
50. O. O. Dosunmu, G. G. Chase, W. Kataphinan and D. H. Reneker, “Electrospinning of Polymer Nanofibres from Multiple Jets on a Porous Tubular Surface”, *Nanotechnology*, Vol. 17 (2006), Number 417, pp. 1123-1127.
51. N. Sasithorn and L. Martinová, “Fabrication of Silk Nanofibres with Needle and Roller Electrospinning Methods”, *Journal of Nanomaterials*, Volume 2014 (2014).
52. B. Robb and B. Lennox, “The Electrospinning Process, Conditions and Control”, *Electrospinning for Tissue Regeneration*, Woodhead Publishing Limited, pp.51-66, ISBN 978-0-85709-291-5 (online), 2011.
53. Ramakrishna, S.; Fujihara, K.; Teo, W.E.; Lim, T.C.; Ma Z.: *An Introduction to Electrospinning and Nanofibers*, ISBN 981-256-415-2, World Scientific Publishing Co. Pte. Ltd., Singapore.
54. Andrady, A.L.: *Science and Technology of Polymer Nanofibers*, John Wiley & Sons, Inc., ISBN 978-0-471-79059-4, the United States of America (2008).
55. J. Du and X. Zhang, “Role of polymer-salt-solvent interactions in the electrospinning of polyacrylonitrile/iron acetylacetonate”, *Journal of Applied Polymer Science*, Vol.109 (2008), Issue 5, pp. 2935-2941.
56. U. Armato, I.D. Pra, C. Migliaresi, A. Motta and K. Kesenci, Method for the Preparation of a Non-Woven Silk Fibroin Fabrics. US Patent 7285637, October 23, 2007.
57. C. Chen, C. Chuanbao, M. Xilan, T. Yin and Z. Hesun, “Preparation of Non-Woven Mats from All-Aqueous Silk Fibroin Solution with Electrospinning Method”, *Polymer*, Vol. 47 (2006), pp. 6322-6327.
58. A. Alessandrino, B. Marelli, C. Arosio, S. Fare, M. C. Tanzi and G. Freddi, “Electrospun Silk Fibroin Mats for Tissue Engineering”, *Engineering in Life Sciences*, Vol. 8 (2008), No. 3, pp. 219-225.
59. S. Sukigaraa, M. Gandhib, J. Ayutsedec, M. Micklusd and F. Kod, “Regeneration of *Bombyx mori* Silk by Electrospinning - Part 1: Processing Parameters and Geometric Properties”, *Polymer*, Vol. 44 (2003), pp. 5721-5727.

60. Z. Liu, F. Zhang, J. Ming, S. Bie, J. Li and B. Zuo, "Preparation of electrospun silk fibroin nanofibres from solutions containing native silk fibrils", *Journal of Applied Polymer Science*, Vol. 132 (2015), Issue 1.
61. J G. Zhang and X M. MO, "Current research on electrospinning of silk fibroin and its blends with natural and synthetic biodegradable polymers", *Frontiers of Materials Science*, Vol. 7 (2013), Issue 2, pp. 129-142.
62. J. Zhou, C B. Cao, X L. Ma and J. Lin, "Electrospinning of silk fibroin and collagen for vascular tissue engineering", *International Journal of Biological Macromolecules*, Vol. 47 (2010), Issue 4, pp. 514-519.
63. M. Garcia-Fuentes, A J. Meinel, M. Hilbe, L. Meinel and H P. Merkle, "Silk fibroin/hyaluronan scaffolds for human mesenchymal stem cell culture in tissue engineering", *Biomaterials*, Vol. 30 (2009), Issue 28, pp. 5068-5076.
64. K. Zhang, L. Fan, Z. Yan, Q. Yu and X. Mo, "Electrospun biomimic nanofibrous scaffolds of silk fibroin/hyaluronic acid for tissue engineering", *Journal of Biomaterials Science Polymer Edition*, Vol. 23 (2012), Issue 9, pp. 1185-1198.
65. L. Li, H. Li, Y. Qian, X. Li, GK. Singh, L. Zhong, W. Liu, Y. Lv, K. Cai, and L.Yang, "Electrospun poly(ε-caprolactone)/silk fibroin core-sheath nanofibers and their potential applications in tissue engineering and drug release", *International Journal of Biological Macromolecules*, Vol. 49 (2011), Issue 2, pp. 223-232.
66. S. Wang, Y. Zhang, H. Wang, G. Yin and Z. Dong, "Fabrication and properties of the electrospun polylactide/silk fibroin-gelatin composite tubular scaffold", *Biomacromolecules*, Vol 10 (2009), Issue 8, pp. 2240-2244.
67. M. A. Woodruff and D. W. Hutmache, "The return of a forgotten polymer-Polycaprolactone in the 21st century", *Progress in Polymer Science*, Vol. 35 (2010), Issue 10, pp. 1217-1256.
68. N. Sasithorn and L. Martinová, "Effect of calcium chloride on electrospinning of silk fibroin nanofibers", *RMUTP Research Journal: Special Issue* (2014), pp. 62-69, ISSN 1906-0432.
69. N. Sasithorn and L. Martinová, Fabrication of Silk Fibroin-Polycaprolactone Blend Fibres using Needleless Electrospinning, *the International Symposium on Fiber Science and Technology (ISF2014)*, Tokyo, Japan (2014).
70. N. Sasithorn and L. Martinová, Needleless Electrospinning of Silk fibroin/ Polycaprolactone Blend Nanofibres, *6th International Conference on Nanomaterials (NANOCON 2014)*, Brno, Czech Republic (2014).
71. F.H. Arnold and G. Georgiou, *Directed Enzyme Evolution: Screening and Selection Methods*, Methods in Molecular Biology, Vol. 230, ISBN-13: 978-1588292865 (2003)
72. T. Hassani, S. Ba and H. Cabana. "Formation of enzyme polymer engineered structure for laccase and cross-linked aggregates stabilization", *Bioresource Technology*, Vol. 128 (2013), pp. 640-645.

73. P. Zapata-Castillo, MdeL. Villalonga-Santana, J. Tamayo-Cortés, G. Rivera-Muñoz and S. Solís-Pereira, "Purification and characterization of laccase from *Trametes hirsuta* Bm-2 and its contribution to dye and effluent decolorization", *African Journal of Biotechnology*, Vol 11, No. 15 (2012), pp. 3603-3611
74. M. Alves Da Silva, M. Helena Gil, J. S. Redinha, Ana M. Oliveira-Brett and J. L. Costa Pereira, "Immobilization of Glucose Oxidase on Nylon Membranes and Its Applications in a Flow-Through Glucose Reactor", *Journal of Polymer Science: Part A: Polymer Chemistry*, Vol. 29 (1991), Issue 2, pp. 275-279.
75. C. Silva, C. J. Silva, A. Zille, G. M. Guebitz, and A. Cavaco-Paulo, "Laccase immobilization on enzymatically functionalized polyamide 6,6 fibres", *Enzyme and Microbial Technology*, Vol. 41 (2007), Issues 6-7, pp. 867-875
76. S.W. Ha, Y. H. Park and S. M. Hudson, "Dissolution of Bombyx mori Silk Fibroin in the Calcium NitrateTetrahydrate-Methanol System and Aspects of Wet Spinning of Fibroin Solution", *Biomacromolecules*, Vol. 4 (2003), pp. 488-496.
77. B. Sun, "Study on the Mechanism of Nylon 6,6 Dissolving Process Using $CaCl_2$/MeOH as the Solvent", *Chinese Journal of Polymer Science,* Vol. 12 (1994), Issue: 1, pp. 57-65.
78. Z. Yang, H. Yin, X. Li, Z. Liu and Q. Jia, "Study on dry spinning and structure of low mole ratio complex of calcium chloride-polyamide 6", *Journal of Applied Polymer Science*, Vol. 118 (2010), Issue 4, pp. 1996-2004.
79. S. De Vrieze, T. Van Camp, A. Nelvig, B. Hagström, P. Westbroek and K. De Clerck, "The effect of temperature and humidity on electrospinning", *Journal of Materials Science*, Vol. 44 (2009), Issue 5, pp. 1357-1362,
80. F. Yener and O. Jirsak, "Comparison between the Needle- and Roller Electrospinning of Polyvinylbutyral", *Journal of Nanomaterials*, vol. 2012 (2012).
81. H. Zhang, L. Li, F. Dai, H. Zhang, B. Ni, W. Zhou, X. Yang and Y.Wu, "Preparation and characterization of silk fibroin as a biomaterial with potential for drug delivery", *Journal of Translational Medicine*, Vol. 10 (2012).
82. N. Amiraliyan, M. Nouri, and M. Haghighat Kish, "Structural Characterization and Mechanical Properties of Electrospun Silk Fibroin Nanofiber Mats", *Polymer Science,* Vol. 52 (2010), No. 4, pp. 407-412, ISSN 0965-545X.
83. K.Zhang, Q.Ye and Z. Yan, "Influence of Post-Treatment with 75% (v/v) Ethanol Vapor on the Properties of SF/P(LLA-CL) Nanofibrous Scaffolds", *International Journal of Molecular Sciences*, 2012 (13), pp. 2036-2047, ISSN 1422-0067.
84. W. Wei, Y. Zhang, Y. Zhao, H. Shao and X. Hu, "Studies on the post-treatment of the dry-spun fibers from regenerated silkfibroin solution: Post-treatment agent and method", Materials and Design, Vol. 36 (2012), pp. 816-822.
85. C. J. Luo, E. Stride and M. Edirisinghe, "Mapping the Influence of Solubility and Dielectric Constant on Electrospinning Polycaprolactone Solutions", *Macromolecules*, vol. 45 (2012), Issue 11, pp. 4669-4680 .
86. J. Lim, C. Ki, J. Kim, K.Lee, S. Kang, H. Kweon and Y. Park, "Fabrication and evaluation of poly(epsilon-caprolactone)/silk fibroin blend nanofibrous scaffold", *Biopolymers*, Vol. 97 (2012), Issue 5, pp. 265-275.

87. N. Sasithorn and L. Martinová, Preparation of Silk Fibroin Electrospun Fibres with Needle and Roller Electrospinning Technique, *the Second International Conference on Advanced Materials, Energy and Environments (ICMEE)*, Yokohama, Japan, (2013), pp. 43-46, ISSN: 1939-7348 Online.